INFORMATION TO USERS

This manuscript has been reproduced from the microfilm master. UMI films the text directly from the original or copy submitted. Thus, some thesis and dissertation copies are in typewriter face, while others may be from any type of computer printer.

The quality of this reproduction is dependent upon the quality of the copy submitted. Broken or indistinct print, colored or poor quality illustrations and photographs, print bleedthrough, substandard margins, and improper alignment can adversely affect reproduction.

In the unlikely event that the author did not send UMI a complete manuscript and there are missing pages, these will be noted. Also, if unauthorized copyright material had to be removed, a note will indicate the deletion.

Oversize materials (e.g., maps, drawings, charts) are reproduced by sectioning the original, beginning at the upper left-hand corner and continuing from left to right in equal sections with small overlaps. Each original is also photographed in one exposure and is included in reduced form at the back of the book.

Photographs included in the original manuscript have been reproduced xerographically in this copy. Higher quality 6" x 9" black and white photographic prints are available for any photographs or illustrations appearing in this copy for an additional charge. Contact UMI directly to order.

UMI

A Bell & Howell Information Company
300 North Zeeb Road, Ann Arbor MI 48106-1346 USA
313/761-4700 800/521-0600

OCEANIC EMISSIONS OF SULFUR:

APPLICATION OF NEW TECHNIQUES

A

THESIS

Presented to the Faculty

of the University of Alaska Fairbanks

in Partial Fulfillment of the Requirements

for the Degree of

DOCTOR OF PHILOSOPHY

By

Clara Jodwalis, B.S., M.S.

Fairbanks, Alaska

August 1998

OCEANIC EMISSIONS OF SULFUR:

APPLICATION OF NEW TECHNIQUES

by

Clara Jodwalis

RECOMMENDED:

Advisory Committee Chair

Department Head, Chemistry and Biochemistry

APPROVED:

Dean, College of Science, Engineering and Mathematics

Dean of the Graduate School

8-27-98

Date

Abstract

Sulfur gases and aerosols are important in the atmosphere because they play major roles in acid rain, arctic haze, air pollution, and climate. Globally, man-made and natural sulfur emissions are comparable in magnitude. The major natural source is dimethyl sulfide (DMS) from the oceans, where it originates from the degradation of dimethysulfoniopropionate (DMSP), a compound produced by marine phytoplankton. Global budgets of natural sulfur emissions are uncertain because of (1) the uncertainty in the traditional method used to estimate DMS sea-to-air flux, and (2) the spatial and temporal variability of DMS sea-to-air flux. We have worked to lessen the uncertainty on both fronts.

The commonly used method for estimating DMS sea-to-air flux is certain to a factor of two, at best. We used a novel instrumental technique to measure, for the first time, sulfur gas concentration fluctuations in the marine boundary layer. The measured concentration fluctuations were then used with two established micrometeorological techniques to estimate sea-to-air flux of sulfur. Both methods appear to be more accurate than the commonly used one. The analytical instrument we used in our studies shows potential as a direct flux measurement device.

High primary productivity in high-latitude oceans suggests a potentially large DMS source from northern oceans. To begin to investigate this hypothesis, we have measured DMS in the air over northern oceans around Alaska. For integrating and extrapolating field measurements over larger areas and longer time periods, we have developed a model of DMS ocean mixing, biological production, and sea-to-air flux of DMS. The model's main utility is in gaining intuition on which parameters are most important to DMS sea-to-air flux. This information, along with a direct flux measurement capability, are crucial steps toward the long-term goal of remotely sensing DMS flux. A remote sensing approach will mitigate the problems of spatial and temporal variability. The new developments in methodology, field sampling, and modeling put forth in this thesis are tools we have used to better understand and quantify sulfur gas emissions from northern oceans, which appear to be a significant source of sulfur to the global atmosphere.

Table of Contents

List of Figures

List of Tables

Acknowledgments

I am fortunate to have had many valuable collaborations and discussions with expert scientists. Special thanks to Don Lenschow of NCAR and Chris Fairall of NOAA for many insightful comments and discussions. This doctoral research at northern latitudes would not have been possible without the contributions of Dave Eslinger and Tom Weingartner of the Institute of Marine Sciences at the University of Alaska Fairbanks. Dave Eslinger worked with us, using his model to develop the DMS model. Tom Weingartner provided a berth, space to work and a heap of enthusiasm aboard the RV *Alpha Helix*. The captains and crews of the RV *Alpha Helix* and RV *Oceanus* also provided expert support, which I truly appreciate.

Funding to do this work was provided by the Office of Naval Research Ocean Chemistry Program, NASA Aerosol Interdisciplinary Program and the Center for Global Change and Arctic System Research at the University of Alaska Fairbanks. For this support, I am grateful.

I proudly thank my family and friends who continue to give me encouragement and understanding. You are terrific!

Thanks to my colleagues Dennis Nicks, Will Cantrel and Dave Veazy, the Renaissance Men. They are a good bunch to do a field campaign with and bounce ideas off of.

Most of all, I thank my advisor, Richard Benner, for steering me away from jargon, garnering funds, and sharing his ideas. He and the rest of my committee members, Richard Stolzberg, Glenn Shaw, Susan Henrichs and Dave Eslinger, have taught me a lot, simply by example.

Chapter 1

Introduction

Sulfur is unique among the panoply of elements. An essential element for organisms, it provides the strong disulfide linkages that give proteins three-dimensional structure. At deep sea hydrothermal vents, oxidation of reduced sulfur is responsible for chemosynthetic primary production without photosynthesis. Sulfur exists naturally in many oxidation states (-II, -I, 0, II, IV, VI), and is found in gaseous, aerosol, aqueous, mineral and organic forms. This leads to sulfur's participation in many oxidation-reduction reactions that have important geochemical consequences. Notably, large sediment reservoirs of FeS_2 result from bacterial reduction in marine sediments. Photochemistry, biology and weathering all play roles in oxidizing sulfur to its highest oxidation state, sulfate (SO_4^{-2}), which is the second most abundant anion in rivers and seawater.

Six valence electrons, six oxidation states, and an electronegativity similar to that of carbon drive sulfur's reactivity. Some ionic bonding with highly electropositive elements occurs, but in nature most sulfur bonding is covalent. The available electrons and mid-range electronegativity of the sulfur atom make possible a multitude of covalent bond types and strengths.

Sulfur-containing aerosol particles and gases are present in ambient air everywhere over land and sea. Although the vast majority of sulfur at any given time is in the lithosphere, the major annual movement of sulfur is by rivers and through the atmosphere [*Harte*, 1988; *Schlesinger* 1991]. This is largely due to the production of volatile, reduced sulfur compounds by biota.

The unique properties of sulfur lead to its reactivity and tendency to form aerosols in the atmosphere. Because of these properties, sulfur gases and aerosols play major roles in acid rain, arctic haze, air pollution, and cloud formation. Sulfur is the major cause of acidity in both natural and polluted rainwater, playing a key role in the

natural weathering of rocks and environmental concerns such as acid rain [*Charlson et al.*, 1992]. In both remote and polluted settings, sulfate in the atmosphere is the dominant component of cloud condensation nuclei (CCN) [*Bigg et al.*, 1984]. This has important consequences for the hydrologic cycle and the earth's radiation balance. Model calculations show that the albedo of clouds over remote oceans increases with increasing CCN number [*Andreae*, 1990]. Sulfate aerosols in the atmosphere may impact climate directly, through light scattering [*Shaw*, 1983], or indirectly, by affecting the formation, amount, lifetime and radiative properties of clouds [*Charlson et al.*, 1994].

Sulfur enters the atmosphere from both man-made and natural sources. Anthropogenic inputs, almost entirely sulfur dioxide (SO_2), result mostly from coal burning and sulfide ore smelting. Current anthropogenic emissions sum to 85 ± 10 Tg S/year [*Andreae*, 1989], and are known to a relatively high degree of accuracy because the sources are known and relatively easy to quantify. On the other hand, natural sulfur is emitted in many forms from a wide variety of very weak sources. Add to this the high spatial and temporal variability of these emissions and calculating a global estimate easily becomes unwieldy and inexact. Natural sulfur emissions to the atmosphere are estimated globally to be 57 Tg S/year with an uncertainty between -50% and +100% [*Charlson et al.*, 1992].

Oceanic dimethyl sulfide (DMS) is thought to be the major natural source of sulfur to the atmosphere. The source is the metabolic release of DMS [*Andreae*, 1990] and its precursor, dimethylsulfoniopropionate (DMSP) [*Turner et al.*, 1988, 1989], from phytoplankton in surface seawater. The global DMS sea-to-air flux is estimated to be 11 - 54 Tg S/year [*Matrai and Keller*, 1993]. The large range reflects the uncertainty in estimations of DMS sea-to-air flux from various parts of the world's oceans, a high degree of spatial and temporal inhomogeneity, and the difficulty in measuring rates of transfer across the air-sea interface. The lack of a direct flux

measuring capability forces workers to use empirically-derived estimates of the flux. Biomass burning and volcanoes release mostly SO_2, about 28 Tg S/year [*Charlson et al.*, 1991]. However, these emissions are episodic and difficult to quantify. Perhaps even more difficult to quantify are the biogenic land sources, due to the heterogeneity of land surfaces, biological variability on many scales and inadequate geographic coverage of existing data. These are estimated to be 20 Tg S/yr, certain to within only a factor of 10 [*Adams et al.*, 1981; *Goldan et al.*, 1987].

Comparable amounts of global sulfur emissions from anthropogenic and natural sources indicate a global sulfur cycle intensely perturbed by human activity. Natural reduced sulfur emissions are largely oxidized by hydroxyl (OH) radical to sulfate that is deposited in precipitation. Anthropogenic emissions of SO_2 to the atmosphere should have the same effect as natural emissions, since this SO_2 is also oxidized to produce sulfate. The magnitude and variability of both sources needs to be understood to determine the significance of either. For example, the relative importance of natural sulfur compounds in the atmosphere, compared to anthropogenic, is important in evaluating the cause of acid rain and the impact of anthropogenic emissions on natural ecosystems.

The atmospheric sulfur cycle is a regional phenomenon. By viewing sulfur emissions on a global or hemispheric scale, regional climate and environmental impacts may be missed. For example, biomass burning is only a minor source of sulfur to the atmosphere, releasing about 2.6 Tg S/yr. However, it is important in tropical regions, where other sulfur emissions are sparse [*Andreae*, 1990]. The patchy distribution of atmospheric sulfur can be explained by the short lifetime of sulfur species in the atmosphere [*Junge*, 1974]. The most important pathway of sulfur through the atmosphere is injection as a low oxidation state gas, followed by removal as oxidation state VI (i.e. SO_4^{2-}) in rainwater. Since the pathway is driven by changes in the chemical oxidation state and physical phase, the lifetime is determined by the kinetics

of the oxidation reactions and the occurrence of clouds and rain. The whole process lasts on the order of hours to days. This results in widely varying atmospheric sulfur gas mixing ratios and sulfate aerosol distributions over the globe.

One, if not the major, uncertainty in understanding the atmospheric sulfur cycle is the surface flux of sulfur species. It is difficult to evaluate the significance of anthropogenic emissions and the impact of natural emissions on climate without being able to quantify natural emissions. Since anthropogenic and natural emissions can be comparable in magnitude, biogenic emissions need to be included in calculations of long-range transport and deposition of sulfur. We have worked to lessen the uncertainty in quantifying natural sulfur emissions on two fronts: 1) flux method development, including field measurements and comparison with current methods, and 2) evaluation of the magnitude of a northern ocean source through screening studies and modeling.

For my doctoral research, I have chosen to focus on marine biogenic sulfur flux and emissions for several reasons. The most compelling reason is that there is a substantial flux of sulfur from the ocean to the atmosphere and, as of yet, no direct way to quantify the flux. The horizontal homogeneity of ocean surfaces offers a good laboratory for studying sulfur gas fluxes, compared to the relative heterogeneity and biological variability of land surfaces. Hence, the ocean is a good starting point for researching the natural sources of sulfur to the atmosphere. The few existing atmospheric sulfur gas measurements from northern ocean regions, along with the high biological primary productivity in these regions, suggests a major contribution of sulfur gases to the atmospheric sulfur budget. The remoteness of these regions avoids the complex pollution chemistry found in populated areas.

Estimates of DMS sea-to-air flux are accurate only to a factor of two, at best [*Andreae,* 1986]. This large uncertainty exists because the commonly used method for estimating DMS flux, the stagnant boundary layer (SBL) method, is indirect -- derived

from an empirical relationship between DMS concentration in seawater and the transfer velocity. Transfer velocities, usually estimated by the radon deficit method, are adjusted for local wind speed and the molecular properties of the diffusing gas. A factor of two uncertainty in DMS gas transfer velocities [*Bates et al.*, 1987] results in flux estimates at least as uncertain.

Richard Benner and I have developed two new methods for estimating DMS sea-to-air flux -- the variance method and the inertial-dissipation method [*Jodwalis and Benner*, 1996]. Both are independent of the commonly used SBL method and have been used successfully for estimating fluxes of other constituents. We used these methods as part of a field campaign during June of 1992 near the Azores, as part of the international experiment known as the Atlantic Stratocumulus Transition Experiment/Marine Aerosol and Gas Exchange (ASTEX/MAGE).

In addition to the flux methods, data from the Azores study were used to develop a new - to our knowledge, the only - method to determine the magnitude and time scale of sulfur gas concentration fluctuations. This information is critical in establishing an experimental design for sample integration time needed to obtain a representative measurement.

In the Azores, we used a sulfur chemiluminescence detector (SCD). The fast response and sensitivity of the SCD make it well suited for direct flux measurements. We showed that the instrument is capable of measuring turbulent-scale-sulfur-concentration fluctuations in the atmosphere, demonstrating its potential as a direct flux measurement instrument. We know of no other instrument with this capability.

The few existing measurements from northern ocean regions of DMS in marine boundary layer (MBL) air [*Aargaard et al.*, 1996; *Ferek and Herring*, 1991] and surface seawater [*Bates et al.*, 1987; *Bürgermeister and Georgii*, 1991] show high levels. To investigate the possibility that the biologically productive waters surrounding Alaska are a significant source of sulfur, atmospheric DMS mixing ratios

in the MBL were measured:

1) aboard the *R/V Alpha Helix* from September 6 through October 4, 1995 in the Chukchi and Bering Seas, and
2) from a land-based research station 6 miles north of Homer, Alaska, overlooking Kachemak Bay, for eleven days in June 1996.

To make these measurements, we interfaced a gas chromatograph to an SCD. For collecting remote shipboard samples for later laboratory analyses, we constructed a remote sampling system that fits into a suitcase.

Since the dominant source of atmospheric DMS is the ocean, understanding the sources and cycling of DMS in surface seawater is important. This is especially evident, considering that only a small percentage of oceanic DMS is vented to the atmosphere [*Bates et al.*, 1994]. Figure 4.3 in Chapter 4 of this thesis is a schematic of the oceanic DMS cycle. The majority of the DMS appears to be cycled through a microbial loop, on time scales from shorter than a day to several days [*Taylor and Kiene*, 1989], depending on the physical environment. The microbial loop is part of a complex food web, involving phytoplankton, zooplankton and bacteria, which governs the distribution and concentration of DMS [*Kiene and Service*, 1991]. Dynamic, biologically-mediated processes result in typically wide fluctuations of DMS in seawater [*Keller*,1989].

Ocean mixed-layer dynamics may play an important role in DMS sea-to-air flux. Mixing, driven by mechanical or thermal destabilization of the water column, replenishes the DMS in surface waters and reinvigorate the biological production by mixing nutrients from below to the surface. The magnitude, duration and frequency of such events could lead to total yearly and regional fluxes of DMS to the atmosphere that are substantially different from what a few samples representing only short time intervals, might indicate.

In collaboration with Dave Eslinger of the University of Alaska Institute of

Marine Science, we have included DMS dynamics in a one-dimensional, mixed-layer model to test the importance of ocean mixed-layer dynamics to DMS sea-to-air flux. Such a model can also be used to assess the importance of parameters affecting DMS flux (e.g., nutrients, salinity, zooplankton grazing) to guide future field-measurement campaigns and provide a more fundamental understanding of the system and how it controls DMS sea-to-air flux.

According to Robert Charlson [1992], a well-known advocate of sulfur's importance in the environment, "the sulfur cycle can only sensibly be studied on a regional basis, and calculation of global budgets will necessarily be a painstaking process of making myriad measurements over a wide range of regions and seasons to allow accurate averaging." A remote sensing approach will be the key to making this process much less painstaking. The possibility exists for using remotely sensed data to locate sources, map distributions, and estimate global-scale fluxes of marine sulfur. Empirical algorithms must be derived using direct surface flux measurements. In a chapter of this thesis [*Jodwalis and Benner,* 1995], we discuss the possibility of developing a satellite-based DMS flux capability and describe a direct surface flux measurement technique that can be used to develop the necessary empirical relationships.

References

Aargaard, K., L. A. Barrie, E. C. Carmack, C. Garrity, E. P. Jones, D. Lubin, R. W. Macdonald, J. H. Swift, W. B. Tucker, P. A. Wheeler, and R. H. Whitner, U.S., Canadian researchers explore Arctic Ocean, *EOS, 77,* (22), 209-216, 1996.

Andreae, M. O., The ocean as a source of atmospheric sulfur compounds, in: The role of air-sea exchange in geochemical cycling, *edited by* Buat-Menard, pp 331-362, D.

Reidel, Norwell, Mass., 1986.

Andreae, M. O., Ocean-atmosphere interactions in the global biogeochemical sulfur cycle, *Marine Chemistry, 30*, 1-29, 1990.

Bates, T. S., J. D. Cline, R. H. Gammon, and S. R. Kelly-Hansen, Regional and seasonal variations in the flux of oceanic dimethylsulfide to the atmosphere, *Journal of Geophysical Research, 92*, (C3), 2930-2938, 1987.

Bates, T. S., R. P. Kiene, G. V. Wolfe, P. A. Matrai, F. P. Chavez, K. R. Buck, B. W. Blomquist, and R. L. Cuhel, The cycling of sulfur in surface seawater of the northeast Pacific, *Journal of Geophysical Research, 99*, (C4), 7835-7843, 1994.

Bigg, E. K., J. L. Gras, and C. Evans, Origin of Aitken particles in remote regions of the Southern Hemisphere, *Journal of Atmospheric Chemistry, 1*, (2), 203-214, 1984.

Bürgermeister, S., and H. W. Georgii, Distribution of methanesulfonate, NSS sulfate and dimethylsulfide over the Atlantic and the North Sea, *Atmospheric Environment, 25A*, (3/4), 587-595, 1991.

Charlson, R. J., J. Langer, H. Rodhe, C. B. Leovy, and S. G. Warren, Perturbation of the norther hemisphere radiative balance by backscattering from anthropogenic sulfate aerosols, *Tellus, 43ab*, 152-163, 1991.

Charlson, R. J., S. E. Schwartz, J. M. Hales, R. D. Cess, J. A. Jr. Coakley, J. E. Hansen, and D. J. Hofmann, Climate forcing by anthropogenic aerosols, *Science, 255*, 423-430, 1992.

Charlson, R. J., and T. M. L. Wigley, Sulfate aerosol and climatic change, *Scientific American*, 48-57, 1994.

Ferek, R. J., and J. A. Herring, Ground-based measurement of DMS in the Arctic atmosphere at Barrow during summer 1991, *Climate Monitoring and Diagnostics Laboratory*, (20), 1991.

Harte, J., *Consider a Spherical Cow: A Course in Environmental Problem Solving*, University Science Books, Mill Valley, California, 1988.

Jodwalis, C. J., and R. L. Benner, On the possibility of remotely sensing global dimethyl sulfide sea-to-air flux, *Polar Record, 31*, (177), 251-256, 1995.

Jodwalis, C. M., and R. L. Benner, Sulfur gas fluxes and horizontal inhomogeneities in the marine boundary layer, *Journal of Geophysical Research, 101*, (D2), 4393-4401, 1996.

Junge, C. E., Residence Time and Variability of Tropospheric Gases, *Tellus, 26*, (4), 477-488, 1974.

Keller, M., Dimethyl sulfide production and marine phytoplankton: The importance of species composition and cell size, *Biological oceanography, 6*, 375-382, 1989.

Kiene, R. P., and S. K. Service, Decomposition of dissolved DMSP and DMS in estuarine waters: Dependence on temperature and substrate concentration, *Marine Ecology Progress Series, 76*, 1-11, 1991.

Kuster, W. C., and P. D. Goldan, Quantitation of the losses of gaseous sulfur compounds to enclosure walls, *Eviron. Sci. Technol., 21*, (8), 810-815, 1987.

Matrai, P. A., and M. D. Keller, Dimethylsulfide in a large-scale coccolithophore bloom in the Gulf of Maine, *Continental Shelf Research, 13*, (8/9), 831-843, 1993.

Schlesinger, W. H., *Biogeochemistry an Analysis of Global Change*, Academic Press, San Diego, 1991.

Shaw, G. E., Bio-controlled thermostatis involving the sulfur cycle, *Climatic Change, 5,* 297-303, 1983.

Taylor, B. F.; Kiene, R. P. *Biogenic Sulfur in the Environment*; Saltzman, E. S.; Cooper, W. J., American Chemical Society: Washington, DC, 1989; pp 202-221.

Turner, S. M., G. L. P. S. Malin, D. S. Harbour, and P. M. Holligan, The seasonal variation of dimethyl sulfide and dimethylsulfoniopropionate concentrations in nearshore waters, *Limnological Oceanography, 33,* (3), 364-375, 1988.

Turner, S. M., Malin, G., and Liss, P. S., Dimethyl sulfide and (dimethylsulfonio)propionate in European coastal and shelf waters, In: *Biogenic Sulfur in the Environment, edited by* Saltzman, E. S. and W. J. Cooper, pp 183-200, American Chemical Society, Washington, DC, 1989.

Chapter 2

Sulfur Gas Fluxes and Horizontal Inhomogeneities in the Marine Boundary Layer[1]

Abstract

Real-time total gaseous sulfur concentrations were measured (sampling frequency 1 Hz) from the R/V *Oceanus* as part of the Atlantic Stratocumulus Transition Experiment/Marine Aerosol and Gas Exchange (ASTEX/MAGE) field campaign in the Azores during June of 1992. The measurements were used to estimate sulfur gas sea-to-air flux, determine the size scale of sulfur gas inhomogeneities in the marine boundary layer, and the timescale of sampling necessary to characterize a meaningful air mass. Using the time scale of sampling and wind speed measurements, the size scale of sampling can also be determined. Sea-to-air sulfur gas flux estimates were obtained using a variance method and the inertial-dissipation method. Values from five 1-hour measurement periods on two different days ranged from 21 to 28 $\mu mol/m^2 \cdot d$ and 11 to 17 $\mu mol/m^2 \cdot d$, respectively. These values are above the range of 1 to 13 $\mu mol/m^2 \cdot d$ reported by Blomquist et al. (this issue) during ASTEX/MAGE, based on the dimethyl sulfide (DMS) concentration in surface seawater, using the stagnant boundary layer model of air-sea exchange. A power spectrum of the sulfur gas time series shows the contribution of each turbulent eddy size to the total signal variance. In a representation of the power spectrum, the area under any portion of the curve is proportional to the variance. From these power spectra we have obtained the fraction of the total variance in ground level sulfur concentration fluctuations as a function of time. The data indicate that

---

[1]Jodwalis, C.M. and R.L. Benner, Sulfur gas fluxes and horizontal inhomogeneities in the marine boundary layer, 1996, *Journal of Geophysical Research*, 101 (D2), 4393-4401.

air samples should be integrated for 1000 s for ground-based measurements.

Introduction

The ocean is the largest natural source of sulfur gases emitted to the atmosphere. This is due to the release of biogenic dimethyl sulfide ($(CH_3)_2S$ or DMS) as the byproduct of the biological activity of marine phytoplankton. The magnitude of this source is uncertain, but estimates based on DMS concentrations in seawater and mass-balance models of the atmospheric sulfur cycle indicate that it is comparable to anthropogenic emissions of sulfur gases [*Andreae et al.*, 1985; *Cullis and Hirschler*, 1980; *Möller*, 1984].

The major constituent, by number concentration, of non-sea- salt marine aerosols is sulfate [e.g. *Clarke et al.*, 1987], of which DMS is the dominant sulfur source [*Bonsang et al.*, 1980]. In recent years, interest in the magnitude of the oceanic source of DMS has heightened, mainly because it is believed to make a significant contribution to the atmospheric aerosol burden. These aerosols that result from the oxidation of DMS may be a factor in global climate change through their influence on the Earth's radiation budget [e.g., *Charlson et al.*, 1987; *Charlson and Wigley*, 1994; *Shaw*, 1983].

Accurate flux measurements are essential in determining global sulfur budgets and the influence of sulfur gases on the atmospheric aerosol burden. This is because fluxes play an important role in all the processes that control chemical cycles (i.e. production, transport, distribution, chemical transformations and removal). One, if not the major, uncertainty in understanding the atmospheric sulfur cycle is the surface flux of sulfur species.

Volatile substances are transferred across the air-sea interface by molecular diffusion and other processes, which are complex and poorly understood. No entirely satisfactory model exists that describes air-sea gas exchange. The most commonly used method for estimating DMS sea-to-air flux is based on *Liss and Slater's* [1974] stagnant boundary layer model of air-sea gas exchange, using DMS seawater concentrations. This

model is also sometimes referred to as the stagnant film model or air-sea gas exchange model. In this model, the flux between liquid and gas phase is determined by the rate of molecular diffusion across a stagnant film. Since the atmosphere is highly undersaturated with respect to the coexisting seawater,

$$\textbf{Flux} \approx v_t\, c_t \qquad (1)$$

where c_l is the seawater concentration of DMS and v_t the transfer velocity.

Transfer velocities, usually estimated by the radon deficit or ^{14}C methods, are adjusted for local wind speeds and the molecular properties of the diffusing gas. A major problem with using wind speed correlations to estimate transfer velocities is that the time scale for wind speed variations (of the order of hours) is much shorter than the time scales used to determine the transfer velocities [*Smethie et al.*, 1985]. This makes estimating gas transfer velocities difficult and uncertain. Another approach is to use wind tunnel studies to make wind speed correlations. *Liss* [1983] gives an overview of results from such studies, and a summary and update is provided by *Liss and Merlivat* [1986]. It is important to keep in mind that the waves generated in wind tunnels are different from ocean waves because of the influence of walls, reflection, and a different turbulence regime. Roughly a factor of 2 uncertainty is typical for values of v_t [*Andreae*, 1986; *Bates et al.*, 1987]. This means that a similar uncertainty in flux estimates using transfer velocities is possible.

Wanninkhof [1992] states, "it is likely that relationships using only wind speed to predict transfer velocities will be flawed." The basis for this statement is that wind speed is not the only factor influencing the gas transfer velocity. Other important factors he mentions include turbulence at the air-water interface, boundary layer stability, surfactants, and bubbles, some of which are not "intimately linked" to wind speed. Parameters which are more closely related to surface turbulence might be better predictors of gas transfer [*Wanninkhof*, 1992].

We have mentioned above just some of the uncertainties involved in using the stagnant boundary layer model to estimate DMS sea-to-air flux. Another, independent method is definitely needed for validation. *Jähne et al.* [1987] have stressed the need for development of new techniques for measuring transfer processes locally and instantaneously. *Andreae* [1986] states that "in view of the large uncertainties associated with the "stagnant film" model, it seems very important that independent methods be developed to test the predictions based on this model."

Estimates based on DMS concentrations in surface seawater, using the stagnant boundary layer model, indicate that the magnitude of DMS sea-to-air flux is highly variable, ranging over a couple of orders of magnitude [*Thompson et al.*, 1990]. Some of this variability could be attributed to higher levels observed in areas of higher biological productivity, and seasonal variations in seawater DMS concentrations. Seawater DMS concentrations also show diurnal behavior [*Andreae et al.*, 1985], which could account for some of the variability in our range of estimates.

We offer sulfur gas sea-to-air flux estimates from two other indirect methods, known as the variance method and the inertial-dissipation method. Both are independent of the commonly used method and have previously been used successfully for estimating fluxes of other scalar constituents [*De Bruin et al.*, 1993; *Edson et al.*, 1991; *Wesely*, 1988]. Since both methods depend on the generation of concentration fluctuations by the action of turbulent eddies on surface fluxes, they require a real-time detection system with adequate sensitivity and resolution to measure turbulent scale fluctuations. The sulfur chemiluminescence detector (SCD) is an ideal instrument for this application because it offers high sensitivity with fast response. Since the SCD measures equimolar responses for all gaseous sulfur species, the surface flux estimates are net surface fluxes. The ramifications of this in regard to sulfur gas sea-to-air flux are discussed in a later section of this paper.

Turbulence is responsible for vertical transport of trace chemical species in the

boundary layer. Real-time measurements can be used to look at turbulence-driven transport because they offer time series showing the perturbations from the mean concentrations due to turbulent eddies. In this study we used a sampling frequency of 1 Hz which allowed us to look for concentration fluctuations due to eddies as small as 5-10 m in size.

In the remote ocean marine boundary layer, the dominant source of sulfur gas is the ocean. This results in a vertical sulfur gas flux up from the ocean surface. Because of this flux, as the wind blows air past the stationary sensor, turbulent eddies manifest themselves as fluctuations in the sulfur concentration time series. The more intense the fluctuation, the greater the variance observed in the time series. The variance can be used to obtain flux estimates because it bears a unique, though indirect, relationship to the sulfur surface flux for a given set of turbulent mixing parameters.

DMS Sea-to-Air Flux Estimations

To use the time series data to estimate net surface flux, we made the following assumptions:

1) DMS was the dominant sulfur species resulting in turbulence driven sulfur concentration fluctuations. Other species, such as sulfur dioxide (SO_2) were assumed to contribute little to the fluctuations. This is reasonable for time periods with no apparent influence from continental sources, in remote ocean regions. This assumption was necessary since the SCD is a total sulfur detection system.
2) We assumed the flow in the atmospheric boundary layer to be horizontally homogeneous and in a steady state on a time scale of 1 hour. According to *Kaimal and Finnigan* [1994], ocean surfaces can come close to the idealized infinite surface where statistical properties are independent of horizontal position; they vary only with height and time.
3) The source of sulfur gases from the ocean was spatially homogeneous.

The variance and inertial-dissipation methods are not entirely independent of each other. Both utilize variance measurements for flux estimation. The variance technique uses direct measurements of total variance to estimate variance production, while the inertial-dissipation method uses variance at high frequencies to estimate variance production by surface flux.

Variance method. This method requires a measurement of the concentration variance in the eddy frequency range important for turbulent transfer. It is based on Monin-Obukhov similarity theory. According to this theory, in the horizontally homogeneous surface layer, the variance of scalars are related to their surface fluxes through universal functions of z/L. L is the Obukhov length and z the measurement height. For example [*Kaimal and Finnigan*, 1994],

$$\frac{\sigma}{|c_*|} = \phi_s\left(\frac{z}{L}\right) \tag{2}$$

where

$$\phi_s\left(\frac{z}{L}\right) = 2\left(1 - 9.5\,\frac{z}{L}\right)^{-\frac{1}{3}} \qquad -2 \le \frac{z}{L} \le 0 \tag{3}$$

$$\phi_s\left(\frac{z}{L}\right) = 2\left(1 + 0.5\,\frac{z}{L}\right)^{-1} \qquad 0 \le \frac{z}{L} \le 1 \tag{4}$$

and $c_* = -F_{c0}/u_*$ is a scaling parameter for constituent c. F_{c0} is the constituent surface flux and u_* the friction velocity. The absolute value of c_* is used because c_* is negative for an upward flux. Furthermore, because the variance must be positive, the sign of c_* is

ambiguous without additional information. The hydrodynamic stability parameters and friction velocities were estimated using the meteorological data collected on board the R/V *Oceanus* as input to an algorithm designed for computing bulk fluxes, supplied by C. Fairall of NOAA, Environmental Technology Laboratory in Boulder, Colorado, (C. Fairall et al., The TOGA CORE bulk flux algorithm, submitted to *Journal of Geophysical Research*, 1994).

Inertial-dissipation method. Because the inertial-dissipation method relies on measurements at high frequencies, which are unaffected by platform motion, it is an attractive technique for estimating air-sea fluxes from ships [*Edson et al.*, 1991]. *Edson et al.* [1991] also point out that measurements made using this method are less affected than covariance measurements (e.g., eddy-correlation method) by distortion of the turbulent flow around obstacles (such as masts, hygrometers, etc.). Furthermore, *Fairall and Larsen* [1986] point out that the dissipation method is more direct than bulk methods (e.g., those that compute chemical fluxes with mean concentrations and a transfer velocity) because it is a true turbulence statistic. According to *Edson et al.* [1991], even though the advantages of the inertial-dissipation technique are well known, questions have been posed regarding the possible anisotropy within the range of frequencies used to calculate the dissipation rates, the accuracy of the similarity functions, the values of constants used (i.e., Kolmogorov and von Kármán), and approximations made in order to use the variance budgets.

Fairall and Larsen [1986] provide an in-depth discussion of this method. This method is also based on Monin-Obukhov theory, which predicts that the dissipation rate of the concentration variance is related to surface flux through another function of z/L. If we know the power at a particular frequency in the inertial subrange, we can reconstruct the whole subrange part of the spectrum using the Kolmogorov variance spectrum form for one-dimensional, isotropic turbulence, S_{xx}, expressed

$$f S_{xx}(f) = \alpha \epsilon^{-\frac{1}{3}} N f^{-\frac{2}{3}} \quad (5)$$

where f is the frequency (cycles per second), α the Kolmogorov constant, ϵ the dissipation rate of turbulent kinetic energy, and N the dissipation rate for the sulfur concentration variance. We can estimate the dissipation rate because the structure function parameter C_x, which is a measure of the correlation of two measurements at different times or distances apart, is related to the dissipation rate through

$$C_x = 4 \alpha \epsilon^{-\frac{1}{3}} N \quad (6)$$

for the inertial subrange.

We have implemented the inertial-dissipation method in terms of the structure function parameter, computing the structure function parameter using the spectral intensity (or power) from the power spectrum at frequency 0.1 Hz. As discussed below, there is no evidence of attenuation in our data at this frequency. Using Taylor's frozen turbulence hypothesis [*Fairall and Larsen*, 1986],

$$C_x = 4\left(\frac{2\pi}{U}\right)^{\frac{2}{3}} f^{\frac{5}{3}} S_x(f) \quad (7)$$

and

$$C_x = (c_*^2)\, z^{-\frac{2}{3}} f\left(\frac{z}{L}\right) \quad (8)$$

where $f(z/L) = 5.5(1\text{-}6.2(z/L))^{-2/3}$ for a scalar quantity under unstable conditions [*Edson et al.*, 1991] (von Kármán constant = 0.4), U is mean wind speed, and $S_x(f)$ is spectral intensity (or power) from the power spectrum, we solved for the scaling parameter c_*.

The flux was then calculated using the relationship

$$c_* = -\frac{F_{c0}}{u_*} \tag{9}$$

Again, the absolute value of c_* was used because the method cannot actually determine the sign of c_*. Combining equations (7), (8), and (9), it becomes evident that a higher power at a particular frequency translates into a higher flux estimate.

Sulfur Gas Horizontal Inhomogeneities in the Marine Boundary Layer

Sampling techniques that rely on short sampling times for measurements of sulfur gas concentrations in the atmosphere do not guarantee an accurate, representative measurement. This is because of the horizontal variability due to turbulence driven concentration fluctuations previously discussed and mesoscale processes. In order to account for the variability due to turbulent mixing, samples need to be collected over a sufficient time-average or horizontal distance. Sampling for horizontal distances less than the size scale of the variability due to turbulent mixing may result in a measurement significantly above or below the true characteristic value for the air mass being sampled. Furthermore, our data give an indication as to whether or not the variations in concentrations observed in time-averaged measurements are due to time dependent changes or simply from sampling at different places in an inhomogeneous air mass.

Fourier transform processing of the sulfur gas concentration times series can provide information on the horizontal homogeneity. The power spectrum of the times series shows the contribution of each eddy size to the total variance. One representation of the power spectrum, that of frequency times power (in units of variance) as a function of log frequency, results in the area under the curve being proportional to the total variance. Integrating the area under the curve, a plot of the fraction of total variance in ground level sulfur concentration fluctuations as a function of sampling time can be obtained. From such plots, the time period necessary to collect a representative sample

that accounts for, say, 90% of the fluctuations caused by turbulence can be determined.

Our study is part of the Atlantic Stratocumulus Transition Experiment/Marine Aerosol and Gas Exchange (ASTEX/MAGE) experiment. This experiment was an attempt to use a Lagrangian sampling scheme in the marine boundary layer (MBL). In order to sample in a Lagrangian framework, a meaningful air parcel of sufficient size has to be characterized and the lifetime of the air parcel has to be longer than the time that the air parcel is followed. The size of the smallest meaningful air parcel for the Lagrangian sampling scheme must be at least as big as the size scale of the variability due to turbulent mixing. Our data give an indication of the smallest size for a meaningful air parcel.

Experiment

The fast response and sensitivity of the SCD, which we used to measure total gaseous sulfur concentrations, are well suited for this experiment. The operation and advantages of the SCD over some of the other sulfur detection systems are described elsewhere [*Benner and Stedman*, 1990, 1994].

Measurements were made from the ship R/V *Oceanus* while it was pointing into the wind located at stationary positions between 27° and 42° N latitude and 16° and 29° W longitude. Samples were collected at a height of 11 m above the ocean surface at a sampling frequency of 1 Hz. Air was transported from the sampling point, the tip of a boom projecting from the bow, to the instrument through a 40-m length of Teflon tubing. We made measurements of zero air followed by calibration span gas the first 3 min of every hour. The data were digitally corrected for zero and span drift prior to any subsequent analysis. In an effort to determine instrument noise, we measured a homogeneous source of sulfur concentrations. In this case, the ship's cabin air worked well.

Using the procedure described by *Lenschow and Raupach* [1991], we have estimated the frequency of half power attenuation, due to attenuation of the signal by the sample tubing, to be 4.5 Hz. This is well above 0.2 Hz, which is the high-frequency end of

the -5/3 slope displayed in the power spectra. Therefore we have concluded that the -5/3 slope for the frequency range of approximately 0.04 to 0.2 Hz corresponds to the inertial subrange region of the turbulence spectrum, which has a characteristic -5/3 slope. Also, we conclude that the flux estimations obtained from our measurements of turbulent fluctuations are not significantly low due to tubing attenuation of the signal.

Our data analysis was limited to time periods when (1) the consequences of the ship's rocking motion were not significant enough to distort the power spectrum, (2) the time series did not show evidence of pollution from ships in the vicinity, (3) adequate, accurate meteorological data were available, and (4) the ship was oriented with its bow into the wind. A malfunctioning zero air valve made it possible for us to determine the period of the ship's rocking motion, since fortuitously, the air flow through this valve varied as the ship rocked back and forth. The resulting pressure change in the instrument was manifested as a concentration fluctuation in the zero air time series. Therefore we were able to obtain the frequency of the ship's rocking motion from the dominant peak(s) in the zero air power spectra. The dominant frequency of the ship's rocking motion was usually close to 0.14 Hz, which corresponds to a period of about 7 s. There are two plausible explanations for why the ship's rocking motion is evident in some of the atmospheric measurement power spectra. It is possible that as the ship went through one rocking cycle, the sampling height above the ocean surface changed. Because there is a DMS flux up from the ocean surface, the concentrations of DMS measured during one rocking cycle would change due to sampling at different heights. This change in sulfur concentrations would show up as a fluctuation of concentration in the sulfur time series having the same frequency as the ship's rocking motion. Another explanation is that sea spray, generated from waves at the ship's bow, caused an artificial release of DMS at the same frequency as the waves and, therefore, the rocking of the ship. This would also show up as a fluctuation in the sulfur time series having a frequency the same as the ship's rocking motion. When seas were the calmest, we did not have this problem.

In addition to the five 1-hour time periods that we estimated the flux under conditions of no apparent influence from continental sources, we also measured the flux during a time period when the air was influenced by continental sources. During this polluted period, deposition of SO_2 would be expected to bias the sea-to-air-flux estimates low, since these methods estimate the net sulfur flux.

Our data show that over 90 % of the variance in the turbulent scale is accounted for by frequencies greater than 0.01 Hz. Based on this, a digital high-pass filter was applied to the data before the flux was estimated. This removed all variance contributions for frequencies less than 0.01 Hz.

Discussion of Results

Figure 2.1 shows a segment of the time series for both cabin air and the atmosphere. Assuming that the cabin air was well mixed, this figure shows a signal-to-noise ratio of 5 to 1. This is more than adequate for flux determinations. If the cabin air was not well mixed, the signal-to-noise ratio would be even larger.

The following interpretation of the power spectrum shown in Figure 2.2 is reasonable for a relatively shallow boundary layer of near neutral stability and low winds. The frequency range from 0.04 to 0.20 Hz corresponds to the inertial subrange with characteristic -5/3 slope. The presence of the inertial subrange indicates that the instrumental technique is capable of adequately resolving turbulence-driven concentration fluctuations. To clearly identify an inertial band, we should look at the next decade of frequencies. Unfortunately, signal attenuation of frequencies higher than about 0.2 Hz does not allow this. The attenuation was due to the response time of the instrument, which is a function of the electronic components and internal tubing. Even though the inertial band cannot be verified in this way, there is strong evidence that the -5/3 slope in Figure 2.2 between frequencies 0.04 and 0.2 Hz correspond to the first decade of the inertial subrange. The evidence includes (1) measurement of instrument noise being white below 0.2 Hz, (2) a signal to noise ratio of approximately 5:1 as shown in Figure 2.1 and

(3) a frequency below 0.2 Hz (normalized frequency close to 0.5 Hz) is reasonable for the onset of the inertial subrange for scalar quantities [*Kaimal et al.*, 1972; *Panofsky and Dutton*, 1984]. The power at frequencies lower than about 0.04 Hz is due to eddies which generate turbulent kinetic energy. Frequencies less than about 0.001 Hz are generally characteristic of mesoscale variability and are of no consequence in a Lagrangian sampling scheme, where the intent is to follow a tagged air parcel with time. Using the conservative requirement of at least 10 fluctuations per sampling period before being confident in the spectral results [*Stull*, 1993], the lowest frequency that can be adequately resolved is about 0.003 Hz. This corresponds to a fluctuation with a period of 6 min. Although the inertial subrange extends to frequencies higher than 0.2 Hz, we have estimated that these frequencies contribute little to the total variance of sulfur concentrations caused by turbulent mixing.

Figure 2.3 is a representation of the power spectrum (using filtered data) which shows the power times frequency plotted as a function of log frequency. This results in the area under the curve being proportional to total variance. As can be seen in Figure 2.3, over 90% of the variance in the turbulent scale is accounted for by frequencies greater than 0.01 Hz and less than 0.2 Hz. In addition, this plot shows the contribution of instrumental noise to the variance. Because the magnitude of the signal is squared in the Fourier transform calculations, the signal-to-noise ratio improves from a ratio of 5:1 shown in Figure 2.1 to 25:1. Therefore, as displayed in , the noise contribution to the total variance becomes very small.

DMS Sea-to-Air Flux Estimations

Sulfur gas sea-to-air flux estimations from both the variance and inertial-dissipation methods gave a range of results higher than those found previously in this region of the world [*Barnard et al.*, 1982; *Berresheim et al.*, 1991; *Van Valin et al.*, 1987] and during ASTEX/MAGE [*Blomquist et al.*, this issue] based on DMS concentration in surface seawater, using the stagnant boundary layer model of air-sea

exchange. *Blomquist et al.'s* [this issue] values range from 1 to 13 μmol/m^2 ·d. Our results are tabulated in Table 1.1.

Since DMS is known to be the dominant sulfur gas emitted from ocean surfaces in remote ocean regions, the total sulfur sea-to-air flux in these areas can be assumed to be equivalent to the DMS sea-to-air flux. Five of the measurement periods used to estimate the sulfur gas sea-to-air flux were made during periods of no obvious signs of anthropogenic pollution in the remote ocean marine boundary layer. Under these conditions, we assumed that the SO_2 fluctuations in the atmosphere were small relative to the fluctuations in DMS. Therefore the measured sulfur concentration fluctuations were essentially due to fluctuations in atmospheric DMS concentrations.

Even though the detector measures total sulfur gases and background carbonyl sulfide (OCS) concentrations are much higher than DMS concentrations in the MBL, the contribution of OCS fluctuations to the measured fluctuations is very small. This is because OCS is uniformly mixed in the MBL due to its long lifetime (for example, greater than 1 year according to *Toon et al.* [1987] and tens of years according to *Finlayson-Pitts and Pitts* [1986]) and small surface fluxes relative to DMS [*Toon et al.*, 1987]. Empirical relationships between residence time and variability [*Junge*, 1974] suggest that OCS should not vary by more than 10%, and is likely closer to 1%. The data of *Maurolis et al.* [1977] have indicated that atmospheric OCS concentrations vary globally with space and time no more than 10%. One could argue that because OCS is long lived, its memory of large-scale influences is long and this can cause concentration fluctuations. We believe that significant fluctuations would only occur along the boundaries of air masses with extreme differences in OCS concentrations. We believe the OCS contribution to our flux estimates is small because the variability of OCS in the marine boundary layer is expected to be rather small on the scale of 30 min [*Bingemer et al.*, 1990].

How atmospheric SO_2 levels change the variance in the sulfur time series is open to question. We do not have simultaneous measurements of atmospheric SO_2 mixing

ratios, but using an average below cloud SO_2 mixing ratio of 104 pptv [*Blomquist et al.*, this issue] from aircraft measurements during ASTEX/MAGE and a deposition velocity of 1 cm/s [*Seinfeld*, 1986], we have estimated the SO_2 flux to the surface to be approximately 3.7 $\mu mol/m^2 \cdot d$. If the SO_2 flux is indeed 15-30 % of the flux estimates in Table 1.1, our DMS sea-to-air flux estimates may be low, since the measured flux would be the sum of DMS flux from the surface and SO_2 flux to the surface. Table 1.1 includes the one time period that we estimated the flux under polluted conditions which resulted in the lowest value for both methods.

In addition to the SO_2 flux to the surface, the oxidation mechanism of the SO_2 may affect the variance in the sulfur time series. For example, contrast a homogeneous oxidation mechanism, such as photochemical oxidation, to oxidation in clouds. For the photochemical case, oxidation of SO_2 would be more uniformly distributed throughout the boundary layer, resulting in a smaller variance (perhaps negligible) in SO_2 concentrations. The oxidation of SO_2 in clouds leads to lower levels of SO_2 in the upper boundary layer. We can only speculate on whether these levels are low enough to affect the variance in the time series when mixed with the air below.

Table 1.1 shows that the range of flux estimates from the variance method is higher than that from the inertial-dissipation method. Although both methods utilize variance measurements, they utilize variances over different frequency ranges. As mentioned earlier, the variance method utilizes variances for frequencies between 0.01 and 0.2 Hz, while the inertial-dissipation method uses a measure of variance at 0.1 Hz. One explanation for the difference in ranges of results is that large-scale inhomogeneous sources of sulfur at the surface affected the variances in the 0.01 to 0.2 Hz region more than at 0.1 Hz, resulting in higher variance method values. On the other hand, we may be losing some variance in the region where we have estimated the scalar dissipation. Other possibilities are that either (1) the atmospheric SO_2 oxidation mechanism, or (2) contribution to the variance from flux at the top of the boundary layer, had a similar affect

on the variances. Considering the explanations mentioned above, both methods might overestimate the flux. But the presence of the characteristic -5/3 slope in the power spectra suggest that if the variance was affected it was only for frequencies lower than the inertial subrange region.

Although the results from the variance method are consistently higher than those from the inertial-dissipation method, a high correlation can be seen. The ratio between the two methods is fairly constant. The empirical constants used in the methods are uncertain by about 20% (C. W. Fairall, personal communication, 1994), which could explain most of the difference between the results of the two methods. Propagation of error analysis estimates uncertainties of 30-35% for both methods.

Sulfur Gas Inhomogeneities in the Marine Boundary Layer

Integrating the area under the curve in Figure 2.3, a plot of the fraction of total variance in ground level sulfur concentration fluctuations as a function of sampling time was obtained, which is shown in Figure 2.4. This plot is typical of the time periods we analyzed on four different days. From the plots, the time period necessary to collect a representative sample can be determined, since they show how long of a sampling time is needed to account for an acceptable percentage of the variance at the turbulent scale. For example, to account for over 95% of the variance, a time period of 100 s should be sufficient. A "safety margin" of a factor of 10 results in a sampling time of 1000 s. We have applied this factor of 10 after considering the rule-of-thumb that micrometeorologists use for determining sampling time. That is, sampling time equals 10 times the period corresponding to the peak in the flux spectrum multiplied by z/U. The peak in the flux spectrum of 36 is at about 0.03 cycles per second. Using the rule of the thumb, a sampling time of 1078 s (18 min) results.

Since turbulence intensity was small relative to the mean wind speed (standard deviation of wind speed less than half of the wind speed), we assumed that the turbulence was "frozen" in time as it passed over the sensor [*Willis and Deardorff*, 1976]. This

allowed for the conversion from a time to spatial scale using Taylor's hypothesis. That is, if an eddy of diameter d is advected at a mean wind speed U, then the time period P for it to pass by a stationary sensor is given by $P = d/U$.

To obtain a representative time-averaged measurement of sulfur gas concentrations in the marine boundary layer, the sample should be collected over a sampling period of approximately 1000 s for ground-based measurements. This corresponds to a horizontal scale of roughly 5 km if the wind speed is 5 m/s. The size scale required to account for the turbulent fluctuations was consistent for the limited cases we investigated on four different days. Likewise, we saw no obvious correlations between this recommended sampling period and sea surface temperature, time of day, wind speed, boundary layer depth, difference between sea surface and air temperatures, or sea state. However, we believe that a more rigorous evaluation including more time periods may uncover some correlations.

Our data show that to obtain a meaningful measurement in the MBL the sample should be integrated over a size scale of approximately 5 km. This would account for all the variability at the turbulent scale and includes a conservative "safety margin." Although our data do not directly answer the question of how large an air parcel should be sampled for a Lagrangian experiment, it is clear that it should be several times larger than 5 km.

Conclusions

Real-time total gaseous sulfur concentration measurements in the marine boundary layer provided sulfur gas time series showing turbulence-driven concentration fluctuations. From these data, sea-to-air sulfur gas flux estimates were obtained using a variance method and the inertial-dissipation method, both of which depend on the generation of turbulent concentration fluctuations by a surface flux. Estimates based on these methods ranged from 21 to 28 $\mu mol/m^2$ d and 11 to 17 $\mu mol/m^2$ d, respectively. The data also provide information on the horizontal inhomogeneity of sulfur gas concentrations in the marine boundary layer due to turbulent mixing. From this, we have determined that air

samples should be integrated for 1000 s for ground based measurements. The size scale of sampling can be estimated by multiplying by the wind speed.

The ASTEX/MAGE data presented here verify that the SCD is capable of resolving the turbulent fluctuations in sulfur gas concentration that are important in transporting the species from one level to another in the boundary layer. The different results from the methods discussed in this paper point even more clearly to the need for a direct measurement technique. We are working on extending this technique for making direct sea-to-air flux measurements using the eddy-correlation method.

Although the two methods that we have used to estimate sea-to-air sulfur flux have their own assumptions and uncertainties, we believe that they introduce an uncertainty no greater than that of the commonly used method. Furthermore, our results provide an independent analysis of the performance of the commonly used stagnant boundary layer model. More work and better techniques are needed to resolve the discrepancies between the methods described.

Acknowledgments

This work was supported by the Office of Naval Research Ocean Chemistry Program under grant ONR N00014-92-J-1296. We would like to thank Byron Blomquist for his efforts in providing logistical support during the field campaign and subsequent discussions of the data, Don Lenschow and Chris Fairall for many insightful comments and discussions both during data analysis and on this manuscript, the anonymous reviewers for their very useful comments, and Chris Fairall for providing a computer program used in our data analysis. These measurements would not have been possible without the professional support provided by the captain and crew of the R/V *Oceanus*. This research is a contribution to the International Global Atmospheric Chemistry (IGAC) Core project of the International Geosphere-Biosphere Programme (IGBP).

Table 1.1 - Sulfur Gas Sea-to-Air Flux Estimates Using the Inertial-Dissipation Method and a Variance Method. The "*" indicates a time period during which air was influenced from continental air (polluted).

Date in 1992	Local Time	Flux Estimate	
		Variance Method	Dissipation Method
June 12	0330-	27.9	16.5
	0830-	26.0	14.8
	1130-	26.8	15.5
June 16 16	1510-	21.2	11.4
June 18	1405-1505*	14.1	9.5
	1105-1205	21.5	11.6

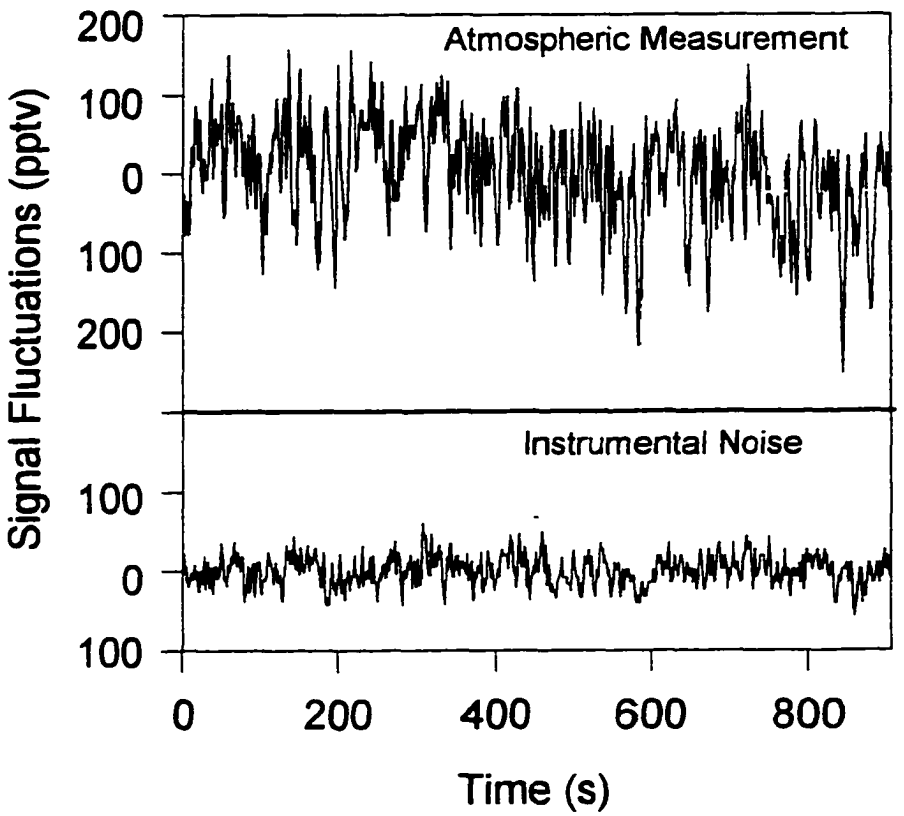

Figure 2.1 - A segment of the sulfur gas time series for both the ship's cabin air and the atmosphere. This shows a signal-to-noise ratio of approximately 5 to 1, which is more than adequate for flux measurements.

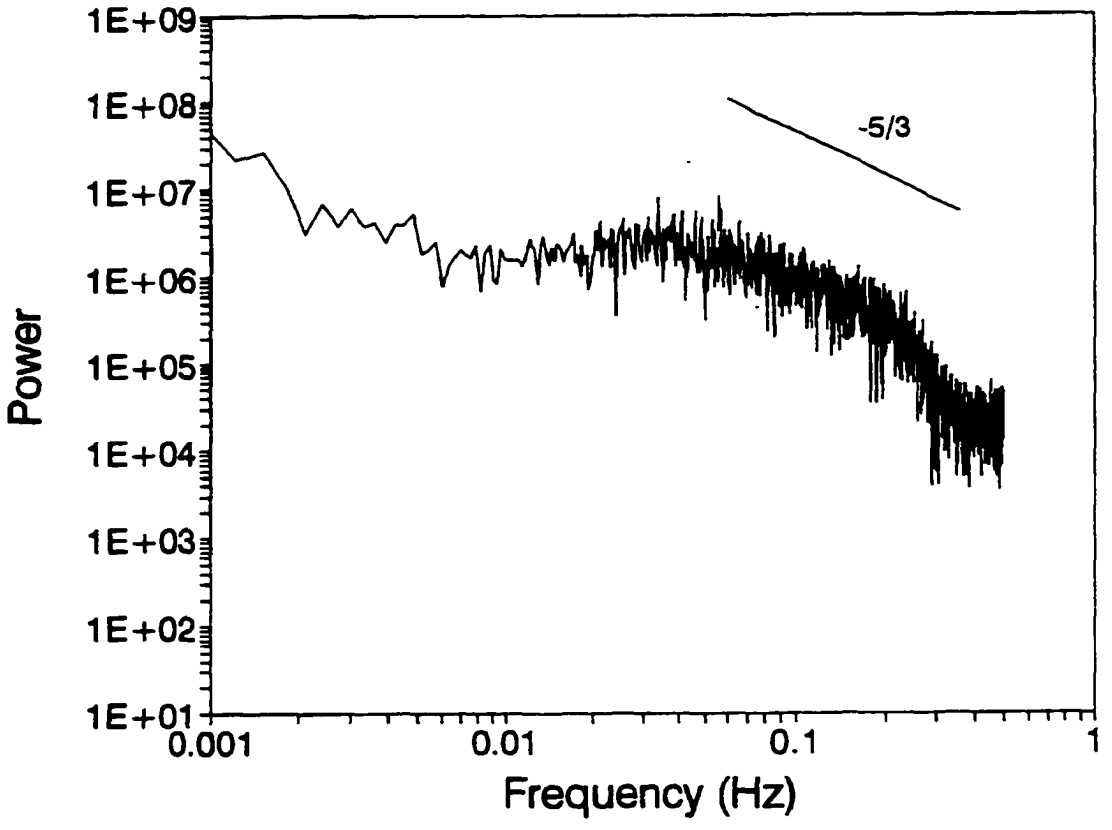

Figure 2.2 - A power spectrum of sulfur gas concentration fluctuations measured during ASTEX/MAGE field campaign. The -5/3 slope indicates that the sulfur detection system resolved fluctuations driven by turbulence in the atmosphere. The falloff in response above approximately 0.2 Hz is due to the response time of the instrument. Frequency is in cycles per second.

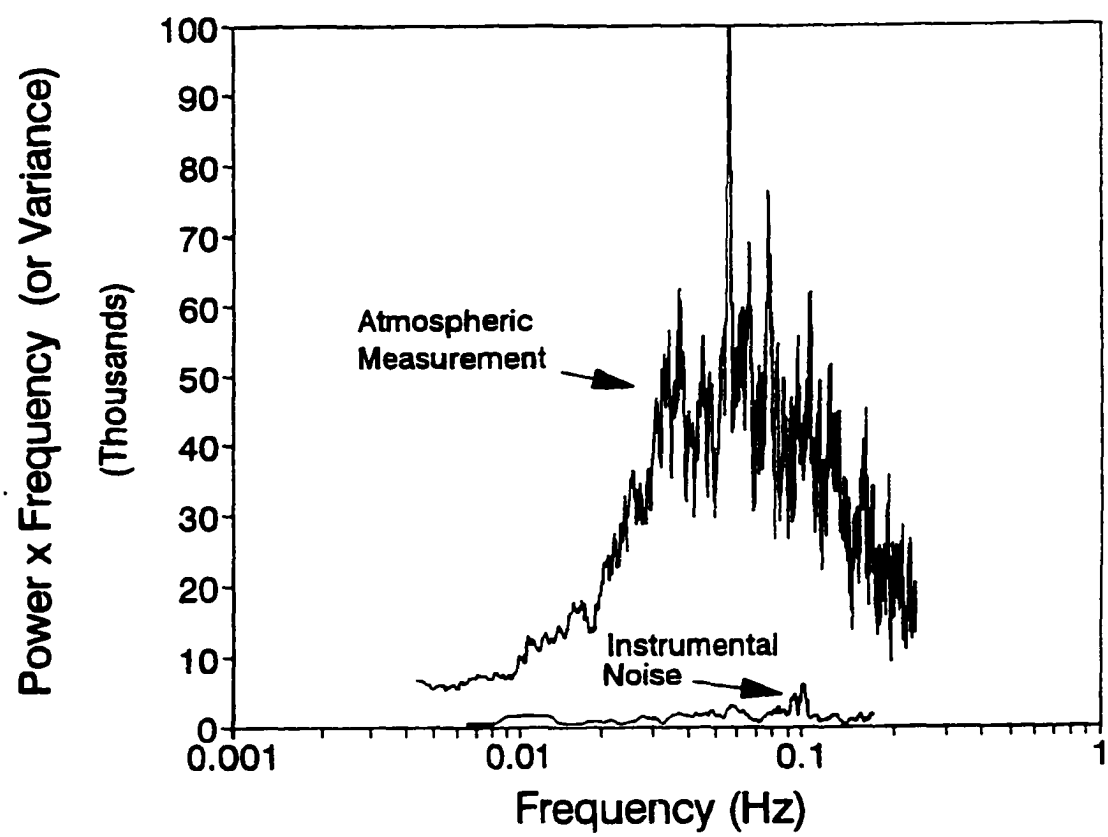

Figure 2.3 - A representation of the power spectrum showing power times frequency plotted as a function of log frequency. The area under the curve is proportional to the total variance.

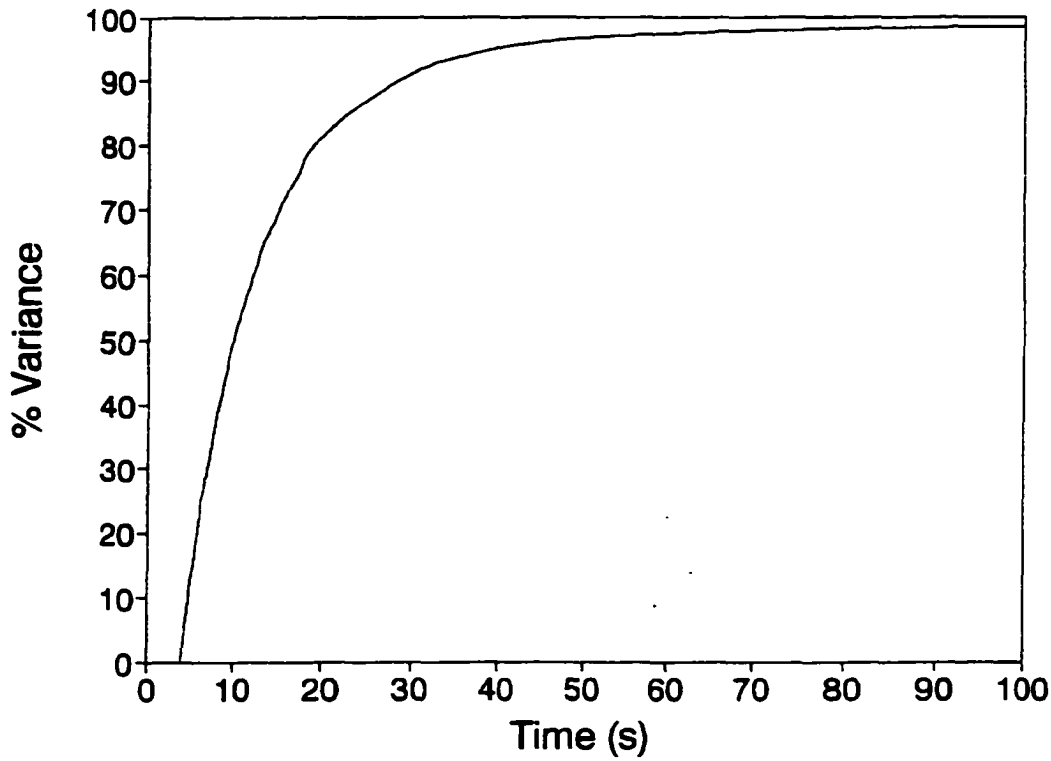

Figure 2.4 - Cumulative variance as a function of sampling time from a ship-based sensor mounted 11 m above the water. This is typical of the plots obtained during the study which indicate that in order to obtain a representative sample of average concentration in the marine boundary layer, sampling should be integrated for 1000 s, which includes a "safety margin" of a factor of 10.

References

Andreae, M. O., The ocean as a source of atmospheric sulfur compounds, *The Role of Air-Sea Exchange in Geochemical Cycling*, edited by Buat-Ménard, pp. 331-362, D. Reidel, Norwell, Mass., 1986.

Andreae, M. O., R. J. Ferek, F. Bermond, K. P. Byrd, R. T. Engstrom, S. Hardin, P. D. Houmere, F. LeMarrec, H. Raemdonck, and R. B Chatfield, Dimethylsulfide in the marine atmosphere, *Journal of Geophysical Research, 90*, 12,891-12,900, 1985.

Barnard, W. R., M. O. Andreae, and W. E. Watkins, The flux of dimethylsulfide from the oceans to the atmosphere, *Journal of Geophysical Research, 87*, 8787-8793, 1982.

Bates, T. S., J. D. Cline, R. H. Gammon, and S. R. Kelly-Hansen, Regional and seasonal variations in the flux of oceanic dimethylsulfide to the atmosphere, *Journal of Geophysical Research, 92*, 2930-2938, 1987.

Benner, R. L., and D. H. Stedman, Field evaluation of the sulfur chemiluminescence detector, *Environmental Science and Technology, 24*, 1592-1596, 1990

Benner, R. L., and D. H. Stedman, Chemical mechanism and efficiency of the sulfur chemiluminescence detector, *Applied Spectroscopy, 48*, (7), 848-851, 1994.

Berresheim, H., M. O. Andreae, R. L. Iverson, and S. M. Li, Seasonal variations of dimethylsulfide emissions and atmospheric sulfur and nitrogen species over the western north Atlantic Ocean, *Tellus, 43B*, 353-372, 1991.

Bingemer, H. G., S. Bürgermeister, R. L. Zimmermann, and H.-W. Georgii, Atmospheric OCS: Evidence for a Contribution of Anthropogenic Sources?, *Journal of Geophysical Research, 95*, 20,617-20,622, 1990.

Blomquist, B. W., A. R. Bandy, and D. C. Thornton, Sulfur gas measurements in the eastern North Atlantic Ocean during the Atlantic Stratocumulus Transition Experiment/Aerosol and Gas Exchange, *Journal of Geophysical Research, 101*, D2, 4377-4392, 1996.

Bonsang, B., B. C. Nguyen, A. Gaudry, and G. Lambert, Sulfate enrichment in marine aerosols owing to biogenic sulfur compounds, *Journal of Geophysical Research, 85*, 7410-7416, 1980.

Charlson, R. J., and T. M. L. Wigley, Sulfate aerosol and climatic change, *Scientific American, 270*, 48-57, 1994.

Charlson, R. J., J. E. Lovelock, M. O. Andreae, and S. G. Warren, Oceanic phyto-plankton, atmospheric sulfur, cloud albedo, and climate, *Nature, 326*, 655-661, 1987.

Clarke A. D., N. C. Ahlquist, and D. S. Covert, The pacific marine aerosol: Evidence for natural acid sulfates, *Journal of Geophysical Research, 92*, 4179-4190, 1987.

Cullis, C. F., and M. M. Hirschler, Atmospheric sulphur: Natural and man-made sources, *Atmospheric Environment, 14*, 1263-1278, 1980.

De Bruin, H. A., W. Kohsiek, and B. J. J. M. Van Den Hurk, A verification of some methods to determine the fluxes of momentum, sensible heat, and water vapour using standard deviation and structure parameter of scalar meteorological quantities, *Boundary Layer Meteorology, 63*, 231-257, 1993.

Edson, J. B., C. W. Fairall, P. G. Mestayer, and S. E. Larsen, A study of the inertial-dissipation method for computing air-sea fluxes, *Journal of Geophysical Research, 96*, 10,689-10,711, 1991.

Fairall, C. W., and S. E. Larsen, Fluxes at the air-ocean interface, *Boundary Layer Meteorology, 34*, 287-301, 1986.

Finlayson-Pitts, B. J., and J. N. Pitts, *Atmospheric Chemistry: Fundamentals and Experimental Techniques*, p. 995, Wiley-Interscience, New York, 1986.

Jähne, B., K. O. Münnich, R. Bösinger, A. Dutzi, W. Huber, and P. Libner, On the parameters influencing air-water gas exchange, *Journal of Geophysical Research, 92*, (C2), 1937-1949, 1987.

Junge, C. E., Residence time and variability of tropospheric trace gases, *Tellus, 26*, 477-

488, 1974.

Kaimal, J. C., and J. J. Finnigan, *Atmospheric Boundary Layer Flows - Their Structure and Measurements*, Oxford Univ. Press, New York, 1994.

Kaimal, J. C., J. C. Wyngaard, Y. Izumi, and O. R. Coté, Spectral characteristics of surface-layer turbulence, *Quarterly Journal of the Royal Meteorological Society, 98*, 563-589, 1972.

Lenschow, D. H., and M. R. Raupach, The attenuation of fluctuations in scalar concentrations through sampling tubes, *Journal of Geophysical Research, 96*, 15,259-15,268, 1991.

Liss, P. S., Gas-transfer: Experiments and geochemical implications, in *Air-sea Exchange of Gases and Particles*, edited by P. S. Liss and W. G. N. Slinn, pp. 241-298, D. Reidel, Norwell, Mass., 1983.

Liss, P. S., and L. Merlivat, Air-sea gas exchange rates: Introduction and synthesis, in *The Role of Air-Sea Exchange in Geochemical Cycling*, edited by P. Buat-Ménard, pp. 113-127, D. Reidel, Norwell, Mass., 1986.

Liss, P. S., and P. G. Slater, Flux of gases across the air-sea interface, *Nature, 247*, 181-184, 1974.

Maroulis, P. J., A. L. Torres, and A. R. Bandy, Atmospheric concentrations of carbonyl sulfide in the southwestern and eastern United States, *Geophysical Research Letters, 4*, (11), 510-512, 1977.

Möller, D., Estimation of the global man-made sulphur emission, *Atmospheric Environment, 18*, 19-27, 1984.

Panofsky, H. A., and J. A. Dutton, *Atmospheric Turbulence Models and Methods for Engineering Applications*, pp. 202 ff., Wiley-Interscience, New York, 1984.

Seinfeld, J. H., *Atmospheric Chemistry and Physics of Air Pollution*, p. 649, Wiley-Interscience, New York, 1986.

Shaw, G. E., Bio-controlled thermostasis involving the sulfur cycle, *Climate Change, 5*,

297-303, 1983.

Smethie, W. M., Jr., T. Takahashi, and D. W. Chipman, Gas exchange and CO_2 flux in the tropical Atlantic Ocean determined from ^{222}Rn and pCO_2 measurements, *Journal of Geophysical Research, 90,* 7005-7022, 1985.

Stull, R. B., *An Introduction to Boundary Layer Meteorology*, Kluwer Acad., Norwell, Mass., 1993.

Thompson, A. M., W. E. Esaias, and R. L. Iverson, Two approaches to determining the sea-to-air flux of dimethyl sulfide: Satellite ocean color and a photochemical model with atmospheric measurements, *Journal of Geophysical Research, 95,* 20,551-20,558, 1990.

Toon, O. B., J. F. Kasting, R. P. Turco, and M. S. Liu, The sulfur cycle in the marine atmosphere, *Journal of Geophysical Research, 92,* 943-963, 1987.

Van Valin, C. C., H. Berresheim, M. O. Andreae, and M. Luria, Dimethyl sulfide over the western Atlantic Ocean, *Geophysical Research Letters, 14,* 715-718, 1987.

Wanninkhof, R., Relationship between wind speed and gas exchange over the ocean, *Journal of Geophysical Research, 97,* 7373-7382, 1992.

Wesely, R. M., Use of the variance techniques to measure dry air-surface exchange rates, *Boundary Layer Meteorology, 44,* 13-31, 1988.

Willis, G. E., and J. W. Deardorff, On the use of Taylor's translation hypothesis for diffusion in the mixed layer, *Quarterly Journal of the Royal Meteorological Society, 102,* 817-822, 1976.

Chapter 3

Measurements of Sulfur Gases in the Air over Alaskan Waters [2]

Abstract

High primary productivity in high latitude oceans suggests a potentially large dimethyl sulfide (DMS) source from northern oceans. We measured atmospheric DMS mixing ratios from aboard the RV *Alpha Helix* from September 6 through October 4, 1995, in the Chukchi and Bering Seas and from a land-based research platform located on the shores of Kachemak Bay between June 6 and 16, and on June 23, 1996. The shipboard sampling involved trapping atmospheric DMS in molecular sieve sampling tubes, followed by analysis in the laboratory using gas chromatography - sulfur chemiluminescence detection (GC-SCD). Most of the shipboard DMS results range from 10 to 100 parts-per-trillion on a volume basis (pptv), but a few are above 150 pptv. The higher levels are interesting, since September is not considered to be a time of peak productivity in the Arctic, and because the highest value (650 pptv) is found in a sample collected near the ice edge. Land-based sampling at Kachemak Bay reveals DMS mixing ratios mostly between 10 and 200 pptv, but several values are significantly higher, exceeding 1,900 pptv on one day. In addition to DMS, other sulfur-containing compounds including carbonyl sulfide, sulfur dioxide, carbon disulfide, and dimethyl disulfide (DMDS) were detected. In some samples the level of DMDS rivals that of DMS. Our results support the hypothesis that northern oceans may contribute significantly to the atmospheric sulfur budget. However, more measurements are needed

---

[2] Jodwalis, C. M., R. L. Benner, T. Weingartner and G. E. Shaw, Measurements of Sulfur Gases in the Marine Boundary Layer on the Alaska Coast, and the Bering and Chukchi Seas, to be submitted in 1998.

to quantify this source.

Introduction

Sulfur gases and particles in the atmosphere play significant roles in acid rain, arctic haze, air pollution, cloud formation and climate. In recent years, atmospheric sulfur has become an integral part of the debate on Earth's changing climate. This is because sulfate aerosols may impact climate directly by scattering light [*Shaw*, 1983], or indirectly, by forming cloud condensation nuclei (CCN) which may modify cloud formation, cloud lifetime and the radiative properties of clouds [*Charlson and Wigley*, 1994]. *Charlson et al.* [1987] go further to suggest that dimethyl sulfide (DMS) may regulate climate via a negative feedback between atmospheric temperature and the amount of DMS produced by marine phytoplankton. *Shaw et al.* [1998] have proposed an alternative feedback mechanism where phytoplankton do not play an active role. Instead, increased sea surface temperatures lead to more deep convection in the atmosphere, pumping DMS laden marine boundary layer (MBL) air into the free troposphere, where DMS is oxidized to CCN which later subside back into the MBL.

Oceanic DMS results from the metabolic release of DMS [*Andreae*, 1985] and its precursor, dimethylsufionoproprionate (DMSP) [*Turner et al.*, 1989], by phytoplankton. Knowledge of this spatially and temporally highly variable source is key to understanding the impacts of atmospheric sulfur since it is the dominant natural source of sulfur to the atmosphere, comparable in magnitude to anthropogenic emissions on a global scale. The vast amount of DMS emitted from the oceans results in sulfate being the major constituent (by number concentration) of non-sea-salt marine aerosols [*Clarke et al.*, 1987]. These aerosols form CCN, the seeds on which the clouds form.

Although the Arctic and subarctic regions constitute a relatively large fraction of the Earth's surface and may make a significant contribution to the global sulfur budget, little is known about the biogenic sulfur gas emissions. *Bürgermeister and Georgii* [1991]

report spring atmospheric DMS concentrations of 390 ± 310 pptv measured on the Island of Sylt, North Sea. August levels were 74 ± 60 pptv. Measurements of DMS and other reduced sulfur compounds in surface water have been reported from the North Sea [*Turner et al.*, 1989] and the Baltic Sea [*Leck and Rodhe*, 1991], and used in DMS sea-air flux estimates. A small number of studies have focused on sulfur gas emissions from high latitude wetland ecosystems in Alaska [*Hines and Morrison*, 1992] and Ontario, Canada [*Nriagu et al.*, 1987]. *Ferek and Herring* [1991] made measurements of DMS and SO_2 in the MBL over the Arctic Ocean north of Barrow and at a ground-based station in Barrow that indicate a seasonal trend of DMS emissions probably due to phytoplankton activity in local waters. Several of their DMS measurements in the MBL exceeded 200 parts-per-trillion on a volume basis (pptv), some of the highest levels they have ever measured, suggesting a strong source in the Arctic. Further evidence of a strong high latitude source comes from several cruises in the Pacific Ocean where the highest seawater DMS concentrations were found between 50°N and 65°N [*Bates et al.*, 1987]. In air over the Atlantic Ocean, *Bürgermeister and Georgii* [1991] found a latitudinal dependence of atmospheric DMS. The highest values they measured, between 45°N and 50°N, were more than twice as high as those measured between 30°S and 45°N. *Aagard et al.* [1996] measured DMS in surface air over the Arctic Ocean between July and September of 1994. They detected mixing ratios above 500 pptv on the Pacific side, over the Chukchi Sea.

In regions of high primary productivity, DMS emissions [*Bates et al.*, 1989] and surface water concentrations [*Andreae and Barnard*, 1984] are generally high. Since ocean areas around Alaska are among the most biologically productive ocean water areas, at least during the summer months [*Schlesinger*, 1991], we hypothesize that these regions may contribute significantly to the global sulfur cycle. To begin to test this hypothesis, we measured atmospheric DMS concentrations:

1) aboard the *R/V Alpha Helix* from September 6 through October 4, 1995 in the

Chukchi and Bering Seas, and

2) from a land-based research station 6 miles north of Homer, Alaska, overlooking Kachemak Bay, during June, 1996.

The main aim of this research is to increase the relatively small data base of atmospheric DMS mixing ratios in the air over northern oceans.

Experimental

Kachemak Bay on-site Atmospheric DMS Measurements

The Kachemak Bay field site is located on the Kenai Peninsula, at about 59° 40' N latitude and 151° 40' W longitude near Homer, Alaska. Figure 3.1 is a map showing the location of the site. At this site, jutting out into Kachemak Bay and lower Cook Inlet, air masses traversing 160 km of ocean are commonly encountered. The mobile laboratory sits above the Bay at an altitude of 210 m, about 120 m inland from the shore break, 9 m from the cliff edge. We sampled air for DMS at various times throughout the day between June 6 and 16, and on June 23, 1996. The area experiences typical land-sea breeze circulation so that at night the air flowed from the land and was not sampled. The data was considered to be clean background air when the wind direction was between 135° and 270°, black carbon concentration was less than 200 ng/m^3, condensation nuclei (CN) number was less than 5000/cm^3, and CN and scanning mobility particle sizer measurements were relatively constant (no sudden large excursions). In addition, data was categorized as clean when 3-day back-trajectories were over the ocean.

The analyses were performed using a Hewlett Packard model 5890 series gas chromatograph (GC) coupled to a sulfur chemiluminescence detector (SCD). The operation and advantages of the SCD over other sulfur detection systems are described by *Benner and Stedman* [1990] and *Shearer* [1992]. Figure 3.2 shows the gas trapping and analysis system used in the present study. DMS samples were collected by cryogenic

preconcentration of 0.90 L of air in a 30 cm length of 1.6 mm diameter FEP Teflon tubing, looped and submerged in liquid nitrogen. Sample air was drawn through a Nafion drier (Permapure Inc., Toms River, New Jersey), to prevent plugging of the cryogenic tube by water, and a potassium iodide trap to remove oxidants. The drier is constructed of 180 cm of 1.6 mm Nafion tubing wound around a screen support immersed in grade 513, 4A molecular sieve desiccant (4-8 mesh). Upon replacing the container of liquid nitrogen with a container of boiling water (while He carrier gas passed through the loop), the sample enters a 0.53 mm megabore, 30-m, 5-μm film DB-1 column, followed by a 5-m section of 0.53 megabore, 1-μm film DB-WAX column [*Barinaga and Farwell*, 1987]. An initial column temperature of 28°C for four minutes, followed by a temperature ramping of 15°C/min to 120°C, provided baseline separation of DMS from other sulfur-containing compounds.

For this experiment, we used a SCD which was constructed in-house by modification of a commercial nitrogen oxides detector (Thermedics TEA model 610, Woburn, Massachusetts). Since both detectors work by measuring the quantity of photons emitted in a chemiluminescent reaction with ozone, few modifications were necessary. We replaced the optical filter and photomultiplier tube to optimize detection for electronically excited SO_2. Since ozone and SO react very readily, the reaction chamber was modified to mix the SO and ozone within the reaction cell, rather than mixing the sample gas and ozone prior to the reaction chamber. For conversion of sulfur containing compounds to SO, we constructed a furnace very similar to the one developed by *Shearer* [1992]. A TECO/SIGMA temperature controller (model MDC4E, Longwood, Florida) controlled the furnace temperature at 800°C.

Sample recovery of DMS was determined frequently during the Kachemak Bay field campaign. When introducing 0.23 ng of DMS in 0.90 L of air (0.090 L/min for 10 min), 94% (standard deviation 12%) of the DMS was recovered. Known amounts of DMS were obtained from a DYNACAL permeation device (VICI Metronics Inc., Santa

Clara, California) maintained at 30.0 ± 0.1 °C in a constant temperature water bath. Multipoint calibrations using the permeation devices were conducted daily to provide linear least-squares calibration equations. Carbonyl sulfide (COS), sulfur dioxide (SO_2), carbon disulfide (CS_2) and dimethyl disulfide (DMDS) were identified based on retention times on the gas chromatographic column.

Bering and Chukchi Seas Atmospheric DMS Measurements using Sample Collection System for Trapping DMS

Since the GC-SCD was not compact and rugged enough to withstand heavy seas and the sampling conditions available to us, we developed a sample collection system for trapping DMS, modeled after the one of *Davison and Allen* [1994]. This allowed us to collect shipboard atmospheric DMS samples and store them for later analysis in our laboratory in Fairbanks, Alaska.

Sampling tubes are constructed of 30 cm lengths of 6.4 mm OD quartz tubing. Before use, the tubes are thoroughly washed with a sequence of acetone, methanol and double deionized water. The center of each cleaned tube contains a 3 cm length of packed molecular sieve 5A (60/80 mesh) held in place by silanized glass wool plugs. *Davison and Allen* [1994] tested a number of adsorbents and scrubbers for DMS recovery. They found 5A molecular sieve to be the superior adsorbent and potassium iodide (KI) crystals were found to be adequate to prevent any DMS losses from oxidants under remote (essentially free of anthropogenic air masses) marine conditions. We also use a KI oxidant scrubber made of a 6 cm length of 6.4 mm OD quartz tubing, an active length of 3 cm, and fitted with silanized glass wool plugs. A Nafion drier is placed before the scrubber and sampling tubes to remove water vapor which could later plug the cryogenic loop on the GC and affect chromatographic separations.

DMS is desorbed from the sampling tubes by heating at 280 °C for 30 minutes. The desorption temperature is maintained by a temperature controller (Omega

Engineering, model CN4400, Stamford, Connecticut) and has been verified by placing a thermocouple in the center of the adsorbent material in a sacrificial sampling tube. The desorbed DMS is collected by cryogenic preconcentration in a 30 cm length of 1.6 mm diameter FEP Teflon tubing, looped and submerged in liquid nitrogen. The sample enters the GC column upon replacing the container of liquid nitrogen with a container of boiling water.

A G-Cal permeation device (GC Industries, Fremont, California), maintained at $30.0 \pm 0.1\,^{\circ}C$ in a constant temperature sand bath, was used for the analyses of the Chukchi and Bering Sea samples in the same manner as the DYNACAL device was used for the Kachemak Bay samples.

Sample losses through the entire sampling apparatus were checked by introducing a known amount of DMS in laboratory air at the inlet and then measuring the recovery from the sampling tube. Recoveries from 24 tests on 12 different tubes, loaded with 0.47 ng DMS, gave an average DMS recovery of 71% with a standard deviation of 9%. .

Over the Bering and Chukchi Seas, samples were collected from the upwind section of the ship's deck. A small suitcase contained the entire sampling apparatus. Included is a small DC pump (Brey model G02, Norcross, Georgia) which draws air through the sampling tubes at 0.40 L/min. Duration of sampling was generally 30 minutes and not less than 20 minutes, while the ship was underway. This amount of time should be sufficient to account for the horizontal variability of turbulence-driven concentration fluctuations, based on the recommendations of *Jodwalis and Benner* [1996], and provide adequate sample for detection down to 9 pptv.

Stipulations of the ships authorization to be in Russian waters precluded docking, except for one day at Providenya, Siberia. Since shipping of samples was not an option, we stored them frozen in a darkened container until analysis. The month-long sampling cruise along with the time intensive nature of sample analysis (one hour/sample) and daily calibration curves, resulted in storage times exceeding one month for some of the samples.

We conducted a study to determine maximum allowable holding times. The results showed a DMS loss of 0.6%/day for up to 43 days. Data from samples analyzed after more than 43 days in storage are flagged and should be viewed as lower limits. No samples were kept more than 60 days after collection.

DMS mixing ratios reported in this manuscript have been adjusted for DMS loss due to storage. We estimate that mixing ratios are accurate to within 15% of the reported value.

Discussion of Results

Bering and Chukchi Sea Atmospheric Samples

The sampling stations and atmospheric DMS measurements from the Bering and Chukchi Seas are plotted on the maps in Figure 3.3 and Figure 3.4. Typically DMS mixing ratios near surface level are on the order of 20 to 200 pptv (parts-per- trillion on a volume basis) depending on many factors, including ocean region and season [*Andreae*, 1990]. Most of the values plotted in Figure 3.3 are in this range, with a few on the high end, above 150 pptv. Two features from the DMS data are especially interesting. One is that relatively high values (>150 pptv) are seen in September, not considered a time of peak productivity in the Arctic. The other is that the highest value, 650 pptv, was found in a sample collected directly at the ice edge. *Aagard et al.* [1996] also found DMS mixing ratios over the Chukchi Sea to be highest at the edge of the ice cover. *Baumann et al.* [1994] suggest that the stress caused by abruptly changing light conditions in marginal ice zones intensifies DMS release. Comparing DMS levels in Antarctic water and sea ice, *Turner et al.* [1995] measured very high levels of DMS in ice, which were 20 to 500 times higher than in the underlying water.

Figure 3.3 suggests a gradient in DMS mixing ratios that decreases from west to east and shows high variability. The reason for the gradient could lie in the biology of the

currents flowing north through the strait. The waters that flow north from the western Bering Sea and coast of Siberia to the western Chukchi Sea are nutrient-rich, having high primary productivity [*Weingartner,* personal communications]. On the contrary, the currents flowing north along the coast of Alaska are relatively low productivity and nutrient poor [*Hansell et al.*, 1993]. This could at least partially explain the trend and the variability seen in the data. However, the variability is not surprising, and could be, in part, a reflection of the short atmospheric lifetime of DMS, suggested by *Chatfield and Crutzen* [1984] to be 8 - 48 hours due to its oxidation by OH and NO_3 radicals. A perhaps more realistic, upper level atmospheric DMS lifetime for northern latitudes, based solely on oxidation by the photochemically driven OH radical, is 3 - 4 days [*Finlayson-Pitts and Pitts*, 1986]. We can conclude that the DMS source is local based on a short lifetime. Time series of atmospheric DMS in the MBL from many locations around the world show considerable variability [*Andreae et al.*, 1985]. Changes in hundreds of pptv are common from one day to the next. We investigate these variations with numerical modeling in Chapter 4 of this thesis.

Dimethyldisulfide (DMDS) appears to be present in about half of the samples collected above the Bering and Chukchi Seas. The relative abundances of DMDS and DMS in the samples containing detectable DMS are plotted in Figure 3.5. Presently, we do not know how quantitative our sample collection system is for DMDS. However, we do know that the SCD has an equimolar sulfur response for all sulfur compounds. Since there are two atoms of sulfur in each molecule of DMDS and one atom of sulfur in each molecule of DMS, we express the amount of DMDS present in the samples as a ratio of half the chromatogram peak area for DMDS to the chromatogram peak area for DMS. In samples where DMS was detected, these ratios ranged from zero, for DMDS not detected, to one. However, comparing DMDS and DMS in terms of the sulfur quantity, the above ratios are multiplied by two, because there are two sulfur atoms for every molecule of DMDS and one sulfur atom per DMS molecule.

To our knowledge, there are no literature reports of DMDS levels rivaling levels of DMS in MBL air. We do not believe that the DMDS found in our samples is an artifact of sampling or a contaminant for many reasons. Firstly, DMDS was present only in air samples and not in the blanks or standards. Also, the amount of DMDS is not correlated to the amount of DMS in individual samples. Only about half of the samples contained DMDS. Groups of samples collected and analyzed on the same day varied in their relative abundances of DMS to the degree that some of the samples contained no DMDS and some contained roughly equal amounts of DMS and DMDS. A chemical mechanism explaining DMDS as a breakdown product or a product liberated from the molecular sieve adsorbent in the sampling tubes is not apparent. Oxidation of mercaptans to disulfides in the presence of oxygen in alkaline solutions is known to occur [*Adewuyi*, 1989]. The possibility that DMDS is a product of mercaptan oxidation in the samples needs to be investigated. Before we can say conclusively that these levels of DMDS are present in the air we need to resample and ensure that our sampling system is quantitative for DMDS, and that DMDS is not an unknown artifact of the sampling procedure.

COS, SO_2, CS_2 and other unidentified sulfur compounds were detected in some of the samples. Since we have not yet determined the efficiency of the sample collection system for trapping these compounds, we are unable to quantify the amounts.

Kachemak Bay Atmospheric Samples

DMS measurements at the Kachemak Bay site offer both ten-day and a one-day time series from a single location. Here the molecular sieve adsorbent system for trapping DMS was not needed, since the GC-SCD was set up in a mobile laboratory, sampling the air coming directly off of the Bay. At typical gas chromatogram for Kachemak Bay air is displayed in Figure 3.6. Figure 3.7 displays the DMS time series. The values cover an even wider range than the Bering and Chukchi Sea samples, from 11 to 1,950 pptv, although most of the Kachemak Bay data are below 200 pptv.

Figure 3.7 (a) shows a downward trend in DMS mixing ratios from June 8 to June 14. During this time, all the DMS mixing ratios were below 200 pptv, except for one value of 250 pptv. Perhaps this period of decreasing DMS mixing ratios is the tail end of the spring phytoplankton bloom?

On June 15, DMS mixing ratios went above 450 pptv. The following day, many measurements were above 450 pptv -- as high as 1,950 pptv early in the day. June 16 was unique in that the day began with the sample site at cloud level. At about 9:00 a.m., before any DMS samples were collected, the clouds rose to the level of the sampling site and total aerosol number decreased from about 3000 to 1000 cm^{-3}. The first three samples, collected while in the cloud, were the three highest mixing ratios of the field campaign -- 1860, 1790 and 1950 pptv, respectively. Aerosol size distributions were bimodal during this time, although the dip between the two modes was close to 150 nm rather than 50 nm which is more typical of clean marine air. If we assume that the top of the cloud is the top of the layer of air in contact with the ocean surface, then we were sampling air in contact with the ocean surface. After the third sample was collected, the winds picked up, decreasing vertical stability, and within an hour the clouds lifted above the sampling site. DMS mixing ratios measured during this period and subsequently -- 341, 1077, 498, 442, and 246 pptv, respectively -- were significantly lower than the first three measurements of the day. Aerosol size distributions were suggestive of clean marine air or a transition to clean marine air for the first four of these five samples. The fifth sample was clearly clean marine air with the dip between modes at 50 nm. Perhaps, as the data and observations suggest, an increase in the height of the top of the layer of air in contact with the ocean surface lead to dilution of mixing ratios near the surface. Diurnal variations in DMS mixing ratios of a factor of approximately 1.4 have been attributed, at least in part, to diurnal variations in boundary layer height at other locations [*Saltzman and Cooper*,1989]. Our interpretation may be an oversimplication, since the layer of air just below cloud top could be decoupled from the ocean surface. We have no data to

refute and verify this, and without vertical profiles of meteorological data to investigate the vertical structure of the air between the ocean surface and the cloud top, we are limited to conjecture. The time series of absolute humidity changes little throughout the sampling period, indicating we are probably sampling the same airmass throughout the sampling period.

The 3-day back-trajectory for June 16 was also unique, indicating a contribution from an air mass traveling south over Cook Inlet. Perhaps air coming from this direction had been significantly influenced by the coastal environment (i.e. tidal flats, different algal species). Tidal heights may also have influenced DMS mixing ratios in the air. The three highest mixing ratios of the field campaign, 1860, 1790 and 1950 pptv, were measured on June 16 during three of the four below average tide events when samples were collected, -2.3, -1.9 and -1.0 m, respectively.

Sulfur compounds other than DMS, such as COS, SO_2, CS_2 and unidentified sulfur compounds, were detected but not quantified in some of the samples. DMDS was found in approximately one third of the samples collected and analyzed at the Kachemak Bay site. The ratios of DMDS to DMS in the samples ranged from zero, indicating not detected, to 0.6 and are plotted in Figure 3.8. The average ratio was 0.2 for the samples containing DMDS. See the section on the Bering and Chukchi Seas sample results for a general discussion on DMDS in the samples.

Conclusions

The portable sample collection system for trapping DMS used in this study is an effective tool for sampling in remote regions, at minimal cost and with few logistical complications. The limited DMS field measurements that do exist, including the results of this study, support the hypothesis that ocean areas around Alaska may contribute significantly to the global sulfur budget. Our results call for a more thorough look into DMS and DMDS emissions from ocean regions around Alaska, potentially a significant

source of sulfur to the atmosphere.

Acknowledgments. This work was supported by the National Aeronautical and Space Administration Aerosol Interdisciplinary Program grant NAGW-3728 and a grant from the Center for Global Change and Arctic System Research at the University of Alaska Fairbanks. These measurements would not have been possible without the professional support provided by the captain and crew of the RV *Alpha Helix*. We especially thank Tom Weingartner for providing a berth and support on the RV *Alpha Helix*.

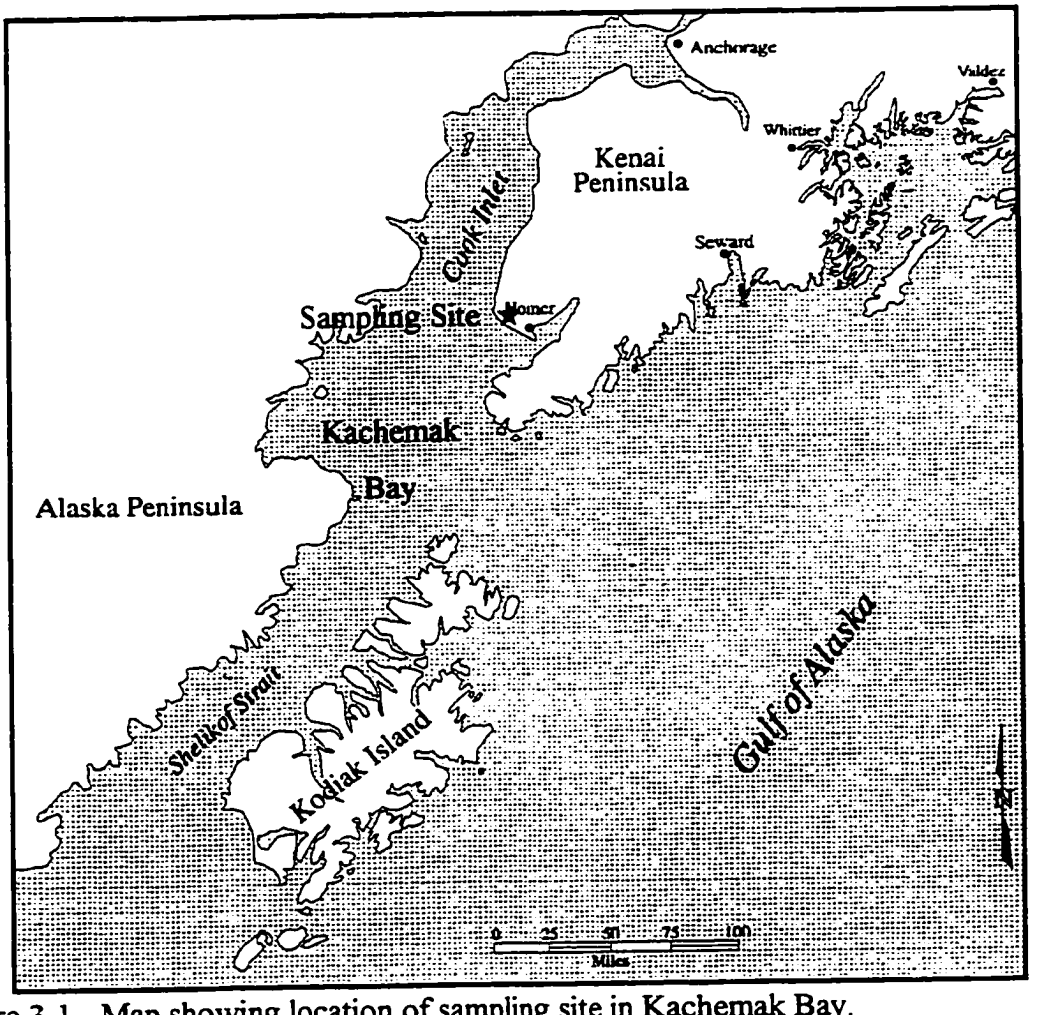

Figure 3.1 - Map showing location of sampling site in Kachemak Bay.

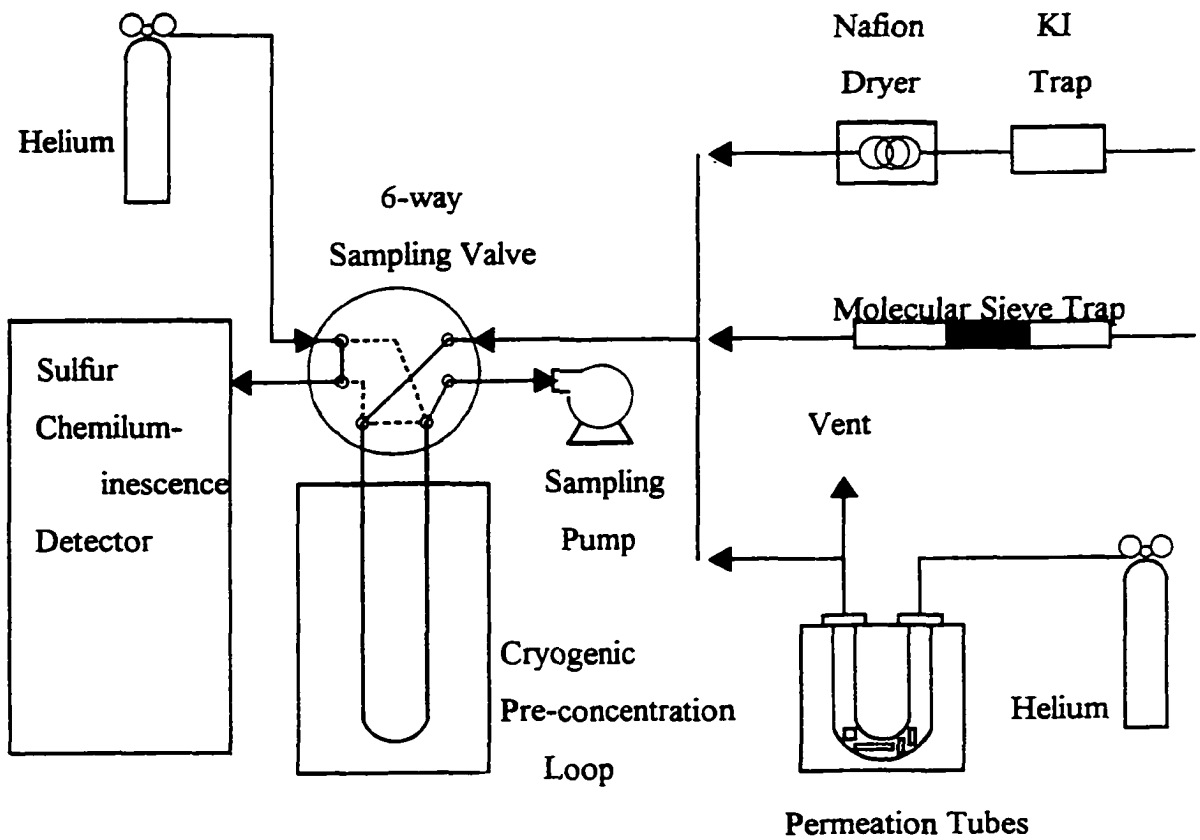

Figure 3.2 - Gas trapping and analysis system used in present study.

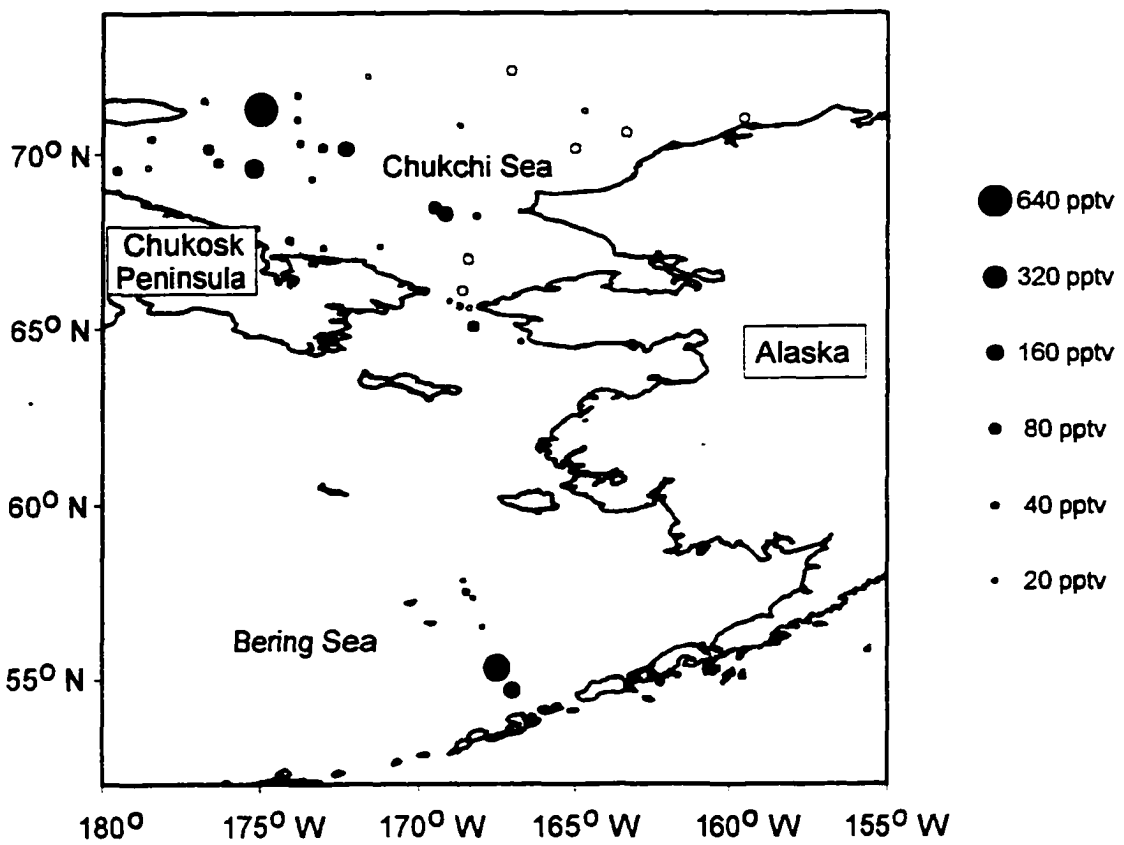

Figure 3.3 - Distribution of atmospheric DMS mixing ratios at sampling stations 1-40 along the cruise track in the Bering and Chukchi Seas. Hollow dots indicate non-detectable levels of DMS sized to indicate the detection limit for each sample.

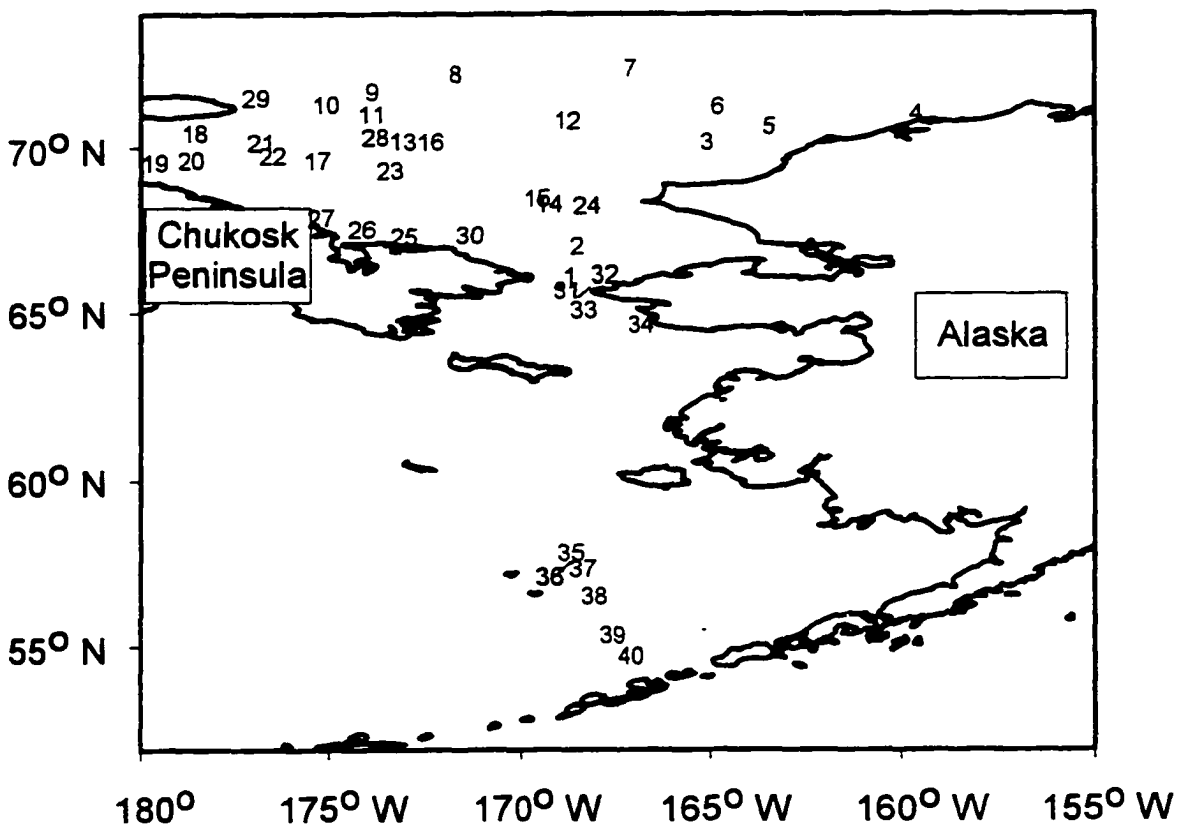

Figure 3.4 - Same as Figure 3.3 except instead of showing DMS mixing ratios, the sampling station numbers 1- 40 are indicated.

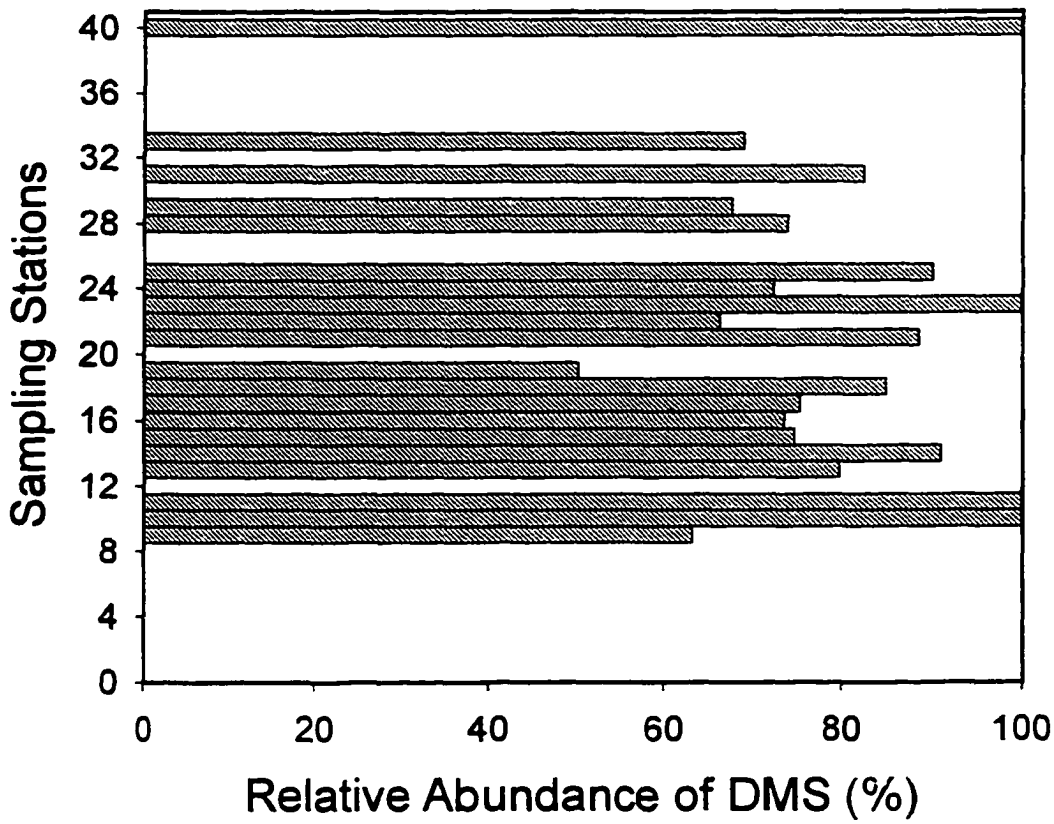

Figure 3.5 - The abundance of DMS relative to the total of DMS + DMDS for individual samples in the Chukchi and Bering Seas. No relative abundances reported for samples with non-detectable DMS and for sampling station 26 where DMDS data was not available.

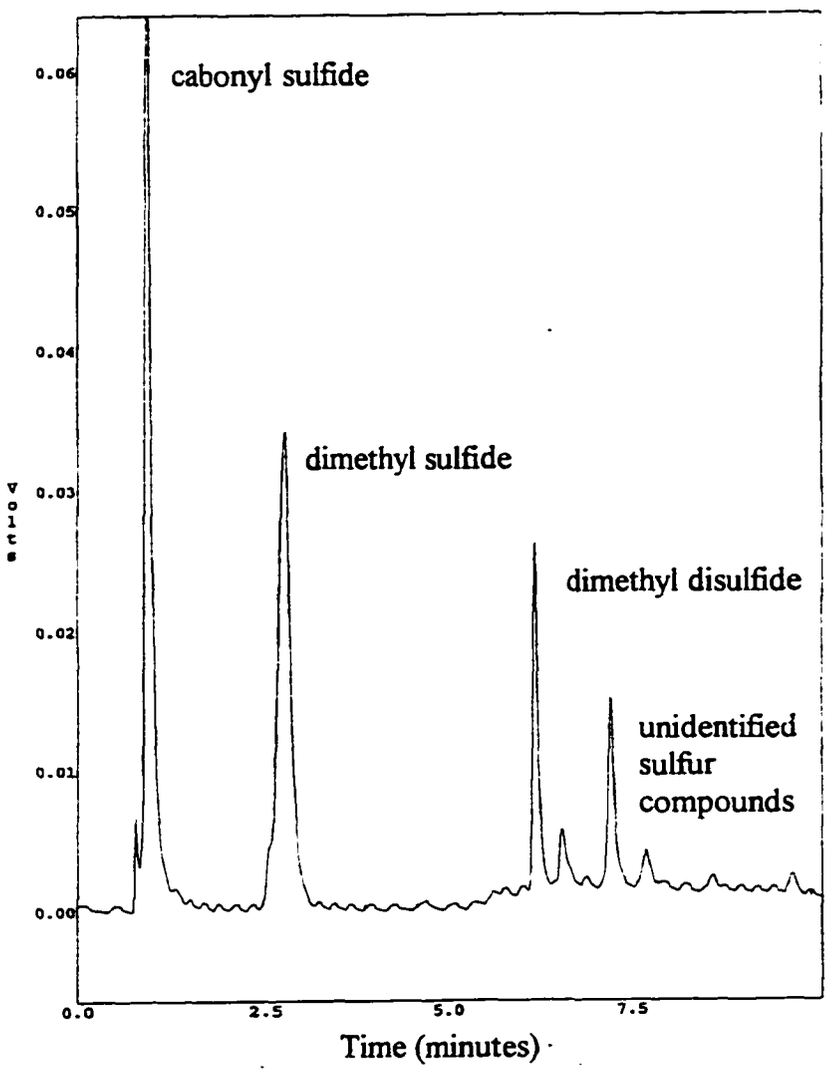

Figure 3.6 - Typical gas chromatogram for Kachemak Bay sampling site. Chromatogram from June 15, 1996 at 12:04 p.m.

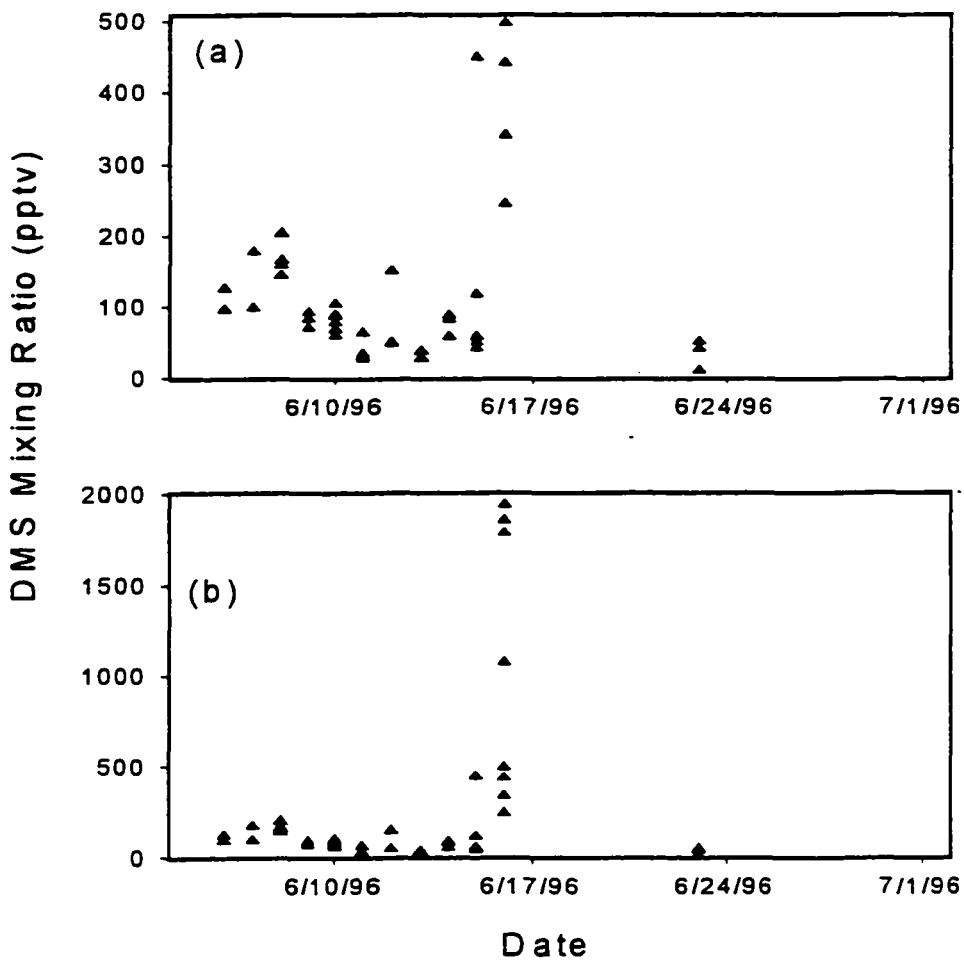

Figure 3.7 - Time series of DMS mixing ratios in air over Kachemak Bay, Alaska (a) below 500 pptv, and (b) below 2,200 pptv.

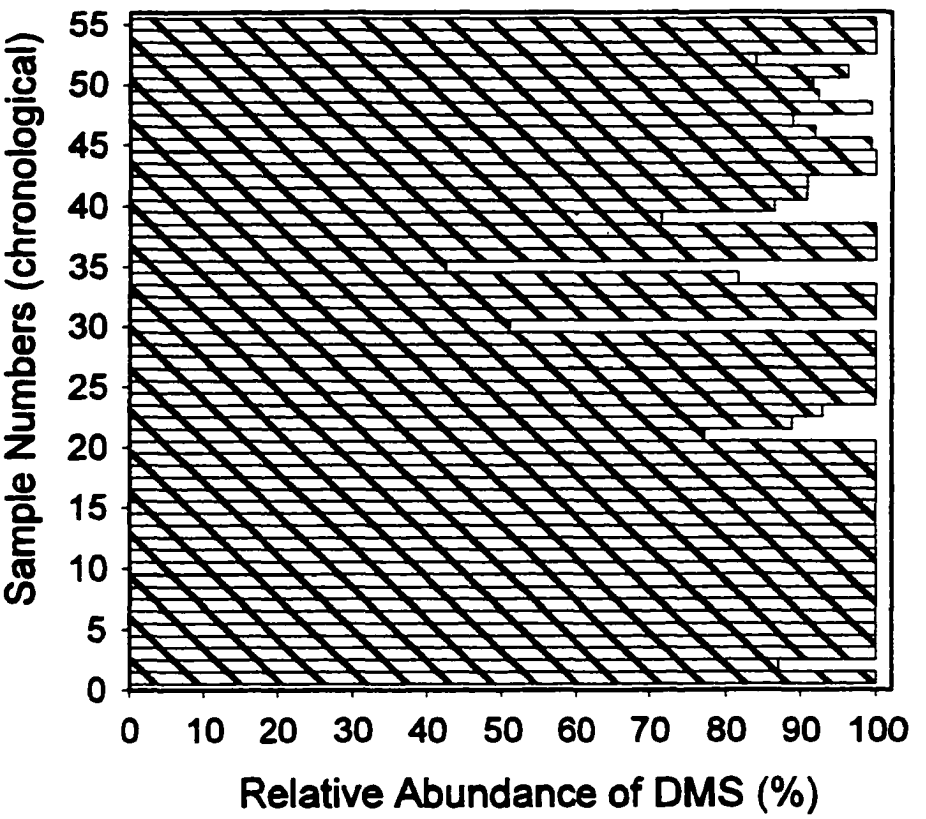

Figure 3.8 - The abundance of DMS relative to the total of DMS + DMDS for individual samples at the Kachemak Bay site. No relative abundances reported for samples with non-detectable DMS.

References

Aargaard, K., L. A. Barrie, E. C. Carmack, C. Garrity, E. P. Jones, D. Lubin, R. W. Macdonald, J. H. Swift, W. B. Tucker, P. A. Wheeler, and R. H. Whitner, U.S., Canadian researchers explore Arctic Ocean, *EOS, 77,* (22), 209-216, 1996.

Adewuyi, Y. G., Oxidation of biogenic sulfur compounds in aqueous media, In: *Biogenic Sulfur in the Environment*, edited by Saltzman, E. S. and W. J. Cooper, pp 529-559, American Chemical Society, Washington, DC, 1989.

Andreae, M. O., Ocean-atmosphere interactions in the global biogeochemical sulfur cycle, *Marine Chemistry, 30,* 1-29, 1990.

Andreae, M. O., R. J. Ferek, F. Bermond, K. P. Byrd, R. T. Engstron, S. Hardin, P. D. Houmere, F. LeMarrec, and H. Raemdonck, Dimethyl sulfide in the marine atmosphere, *Journal of Geophysical Research, 90,* (D7), 12,891-12,900, 1985.

Barinaga, C. J., and S. O. Farwell, Noncryogenic FSOT column separation of sulfur-containing gases, *Journal of High Resolution Chromatography & Chromatography Communications, 10,* 538-543, 1987.

Barnard, W. R., M. O. Andreae, and R. L. Iverson, Dimethylsulfide and *Phaeocystis poucheti* in the southeastern Bering Sea, *Continental Shelf Research, 3,* (2), 103-113, 1984.

Bates, T. S., A. D. Clarke, V. N. Kapustin, J. E. Johnson, and R. J. Charlson, Oceanic dimethylsulfide and marine aerosol: Difficulties associated with assessing their covariance, *Global Geochemical Cycles, 3,* (4), 299-304, 1989.

Bates, T. S., J. D. Cline, R. H. Gammon, and S. R. Kelly-Hansen, Regional and

seasonal variations in the flux of oceanic dimethylsulfide to the atmosphere, *Journal of Geophysical Research, 92,* (C3), 2930-2938, 1987.

Baumann, M. E. M., F. P. Brandini, and R. Staubes, The influence of light and temperature on carbon-specific DMS release by cultures of *Phaeocystis antarctica* and three antarctic diatoms, *Marine Chemistry, 45,* 129-136, 1994.

Benner, R. L., and D. H. Stedman, Field evaluation of the sulfur chemiluminescence detector, *Environ. Sci. Technol., 24,* (10), 1592-1596, 1990.

Bürgermeister, S., and H. W. Georgii, Distribution of methanesulfonate, NSS sulfate and dimethylsulfide over the Atlantic and the North Sea, *Atmospheric Environment, 25A,* (3/4), 587-595, 1991.

Charlson, R. J., and T. M. L. Wigley, Sulfate aerosol and climatic change, *Scientific American* , 48-57, 1994.

Charlson, R. J., J. E. Lovelock, M. O. Andreae, and S. G. Warren, Oceanic phytoplankton, atmospheric sulphur, cloud albedo and climate, *Nature, 326,* 655-661, 1987.

Chatfield, R. B., and P. J. Crutzen, Sulfur dioxide in remote oceanic air: Cloud transport of reactive precursors, *Journal of Geophysical Research, 89,* (D5), 1984.

Clarke, A. D., The Pacific marine aerosol: Evidence for natural acid sulfates, *Journal of Geophysical Research, 92,* (D4), 1987.

Davison, B. M., and A. G. Allen, A method for sampling dimethylsulfide in polluted and remote marine atmospheres, *Atmospheric Environment, 28,* (10), 1994.

Ferek, R. J., and J. A. Herring, Ground-based measurement of DMS in the Arctic

atmosphere at Barrow during summer 1991, *Climate Monitoring and Diagnostics Laboratory* , (20), 1991.

Finlayson-Pitts, B. J., and J. N. Pitts, *Atmospheric Chemistry: Fundamentals and Experimental Techniques*, Wiley-Interscience, New York, 1986.

Hines, M. E., and M. C. Morrison, Emissions of biogenic sulfur gases from Alaska tundra, *Journal of Geophysical Research, 97,* (D15), 16,703-16,707, 1992.

Jodwalis, C. M., and R. L. Benner, Sulfur gas fluxes and horizontal inhomogeneities in the marine boundary layer, *Journal of Geophysical Research, 101, D2,* 4393-4401, 1996.

Leck, C., and H. Rodhe, Emissions of marine biogenic sulfur to the atmosphere of northern Europe, *Journal of Atmospheric Chemistry, 12,* pp. 63-86, 1991.

Nriagu, J. O., D. A. Holdway, and R. D. Coker, Biogenic sulfur and the acidity of rainfall in remote areas of Canada, *Science, 237,* 1189-1192, 1987.

Shaw, G. E., Bio-controlled thermostatis involving the sulfur cycle, *Climatic Change, 5,* 297-303, 1983.

Shearer, R. L., Development of flameless sulfur chemiluminescence detection: application to gas chromatography, *Analytical Chemistry, 64,* 2192-2196, 1992.

Turner, S. M., Malin, G., and Liss, P. S., Dimethyl sulfide and (dimethylsulfonio)propionate in European coastal and shelf waters, In: *Biogenic Sulfur in the Environment*, edited by Saltzman, E. S. and W. J. Cooper, pp 183-200, American Chemical Society, Washington, DC, 1989.

Turner, S. M., P. D. Nightingale, W. Broadgate, and P. S. Liss, The distribution of

dimethyl sulphide and dimethylsulphoniopropionate in Antarctic waters and sea ice, *Deep-Sea Research II, 42,* (4-5), 1059-1080, 1995.

Chapter 4

Modeling of Ocean Mixing, Biological Production and Dimethyl Sulfide Sea-to-Air Flux for High Latitude Regions[3]

Introduction

Atmospheric sulfate, produced from oceanic DMS emitted to the atmosphere, potentially affects the Earth's radiation balance, and hence the climate. DMS is oxidized in the atmosphere to aerosols, which may impact climate directly through light scattering [*Shaw*, 1983] or indirectly through their role as cloud condensation nuclei (CCN) affecting cloud formation, lifetime and reflectivity [*Charlson et al.*, 1987]. Over remote and polluted regions sulfate is the main component of CCN [*Bigg et al.*, 1984]. Sulfate also dominates (by number concentration) in non-sea-salt marine aerosols [*Clarke et al.*, 1987]. The sulfate in these non-sea-salt marine aerosols originates mostly from dimethyl sulfide (DMS) emitted from the oceans [*Bonsang et al.*, 1980].

DMS is present in surface seawater due to the release of DMS [*Andreae*, 1990] and its precursor, dimethylsulfoniopropionate (DMSP) [*Turner et al.*, 1989], by phytoplankton that may use it to regulate osmotic pressure in their cells. Complex biological cycling, interacting with a complex physical environment, results in seawater DMS concentrations which vary widely over time and space. The factors influencing the release of DMS into the water are not clearly understood. Possible mechanisms include algal senescence, zooplankton grazing activity and metabolic release by phytoplankton [*Nguyen et al.*, 1988; *Turner et al.* 1988; *Dacey and*

---

[3] Jodwalis, C. M., D.L. Eslinger and R. L. Benner, Modeling of Ocean Mixing, Biological Production and Dimethyl Sulfide Sea-to-Air Flux, to be submitted 1998.

Wakeham 1986; *Leck et al.* 1990]. DMS is removed from the water column by ventilation to the atmosphere, microbial consumption and oxidation (microbial degradation), photo-oxidation, and particle adsorption [*Liss*, 1983; *Kiene and Bates*, 1990; *Leck and Rodhe*, 1991; *Brimblecombe and Shooter*, 1986; *Shooter and Brimblecombe*, 1989]. The rates of microbial degradation and photo-oxidation of DMS are very poorly understood [*Bates et al.*, 1994], although the former is currently considered the major sink of oceanic DMS [*Kiene and Bates*, 1990; *Leck et al.*, 1990; *Bates et al.*, 1994]. It appears that DMS loss by particle adsorption and sedimentation is very small [*Brimblecombe and Shooter*, 1986] and that only a small percentage of DMS in the water column is emitted to the atmosphere [*Bates et al.*, 1994] . In other words, the production rate of DMS in the ocean water is large compared to the small amount of DMS that is emitted to the atmosphere. However, under conditions of substantial vertical mixing, such as high wind stress or convective mixing, there is a potential for enhanced DMS emissions.

Wide excursions in atmospheric mixing ratios are common at many locations throughout the world [*Andreae et al.*, 1985]. Orders of magnitude differences may exist from one day to the next at the same location [*Kwint and Kramer*, 1995]. Our measurements of atmospheric DMS mixing ratios from Kachemak Bay, Alaska, and the Bering and Chukchi Seas also exhibit high spatial and temporal variability [Chapter 3 of this thesis]. Variability in DMS air mixing ratios could result from a combination of many factors, including: (1) marine source strength; (2) meteorological parameters, such as boundary layer mixing height, or wind speed, which affect mass transfer rates; (3) pathway of airmass and time it spends over the ocean; (4) influence of the coastal environment; (5) differing rates of oxidation; and (6) fluctuations in DMS sea-to-air flux. No one has looked in detail at the relationship between atmospheric DMS mixing ratios and any of these factors.

In addition to high variability in DMS mixing ratios above the Bering and

Chukchi Seas, we observed high levels of DMS in September, generally not considered to be a very productive time of the year in the Arctic. These two observations lead us to consider another factor that influences DMS mixing ratios and DMS sea-to-air flux, that is ocean mixed layer dynamics. Decreasing sea surface temperatures in the autumn at high latitudes and strong wind events typically lead to deepening of the ocean mixed-layer depth. This enhanced mixing could bring DMS from below to the surface, increasing the amount ventilated to the atmosphere.

In this work we explore the extent to which ocean mixed-layer dynamics influences the day-to-day and seasonal cycles of DMS sea-to-air flux in high-latitude regions. To gauge the role of ocean mixed-layer dynamics on DMS sea-to-air flux, we use a computer model. The model has been used to evaluate what parameters are most important to DMS sea-to-air flux. These results can help to improve the design of field experiments and the accuracy of DMS sea-to-air flux estimations. The model also may prove useful in extending DMS sea-to-air flux estimates to climatic regimes or extreme weather conditions not conducive to field sampling, and indicate areas where temporal and spatial coverage need to be improved.

This modeling study supplements efforts to assess the magnitude of DMS emissions from high latitude oceans. High primary productivity in ocean regions surrounding Alaska [*Hood and Kelley*, 1974], such as Prince William Sound, the Gulf of Alaska and the Bering Sea, suggest significant potential for DMS emissions from these waters. Field measurements of atmospheric DMS above northern oceans [*Aagaard et al.*, 1990; *Ferek and Herring*, 1991; Chapter 3 of this thesis] and seawater DMS concentrations in northern oceans [*Bates et al.*, 1987; *Bürgermeister and Georgii*, 1991] also suggest a potentially important source of sulfur to the atmosphere from high latitude oceans.

The Model

We are using a biophysical model of the well-mixed ocean layer under meteorological forcing to investigate the importance of mixed layer dynamics on daily and seasonal DMS sea-to-air flux in Prince William Sound (PWS) and the northern Gulf of Alaska. The physical component of the model is based on the model of *Pollard et al.* [1973] as modified by *Thompson* [1976]. Eslinger and Iverson [in press] have built upon Thompson's work to construct a model of the spring phytoplankton bloom in the Bering Sea. Eslinger's [in preparation] model of phytoplankton and zooplankton variability in PWS went a step further than the model, extending the model to cover a whole year, thus providing insight into seasonal and interannual variability.

Eslinger's [in preparation] PWS model has been extensively validated by field data [Eslinger, in preparation; Eslinger and Iverson, in press]. The Eslinger PWS model accurately simulated the timing and magnitude of the phytoplankton and zooplankton blooms in three out of four years for which field data were available. Actual sea surface temperatures also agreed well with model results over the course of an entire year. The model accurately simulates springtime phytoplankton dynamics in the Bering Sea and the Mid-Atlantic Bight. The model's high vertical resolution is credited for this success. Both models show that small differences in the meteorological forcing can significantly affect timing, duration, and character of the bloom - spatially, interannually and temporally. For example, warm, calm springs lead to short, intense phytoplankton blooms, whereas, colder, stormy springs lead to longer phytoplankton blooms [Eslinger, personal communication]. Although the ocean cycling of DMS is not directly correlated to phytoplankton biomass, they are related since oceanic DMS is a result of phytoplankton metabolism.

The model of Eslinger [in preparation] serves as the basis for this work. We have incorporated mixing and DMS production and loss terms in this model. The DMS model domain is the upper 100 m of a significantly deeper water column.

Vertical resolution is 2 meters, and temporal resolution is 2 hours. The meteorological parameters driving the model are: 1) measured wind velocity, air temperature, and relative humidity measurements from buoys and National Weather Service surface observations, 2) solar radiation, calculated by the model, using the method of *Frouin et al.* [1989], and 3) cloudiness, assumed to be constant at 70% coverage. Vertical mixing, which is controlled by the balance between the kinetic energy available for additional mixing and the potential energy cost of overcoming the existing stratification, is calculated to occur according to a Froude number criterion [*Thompson*, 1976]. A full description of the 1-D physical model can be found in *Eslinger* [1990]. The DMS model biology includes essential nutrients (nitrate, ammonium and silica), zooplankton (large *Neocalanus*-type and small *Pseudocalanus*-type copepods), and two types of phytoplankton (diatoms and flagellates). Production of DMS by these species is offset, at least in part, by bacteria that consume DMS. Figure 4.1 shows the processes incorporated into the model schematically. In the DMS model, DMS sea-to-air flux is calculated as a function of DMS concentration in the top two meters of the water column and a transfer velocity modeled as a function of wind speed [*Liss and Merlivat*, 1986].

Model output consists of: 1) DMS concentrations at two meter increments in the upper 100 m of the water column every two hours, 2) daily DMS sea-to-air flux, and 3) cumulative DMS sea-to-air flux, from early March through year's end. Results showing interannual variability come from 1993 and 1996 model runs driven by meteorological data from the C-Lab Buoy in PWS. One other buoy in PWS, designated Mid-sound, provided meteorological data used to investigate spatial variability for 1996. The model was also run using 1995 meteorological data from Middleton Island, a site just outside PWS which is representative of the Gulf of Alaska. Figure 4.2 shows the buoy and Middleton Island site locations.

DMS Component

Presently identified pathways involved in cycling of DMS in ocean water are diagramed in Figure 4.3. In the DMS model, we include, as parameters, the significant pathways that are known to exist and for which some measurements are available. "Base values" for each parameter were chosen to best represent the area of study. These base values were then varied to quantify the sensitivity of the calculated flux to each parameter. Table 4.1 summarizes the DMS model parameters, base values and ranges. A comprehensive discussion of the parameters, their uncertainties and ranges, and the chosen base values follows. Keep in mind that none of the DMS production or loss rates come from studies of high latitude systems because they are currently not available. This introduces yet more uncertainty in quantifying the pathways for the DMS model. There is a definite need for measurements of DMS cycling rates in high latitude systems.

DMS production. *Keller et al.* [1989] report cellular concentrations of DMSP for 12 classes of phytoplankton, noting that the highest levels are found in the classes Dinophyceae (dinoflagellates) and Prymnesiophyceae (including coccolithophorids). These two phytoplankton classes are representative of the flagellated phytoplankton found in high latitude ocean regions. The variability of DMSP cellular concentrations among species within each class is tremendous, ranging from 3.28 to 260 μmoles DMSP cm^{-3} (cell vol) for species in the Prymnesiophyceae and from 0.01 to 2201.5 μmoles DMSP cm^{-3} (cell vol) among the Dinophyceae [*Keller et al.*, 1989]. *Wakeham and Dacey* [1989] estimate that the turnover of intercellular DMSP (releasing DMS into seawater) is about 1% per day. Using this turnover rate and the range of 0.01 to 2201.5 μmoles DMSP cm^{-3} (cell vol) provided by *Keller et al.* [1989], we estimate daily metabolic release to be between 0 and 22 x 10^{-3} mol DMS L^{-1} (cell vol) d^{-1} for flagellates.

We calculated the daily metabolic release of DMS for the dinoflagellate

Gymnodinium nelsoni and the coccolithophorid *Hymenomonas carterae* using DMS production rates and approximate cell volumes reported from laboratory studies of *Dacey and Wakeham* [1986] and *Vairavamurthy et al.* [1985]. *G. nelsoni* produces 0.96 x 10^{-3} mol DMS L^{-1} (cell vol) d^{-1} and *H. carterae* 1.6 x 10^{-3} mol DMS L^{-1} (cell vol) d^{-1}. *G. nelsoni* contains 2.96 x 10^{1} μmoles DMSP cm^{-3} (cell vol) [*Keller et al.*, 1989], which is in the low end of the range for dinoflagellates. This suggests that the metabolic release of DMS by *G. nelsoni* may also be low compared to other dinoflagellates. Therefore we justify using a slightly higher metabolic release rate of 5 x 10^{-3} mol DMS L^{-1} (cell vol) d^{-1} in the DMS model. This is a conservative number which is within the range of 0 and 22 x 10^{-3} mol DMS L^{-1} (cell vol) d^{-1}. Furthermore, this metabolic release rate gives a reasonable DMS sea-to-air flux and DMS seawater concentrations that are within the range of measurements. This will be discussed in the results.

Field data of *Liss et al.* [1994] show that cellular concentrations of DMSP in diatoms are about 6% those of flagellates. Lab culture studies of *Keller et al.* [1989] are in general agreement. Therefore, we have set the metabolic release rate of DMS by diatoms at 0.3 x 10^{-3} mol DMS L^{-1} (cell vol) d^{-1} in the DMS model, with a range from 0 to 1.3 x 10^{-3} mol DMS L^{-1} (cell vol) d^{-1}.

Release of DMS by phytoplankton during the growth phase (herein referred to as metabolic release) is small compared to DMS release during senescence. The senescent phase is associated with the degradation of the organic matter synthesized during the growth phase. Maximum production of DMS often occurs after a phytoplankton bloom [*Ngyuen et al.*, 1988; *Stefels and van Boekel*, 1993; *Leck et al.*, 1990; *Matrai and Keller*, 1993], probably due to cell death followed by disintegration. *Stefels and van Boekel* [1993] followed DMS production in the senescent phase of a *Phaeocystis* sp. batch culture. Measurements in cultures that had completely died (all cells lysed) showed that 73% of the total DMSP had been converted to DMS during the

senescence phase. They also found that the intracellular DMSP concentration of *Phaeocystis* sp. increased more than 2-fold during the transition from exponential growth phase to stationary growth phase. *Nguyen et al.* [1988], experimenting with natural phytoplankton assemblages, reported that the ratio of DMS concentrations in water during the senescence phase to that during the growth phase was 7 for diatom species and 26 for a flagellate species. We use the factors of *Nguyen et al.* [1988], to derive DMS release rates during senescence because natural assemblages are likely to be more representative of actual populations. However, the batch culture results help to define an approximate range, between two times and 73 times the daily metabolic release rate. As a result of zooplankton grazing, release of DMS by diatoms is 7 times greater than 0.3×10^{-3} mol DMS L^{-1} (cell vol) d^{-1} and release of DMS by flagellates is 26 times greater than 5×10^{-3} mol DMS L^{-1} (cell vol) d^{-1}. This amounts to 2.1×10^{-3} mol DMS L^{-1} (cell vol) d^{-1} and 130×10^{-3} mol DMS L^{-1} (cell vol) d^{-1}, for diatoms and flagellates respectively. Ranges are estimated to be from 0.6×10^{-3} to 22×10^{-3} mol DMS L^{-1} (cell vol) d^{-1} for diatom species and 10×10^{-3} to 360×10^{-3} mol DMS L^{-1} (cell vol) d^{-1} for flagellates.

Grazing of zooplankton greatly increases DMS release by phytoplankton and is likely an important factor in the natural environment [*Dacey and Wakeham*, 1986]. In the sea, grazing is the main cause of phytoplankton mortality [*Turner et al.*, 1988]. *Leck et al.* [1990] have found a significant correlation between copepod and total zooplankton biomass, and ambient DMS concentration. A couple of research groups have worked to quantify this relationship. To test whether grazing by the antarctic krill *Euphausia superba* on phytoplankton enhanced DMS production, *Daly and DiTullio* [1993] performed experiments with bottles containing antarctic seawater and phytoplankton. They found that addition of 3 krill to the bottles resulted in a greater than threefold increase in DMS production. Performing similar experiments in the laboratory, *Dacey and Wakeham* [1986] and *Vairavamurthy et al.* [1985] investigated

the production of DMS during grazing by the marine copepods *Labidocera aestiva* and *Centropages hamatus* on the phytoplankton species *Gymnodinium nelsoni*. They found that about one-third of the total DMSP in phytoplankton is released and converted to DMS during grazing. We use this fraction provided by *Dacey and Wakeham* [1986] to derive the base value for DMS release used in the model. The total DMSP in *G. nelsoni* can be estimated by multiplying the daily metabolic release rate of 5×10^{-3} mol DMS L^{-1} (cell vol) d^{-1} by 100 days, since daily metabolic release of DMS is roughly 1% of the intracellular DMSP from DMS-producing phytoplankton [*Wakeham and Dacey,* 1989]. This gives 500×10^{-3} mol DMS L^{-1} (cell vol), a third of which is 170×10^{-3} mol DMS L^{-1} (cell vol). We estimate the lower limit of the uncertainty to be 3 times greater than the daily metabolic release rate, based on the experiments of *Daly and DiTullio* [1993], resulting in 15×10^{-3} mol DMS L^{-1} (cell vol). The higher limit can be no more than the total intracellular DMSP from DMS-producing phytoplankton, which is 500×10^{-3} mol DMS L^{-1} (cell vol) in the DMS model. Following the same logic, we estimate that the amount of DMS released upon zooplankton grazing of diatoms is 10×10^{-3} mol DMS L^{-1} (cell vol), with a range of 0.6×10^{-3} to 30×10^{-3} mol DMS L^{-1} (cell vol).

Cell disruption due to grazing or senescence also releases DMSP from phytoplankton. Free DMSP (DMSP not contained in phytoplankton cells) may be converted to DMS through microbial transformation [*Taylor and Kiene,* 1989]. Figure 4.3 shows these pathways from algal DMSP to free DMSP and from free DMSP to DMS. It is currently not possible to quantify these pathways due to lack of measurements.

Andreae [1986] suggests that the enzymatic release rate of DMS from DMSP in algae is subject to increase as a result of external stress on the organism, such as salinity changes, physical disturbance and tidal exposure. However, the data on salinity are inconclusive. In a few species of phytoplankton, intracellular DMSP has

been observed to increase, but only during extreme salinity changes [*Keller et al.*, 1989].

In ocean waters, microbes convert DMSO, an electron acceptor, to DMS [*Taylor and Kiene*, 1989]. Although DMSO concentrations are generally higher than those of DMS and represent a major pool of dissolved sulfur, there is little reliable information on the importance of this pathway [*Simo et al.*, 1995]. For this reason this pathway has not been included in the DMS model.

DMS loss. DMS loss in surface seawater is a result of emission to the atmosphere [*Liss*, 1983], photo-oxidation to DMSO [*Brimblecombe and Shooter*, 1986], particle adsorption [*Shooter and Brimblecombe*, 1989] and microbial oxidation and consumption (microbial degradation) [*Kiene and Bates*, 1990; *Leck and Rodhe*, 1990]. The latter appears to be the major loss process with DMS turnover times on the order of days [*Kiene and Bates*, 1990; *Kiene and Service*, 1991; *Leck et al.*, 1990].

Our literature search uncovered one reference quantifying the loss of DMS in seawater due to photo-oxidation. *Brimblecombe and Shooter* [1986] examined coastal seawater samples and found that sunlight photo-oxygenates DMS with a first order rate constant of 9.0×10^{-2} hr^{-1}. Assuming that photo-oxidation takes place in the first meter of the oceans, for about one third of the time, the loss rate of DMS by photo-oxidation is approximately the same as the rate of loss to the atmosphere. It is difficult to put a range on the loss rate, because the samples of coastal seawater used in the experiment may not be typical, the wavelength dependence of the photosensitized oxidation has not been characterized and no other measurements are available.

Loss of DMS to the deep sea by particle adsorption and sedimentation appears to be of little consequence compared to other loss mechanisms. The value of 0.001 Tg(S) lost to the deep sea each year through particle adsorption is negligible compared to the loss to the atmosphere which is about 17-30 Tg(S) $year^{-1}$ [*Shooter and Brimblecombe*, 1989]. Therefore, we have not included this process in the model.

Biological loss and production of DMS are coupled, and are believed to be the main factor in controlling seawater DMS concentrations [*Simo et al*, 1995; *Kwint and Kramer*, 1995; *Kiene*, 1992]. The end-products of microbial consumption and oxidation (microbial degradation) are sulfate and carbon dioxide, or DMSO [*Taylor and Kiene*, 1989].

Seawater incubation experiments have been used to estimate DMS microbial degradation rates. *Bates et al.* [1994] incubated water samples with 500 μM chloroform. Chloroform (500μM) inhibits microbial degradation of DMS in sea water, whereas DMS production is not affected [*Bates et al.*, 1994; *Kiene and Bates*, 1990]. Therefore the difference in DMS production between incubated samples with and without chloroform is the degradation of DMS by microbes.

In the DMS model, we have chosen to use a microbial degradation rate of 0.1 nM DMS d^{-1}. This is the lowest value in the range of 0.1 to 3 nM d^{-1} reported by *Kiene* [1992] from Sargasso Sea and eastern Pacific samples. *Kiene and Bates* [1990] report depth integrated net loss values from 1.1 to 55 nM d^{-1} for samples from 5 m depths in the same area in the eastern Pacific. *Simo et al.* [1995] report a range of 8 to 9 nM d^{-1} at 30 and 50 m depth for samples from the western Mediterranean Sea. At 5 m and 80 m depths they found no net losses. *Simo et al.* [1995] cautions that the microbial degradation rate values are possibly overestimated, since chloroform has been found to desorb DMSP from particulate surfaces, thereby enhancing DMS formation. These ranges are in general agreement with the observations of *Bates et al.*, [1994] *Gabric et al.* [1993] and *Kiene and Service* [1991] that at least two-thirds of oceanic DMS is consumed by microbes. In *Bates et al.*'s [1994] Pacific study off the Washington State Coast, during a period of no vertical mixing, they found only 1% of the oceanic DMS was vented to the atmosphere and a similar amount was lost due to photo-oxidation. Microbial degradation rates reported by *Kiene and Bates* [1990] were also more than 10 times higher than the loss of DMS to the atmosphere through air-sea

exchange.

A low value from the reported ranges of DMS microbial degradation may be more realistic for high latitude environments. Some studies have found that bacterial metabolism is suppressed at low temperatures [*Pomeroy and Wiebe*, 1988; *Kiene and Bates*, 1990], suggesting net loss of oceanic DMS by microbes may be lower in colder climates. If this is the case, it could explain the extremely high DMS concentration measured by *McTaggart and Burton* [1992] in Antarctic waters and the relatively high DMS concentrations found in the Bering Sea and the Gulf of Alaska compared with tropical Pacific waters [*Bates et al.*, 1992].

Diffusivity. DMS is mixed vertically in the ocean by eddy diffusion and to a much lesser extent, molecular diffusion. Molecular diffusion is important in the DMS model because it is needed for the gas exchange calculation. In the DMS model, we use the value of 4.71 x 10^{-2} m^2 hr^{-1} [*Wakeham and Dacey*, 1989] for the eddy diffusivity and the value of 6.46 x 10^{-6} m^2 hr^{-1} for the DMS molecular diffusivity [*Andreae*, 1985; *Barnard et al.*, 1982].

Sensitivity Analysis

A sensitivity analysis was performed to identify the parameters most important to DMS seawater concentrations and DMS sea-to-air flux. Sensitivity of DMS sea-to-air flux to changes in photo-oxidation, zooplankton grazing, microbial loss, flagellate and diatom production of DMS, and eddy diffusivity were all quantified. The analysis consisted of running the model at one-half and twice the base parameter values, changing one parameter at a time. For six different parameters this meant thirteen model runs, total. We used the annual cumulative DMS sea-to-air flux from the model runs to evaluate sensitivity of the results to changes in the parameters.

Discussion of Results

In light of the large uncertainties associated with the parameters in the DMS

model, interpretation of the model results are qualitative rather than quantitative. For example, we avoid making any conclusions that rely on absolute quantities, such as the integrated DMS sea-to-air flux. Instead, we evaluate trends or differences from season to season and place to place. For each parameter only very few measurements exist and the measurements that do exist come almost exclusively from mid and low-latitude systems. Add to this the physical and biological complexity that exists in nature, and we can at best only draw conclusions based on qualitative comparisons.

Given the high degree of uncertainty in the magnitude of all the parameters used in the model, it is important to check to see that the model output is close to what is seen in nature. We have compared model output to the few data available to ensure that the model results are reasonable.

The magnitude of DMS seawater concentrations from the model are reasonable when compared to field measurements. DMS concentrations from 1 to 10-m depth in the model are within the range of approximately 0.2 to 40 nM DMS generally found in surface seawater [*Bates et al.*, 1994]. Higher concentrations, up to 60 nM, are seen at approximately 20-m depth in the model. High concentrations have also been reported in field data. *Bates et al.* [1992] measured a maximum of 90 nM DMS at 5-m depth in the North Pacific. In Antarctic waters, *Gibson et al.* [1990] detected 300 nM at approximately 30-m depth.

The changes in DMS seawater concentrations with depth resulting from the model runs are well within the variations that exist in nature. Model results show the DMS maximum most often at about 20 m depth, generally between 20 to 40 nM, gradually decreasing to about 1 nM at around 50 meters. However, DMS maxima do appear between 0 and 40 m depths in the model run results. In nature, the vertical distribution of DMS in seawater typically displays a maximum at, or a few meters below, the sea surface, and a sharp decrease in DMS concentration near the level of 1% light transmission [*Andreae*, 1990]. *Nguyen et al.* [1978] were the first researchers

to report DMS water column profiles. They found one profile with a maximum at 10 m, another profile showed a maximum at 30-32 m depth and a third showed a continual decrease in DMS with depth, from 0 to 130 m. They concluded from the data that the depth of the DMS maximum could vary, which could explain the existence of sometimes very high surface DMS concentrations. Vertical distributions of DMS concentrations measured at high latitudes are also in general agreement with the DMS model results. In July, east of Orkney (58°58'N, 02°00'W) *Turner et al.* [1988] measured a DMS maximum of 14 nM at 10 m depth which gradually decreased to about 1 nM at 40 m depth. In May, Bering Sea shelf waters had DMS maxima from 1.5 to 6.5 nM, generally between 2 and 5 meters below the surface *Barnard et al.* [1984]. DMS levels remained constant down to 30-50 m depth.

Sensitivity Analysis

The sensitivity analysis revealed that DMS sea-to-air flux was most sensitive to flagellate production of DMS, microbial degradation, zooplankton grazing and photo-oxidation of DMS. These parameters are thus potentially important to the DMS seawater concentrations which drive DMS sea-to-air flux. Figure 4.4 displays the results of the sensitivity analysis.

The two parameters that are least well-quantified and most important to flux are flagellate production of DMS and microbial degradation. Changing the flagellate production of DMS affected the model results more than changing any of the other parameters. Varying flagellate production of DMS, estimated to be 5 x 10^{-3} mol DMS L^{-1} (cell vol) d^{-1}, by a factor of two resulted in changes of similar magnitude in the cumulative DMS sea-to-air flux. The uncertainty in this parameter ranges from 0 to 22 x 10^{-3} mol DMS L^{-1} (cell vol) d^{-1}.

The sensitivity analysis showed about a 15% change in cumulative DMS sea-to-air flux with a factor of two change in the microbial degradation base value of 0.1 nM d^{-1}. When we ran the model for a biological degradation value of 1 nM d^{-1}, which is

within the observed range of 0.1 to 55 nM d^{-1}, cumulative flux went from 1020 to 320 μmol m^{-2} yr^{-1}. If microbial degradation is much greater than 1 nM d^{-1}, the model would predict no DMS efflux (and near-zero DMS concentrations). Since a significant flux of DMS does exist in nature, microbial degradation cannot be this high in the DMS model. It is clear that microbial degradation is a very important parameter controlling DMS seawater concentrations and that more measurements are needed.

When photo-oxidation of DMS was changed by a factor of two in the sensitivity analysis, cumulative DMS sea-to-air flux changed by about 30%. This indicates that photo-oxidation is an important loss mechanism for DMS in the oceans, and hence important to DMS sea-to-air flux. There is some uncertainty associated with *Brimblecombe and Shooter's* [1986] photo-oxidation loss rate of DMS used in our model. Furthermore, it is the only photo-oxidation rate available. *Brimblecombe and Shooter* [1986] mention that they do not know if the rate they measured is at all typical and that the lack of information on the wavelength dependence makes it difficult to determine how far into surface waters photochemical activity will penetrate.

When zooplankton grazing on DMS was changed by a factor of two in the sensitivity analysis, cumulative DMS sea-to-air flux changed by about 20%. This indicates that zooplankton grazing also significantly affects DMS efflux from the ocean, although probably not as much as microbial degradation or flagellate production.

Changing diatom production of DMS or eddy diffusivity by a factor of two resulted in only small changes in the model results. Therefore, we conclude that diatom production of DMS is not an important production mechanism for DMS release in this model and that a change in the eddy diffusivity, even by an order of magnitude, would not significantly affect flux of DMS in the model.

Seasonal Variability

From the beginning of the year until early March, the waters of the Gulf of

Alaska and PWS are generally well mixed, and phytoplankton biomass is at a relatively low level. During this period, nutrients are high because primary productivity is low. With the onset of spring, the phytoplankton biomass increases rapidly in the nutrient rich waters. This bloom results in an increase of DMS seawater concentration.

Figure 4.5 shows monthly average DMS model sea-to-air flux results from early March until year's end, for the site near Middleton Island - 1995, the C-Lab buoy - 1993 and 1996, and Mid-sound buoy - 1996. The most notable feature in Figure 4.5 is the bimodal nature of the sea-to-air flux. A relatively long period of high flux in the spring and a period of high flux in autumn is separated by several months of low summer flux.

As the year progresses to summer, sea surface temperatures rise and the ocean waters become stably stratified, isolating water (and DMS) at depths from the surface. In these stratified waters, nutrients are not readily replenished and therefore become depleted as the bloom uses the nutrients. Time series of actual seawater temperature profiles are available for the C-Lab buoy in 1993 and 1996 and are displayed in Figure 4.6. Since salinity variations with depth here are small, density is primarily a function of temperature and so the temperature profiles reliably indicate the mixed layer depth. A stably stratified surface layer sets up in the summer months only, followed by a breakdown of stratification in the fall.

Model results showing daily average DMS sea-to-air flux are shown in Figure 4.7. In this figure, the excursions in flux during the summer months (June, July and August) are indicated by an asterisk. These excursions correlate with high wind events, which for a short time deepen the mixed layer, bringing the higher DMS seawater concentrations at depth to the surface. The correlations of high DMS sea-to-air flux with high wind events can be seen by comparison with the time series of the actual wind speeds for the site near Middleton Island - 1995, the C-Lab buoy - 1993 and 1996, and Mid-sound buoy - 1996, shown in Figure 4.8. In this figure, the three or

four highest wind speed occurrences during the summer months (June through August - day 153 to 245 of the year) are indicated by asterisks.

High winds are often associated with extreme weather conditions not conducive to sampling. Lack of measurements during these periods may lead to a bias in regional DMS sea-to-air flux estimates. The correlations between high wind events and excursions in DMS sea-to-air flux seen in the DMS model results need to be considered when designing field experiments.

High DMS sea-to-air flux is maintained by high DMS concentrations in the water column. In turn, what maintains high DMS concentrations in the water column are: 1) high concentrations of phytoplankton that produce DMS (i.e. high primary productivity), 2) frequent mixing of nutrients into the surface layer from below and 3) large zooplankton populations. To better illustrate the interplay of DMS mixing and sea-to-air flux, phytoplankton population and DMS production, and zooplankton grazing, we have plotted the seawater profiles of DMS, flagellates and zooplankton in 10-day increments for each of the four model runs. Figure 4.9, Figure 4.10 and Figure 4.11 show these plots for the C-Lab - 1993 model run. The same series of plots for the other three model runs can be found in the Appendix. Comparison of these profiles from the C-Lab buoy - 1993 model run with the time series of DMS sea-to-air flux, wind speed and seawater temperature profiles provides insight into how the parameters in the model affect DMS seawater concentrations and flux. For example, large excursions in DMS sea-to-air flux during the summertime, which correlate with high wind speed events, are a result of increased wind-driven mixing. Increased mixing to about 10 m depth is evident in the day 150-160 and day 220-230 time intervals in Figure 4.9. The two largest excursions in the summer DMS sea-to-air flux and the highest wind speed events occur during these two intervals.

Looking at yet greater detail, the model provides some interesting results. Notice the excursion in summertime DMS sea-to-air flux at about day 185 in the C-Lab

- 1993 model run shown in Figure 4.7. This excursion correlates with a high wind event on that day, shown in Figure 4.8. Although another high wind event of similar magnitude follows within days, no corresponding excursion in DMS sea-to-air flux can be seen. This is likely due to most of the DMS being vented during the previous high wind event of day 185 and the stratification preventing DMS from being replenished to the surface waters. The short time period between these two wind events does not allow enough time for phytoplankton to regenerate DMS in the upper water column. High wind events are therefore necessary, but not sufficient, to produce an excursion in summer DMS sea-to-air flux.

At the latitudes of the Gulf of Alaska and PWS, the end of August generally marks the time of decreasing sea surface temperatures and increasing wind speeds. Both factors typically lead to a deepening of the mixed-layer depth, the former through thermal destabilization and the latter by mechanical mixing. This enhanced mixing redistributes the DMS vertically, bringing DMS from below to the surface, increasing the amount of DMS available to exchange with the atmosphere. The enhanced mixing also brings nutrients from below to the surface, which results in a secondary bloom, increasing DMS seawater concentrations through increased biological production.

We measured high DMS mixing ratios in marine boundary layer air above the Bering and Chukchi Seas during September and October of 1995 [Chapter 3 of this thesis]. These observations, concurrent with autumnal thermal destabilization of the water column, led us to hypothesize that ocean mixed layer dynamics strongly influence DMS sea-to-air flux. Part of the impetus for developing the DMS model is to test this hypothesis.

Average monthly DMS sea-to-air flux was highest in October for the C-Lab - 1993 model run, as shown in Figure 4.5. Between days 260 and 270, shown in Figure 4.9, high surface concentrations of DMS develop as a result of increased primary productivity shown in Figure 4.10, and the onset of seasonal mixing shown in Figure

4.6. High DMS surface concentrations and flux persist for another 20 days as shown in Figure 4.7 and Figure 4.9, getting a boost from increased primary productivity and continued mixing. The bloom is clearly seen in Figure 4.10. High DMS flux is linked to high surface DMS concentrations that depend on both mixing and primary production.

For the other two buoy model runs the largest monthly average DMS sea-to-air flux also occurs in October. For the C-Lab buoy - 1996 model run, the high October flux coincides with autumnal breakdown in ocean stratification, which can be seen in the seawater temperature profile of Figure 4.6, starting at about day 270. A seawater temperature profile is not available for the Mid-sound Buoy - 1996 model run. However, sustained, very deep mixing at about day 280 is evident in the DMS and flagellate profiles shown in Figure 4.12 and Figure 4.13 for the mid-sound. Very deep mixing is also evident for the C-Lab Buoy - 1996 model run in Figure 4.12, Figure 4.13, and Figure 4.14, but the DMS concentrations and primary productivity are considerably less. The low DMS concentrations and primary productivity may explain the spatial variability in the magnitude of autumnal DMS sea-to-air flux from the 1996 sites. High DMS concentrations resulting from high primary productivity, as well as deep mixing, contribute to the high DMS sea-to-air flux. Relatively high flux coinciding with the breakdown in density stratification implicates ocean mixed layer dynamics as playing a key role in DMS sea-to-air flux late in the year.

Most of the measurements of DMS in marine boundary layer air and DMS sea-to-air flux have been made in the spring and summer. The DMS model results clearly show that at high latitudes a significant DMS sea-to-air flux is likely to occur in the fall, as well as in the spring. For accurate annual (or seasonal) estimates of regional DMS sea-to-air emissions from high latitude regions, fall measurements are necessary.

Annual flux. Figure 4.15 shows cumulative DMS sea-to-air flux model results from early March through December. For the three buoy model runs, the cumulative

flux in the second half of the year is greater than that in the first half of the year. That is, assuming daily DMS sea-to-air flux for January and February is close to zero, the cumulative flux for the second half of the year ranges from a factor of 1.2 to 2 times higher than that for the first half of the year. The Middleton Island - 1995 site model run is different from the other buoy model runs. For the Middleton Island - 1995 model run, the largest monthly DMS sea-to-air flux occurs in April and the DMS sea-to-air flux for the first half of the year is two times greater than the DMS sea-to-air flux for the second half of the year. The reason for the disparity in the results for the Middleton Island - 1995 model run could be the difference in meteorology early in the year. The spring of 1995 was cold and stormy, leading to a well-mixed ocean surface layer, more primary productivity and a long phytoplankton bloom. In contrast, the springs of 1993 and 1996 were warm and calm with intense phytoplankton blooms. This difference in meteorology early in the year, and the resulting character of the phytoplankton bloom, may explain the difference in timing and seasonality of the dominant DMS sea-to-air flux.

Conclusions

The DMS model results are well within the variations of DMS seawater concentrations and DMS seawater profiles found in natural systems. While this indicates that the model may be a reasonable representation of processes governing DMS concentrations and fluxes in the ocean, the model contains many adjustable parameters that are poorly constrained by the available data.

Field studies described in the literature are just beginning to uncover the complexity of DMS ocean cycling. Our sensitivity analysis revealed that flagellate production of DMS and microbial degradation are probably important processes in controlling seawater DMS concentrations and ultimately DMS sea-to-air flux. Zooplankton grazing and photo-oxidation are also significant, but to a lesser degree.

The importance of these parameters in the oceanic DMS cycle calls for more research.

One difficulty in this modeling study was in setting ranges for the parameters. Unfortunately, all the DMS production and loss rates used in the DMS model have large uncertainties. Furthermore, field data on these parameters from northern high latitudes are virtually nonexistent, which introduces even more uncertainty. Measurements of DMS production and loss rates in northern latitude oceans need to be made.

Another reason for the difficulty in setting ranges for some of the parameters, besides the lack of measurements, was the use of different measurement units by experimenters. For example, it would have been useful to have a well-defined conversion from cellular concentrations of DMSP to daily metabolic release of DMS, since there is extensive data on cellular concentrations of DMSP for numerous species within the 12 phytoplankton classes. It is recommended that experimenters could pay more attention on how they report data by considering how the data might be used.

Despite the large uncertainties associated with the parameters in the DMS model, we can still use the model to investigate this under-sampled system in qualitative terms. Information can be gleaned from trends and relative differences seen in the model results.

At northern high latitudes, there appears to be a significant DMS sea-to-air flux in the fall as well as in the spring. This flux is likely the result of the water column mixing caused by high wind events and thermal destabilization of the water column. The mixing reinvigorates the biological production by bringing nutrients from below to the surface, and also transports existing DMS from deeper water, thus replenishing the DMS in surface waters and increasing the amount of DMS ventilated to the atmosphere. However, deep mixing alone is not enough to sustain the flux. High surface DMS concentrations, maintained by high primary productivity and nutrient levels, are also necessary.

Summer pulses in DMS sea-to-air flux correspond to high wind events which result in increased mixing. High wind events alone are not sufficient to result in a high DMS sea-to-air flux. High surface concentrations of DMS are also needed.

Periods of ocean mixing (i.e. storms, high winds, breakdown of stratification late in the summer season) are often overlooked, inadvertently or out of necessity, in field campaigns. Ocean mixed layer dynamics can cause the high DMS sea-to-air flux observed late in the year at northern latitudes and sudden high excursions in DMS sea-to-air flux at any time of the year. Field measurement campaigns and estimates of the contribution of northern latitude oceans to the global sulfur budget need to include measurements during these mixing events to obtain unbiased DMS sea-to-air flux estimates. This means that extrapolation (spatial and temporal) of a few measurements during a limited field season to longer periods has enormous uncertainties. Furthermore, parameterizations used to estimate emissions of such a highly variable gas as dimethyl sulfide must include ocean mixed-layer dynamics.

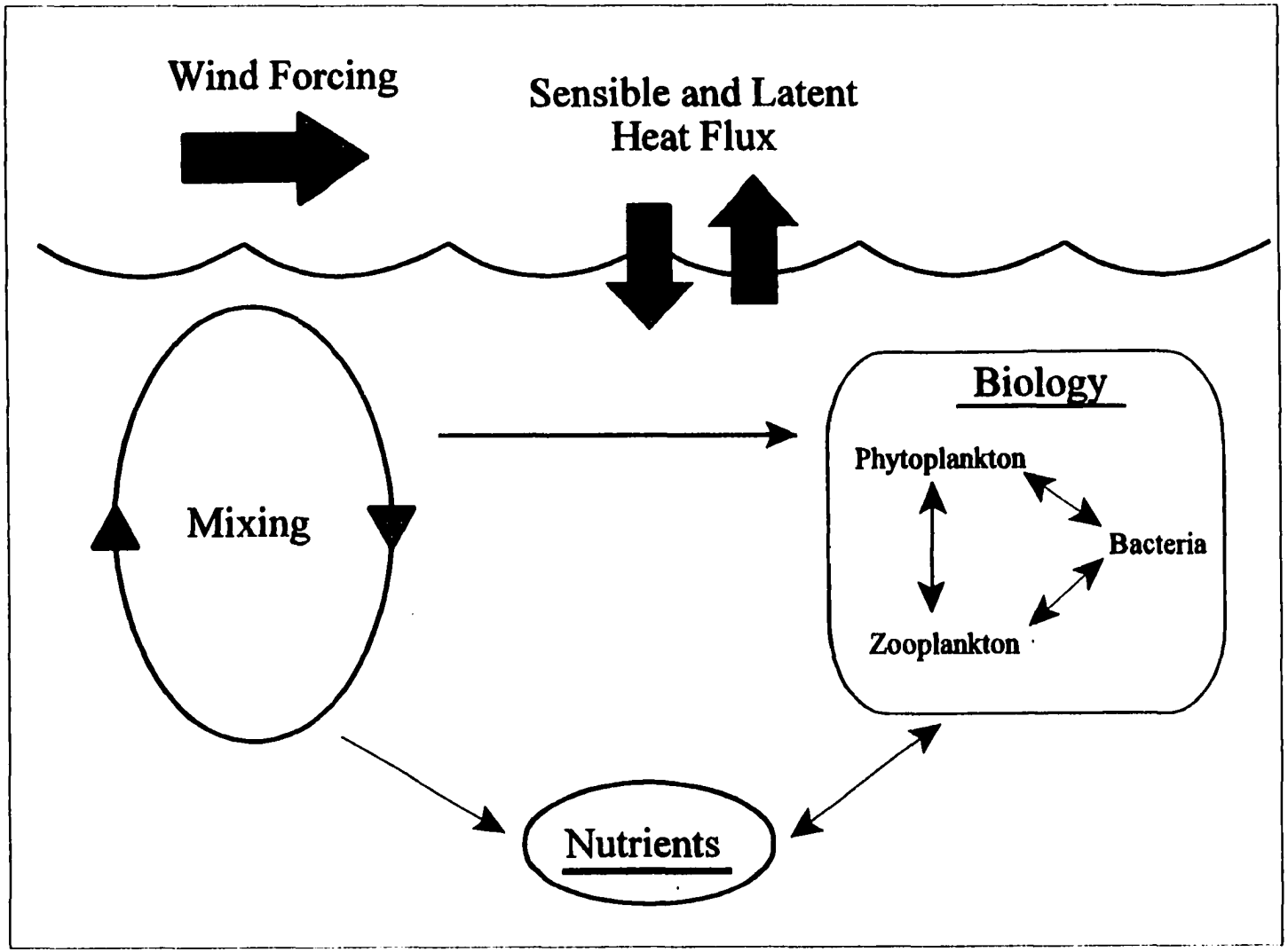

Figure 4.1 - Physical processes included in the original model by Eslinger [*Eslinger, in preparation*].

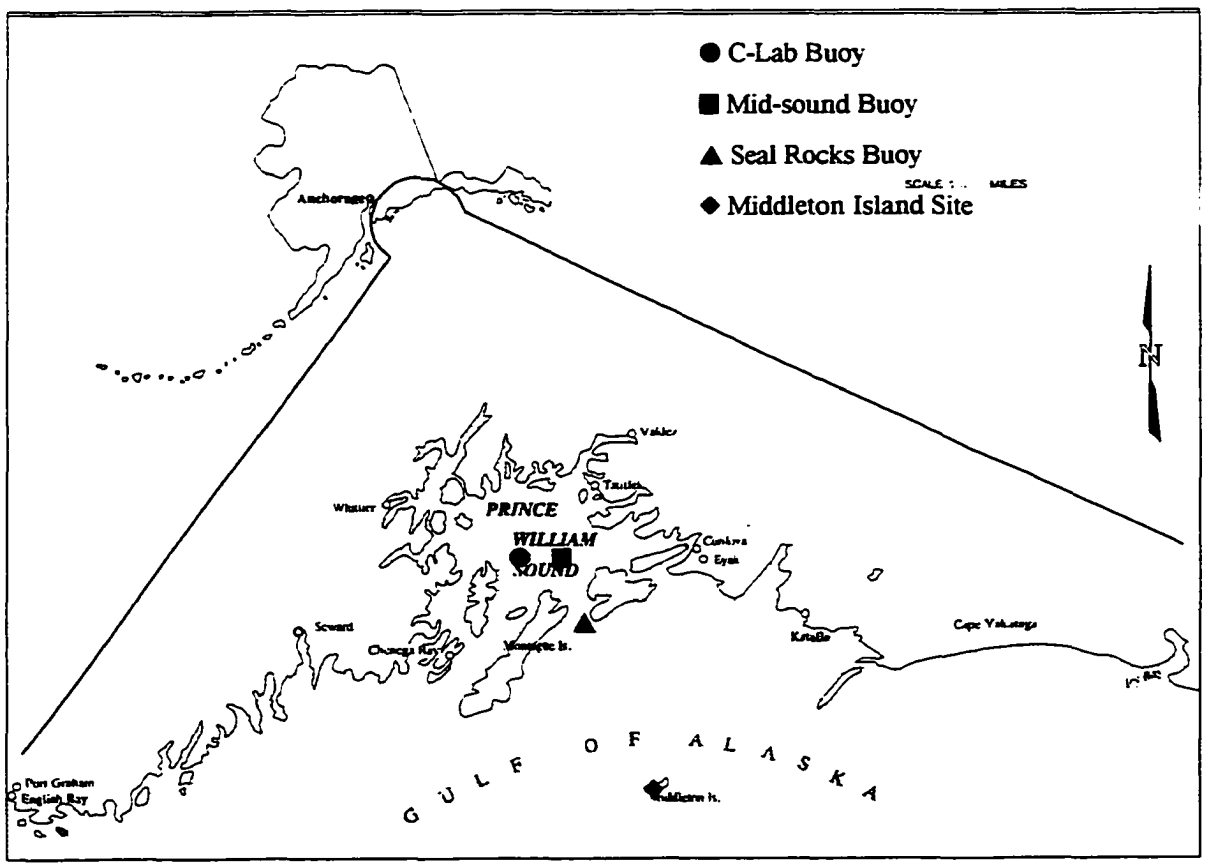

Figure 4.2 - Location of buoys and Middleton Island site.

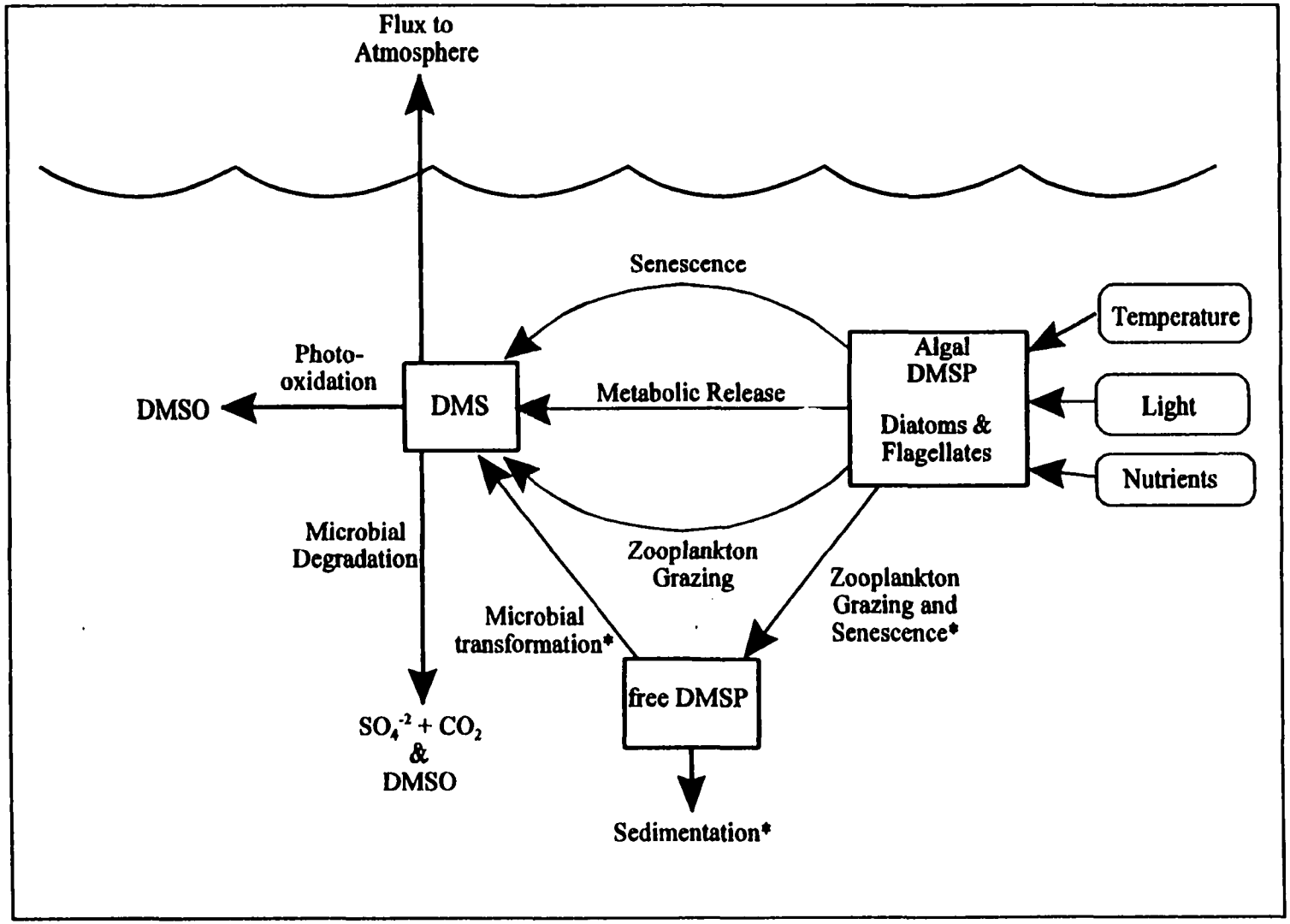

Figure 4.3 - Processes involved in cycling DMS in ocean water. The asterisk (*) designates process not included in DMS model.

Table 4.1: Model Parameters for a 100-m Mixed Layer. For references see the text.

Parameter	Value	Range	Units
DMS Loss			
DMS → atmosphere	k $[DMS]_{seawater}$		μmol $m^{-2} d^{-1}$
DMS → DMSO (photo-oxidation)	9.0×10^{-2}		hr^{-1}
DMS particle adsorption → deep sea	10 *		ng S $m^{-2} d^{-1}$
Microbial degradation	0.1	0.1 - 55	nM d^{-1}
(Consumption - DMS → $SO_4^{-2} + CO_2$)			
(Oxidation - DMS → DMSO)			
DMS Production			
Algal DMSP → DMS			
(flagellates - metabolic release)	5×10^{-3}	$0 - 22 \times 10^{-3}$	mol DMS L^{-1} (cell vol) d^{-1}
(diatoms - metabolic release)	0.3×10^{-3}	$0 - 1.3 \times 10^{-3}$	mol DMS L^{-1} (cell vol) d^{-1}
(flagellate senescence)	2.1×10^{-3}	$0.6 \times 10^{-3} - 22 \times 10^{-3}$	mol DMS L^{-1} (cell vol) d^{-1}
(diatom senescence)	130×10^{-3}	$10 \times 10^{-3} - 360 \times 10^{-3}$	mol DMS L^{-1} (cell vol) d^{-1}
(zooplankton grazing - flagellates)	170×10^{-3}	$15 \times 10^{-3} - 500 \times 10^{-3}$	mol DMS L^{-1} (cell vol)
(zooplankton grazing - diatoms)	10×10^{-3}	$0.6 \times 10^{-3} - 30 \times 10^{-3}$	mol DMS L^{-1} (cell vol)
Other			
DMS Molecular Diffusivity	6.46×10^{-6}		$m^2 hr^{-1}$
Eddy Diffusivity	4.71×10^{-2}		$m^2 hr^{-1}$

k = transfer velocity; calculated as a function of wind speed [*Liss & Merlivat*, 1986]

* This value represents 0.001 Tg(S) to the deep sea each year, which is negligible compared to loss to the atmosphere which is about 17-30 Tg(S) $year^{-1}$ [*Shooter & Brimblecombe*, 1989], therefore we have not included this parameter in the model.

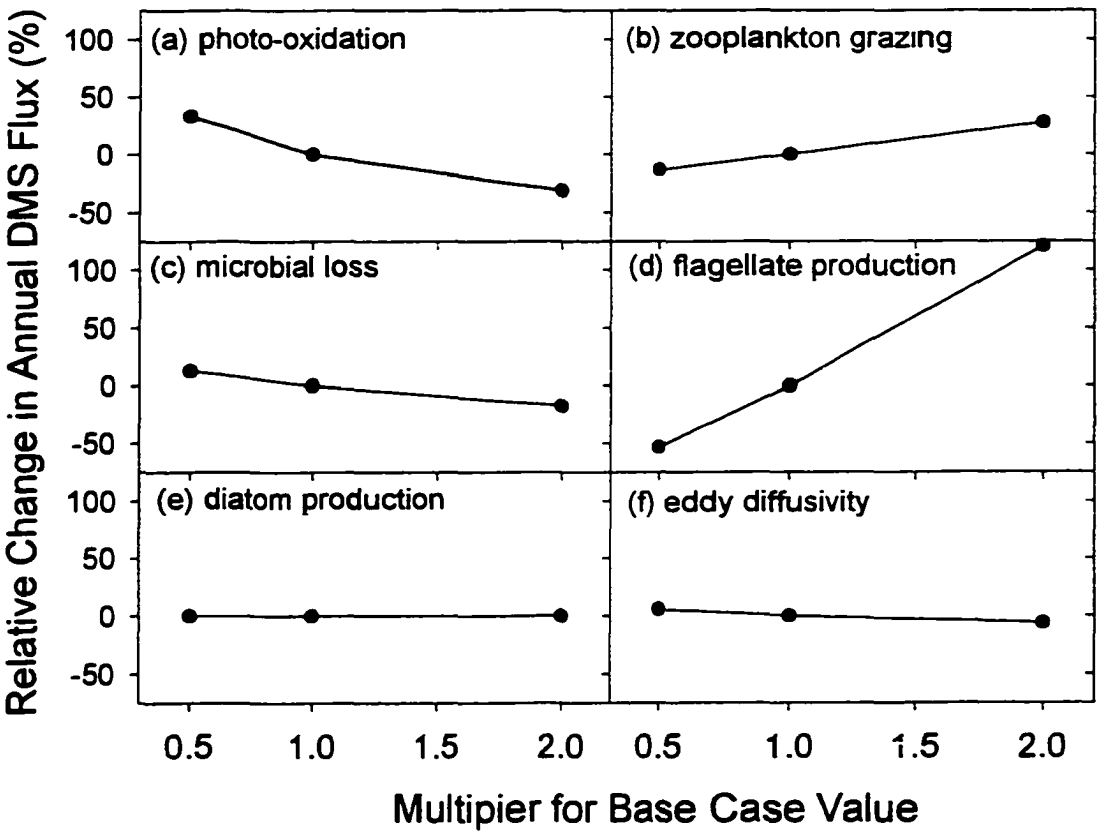

Figure 4.4 - Sensitivity analysis results showing relative change (%) in annual DMS flux when changing, by a factor of 0.5 and 2.0, the base value for (a) photo-oxidation, (b) zooplankton grazing, (c) microbial loss, (d) flagellate production of DMS, (e) diatom production of DMS, and (f) eddy diffusivity.

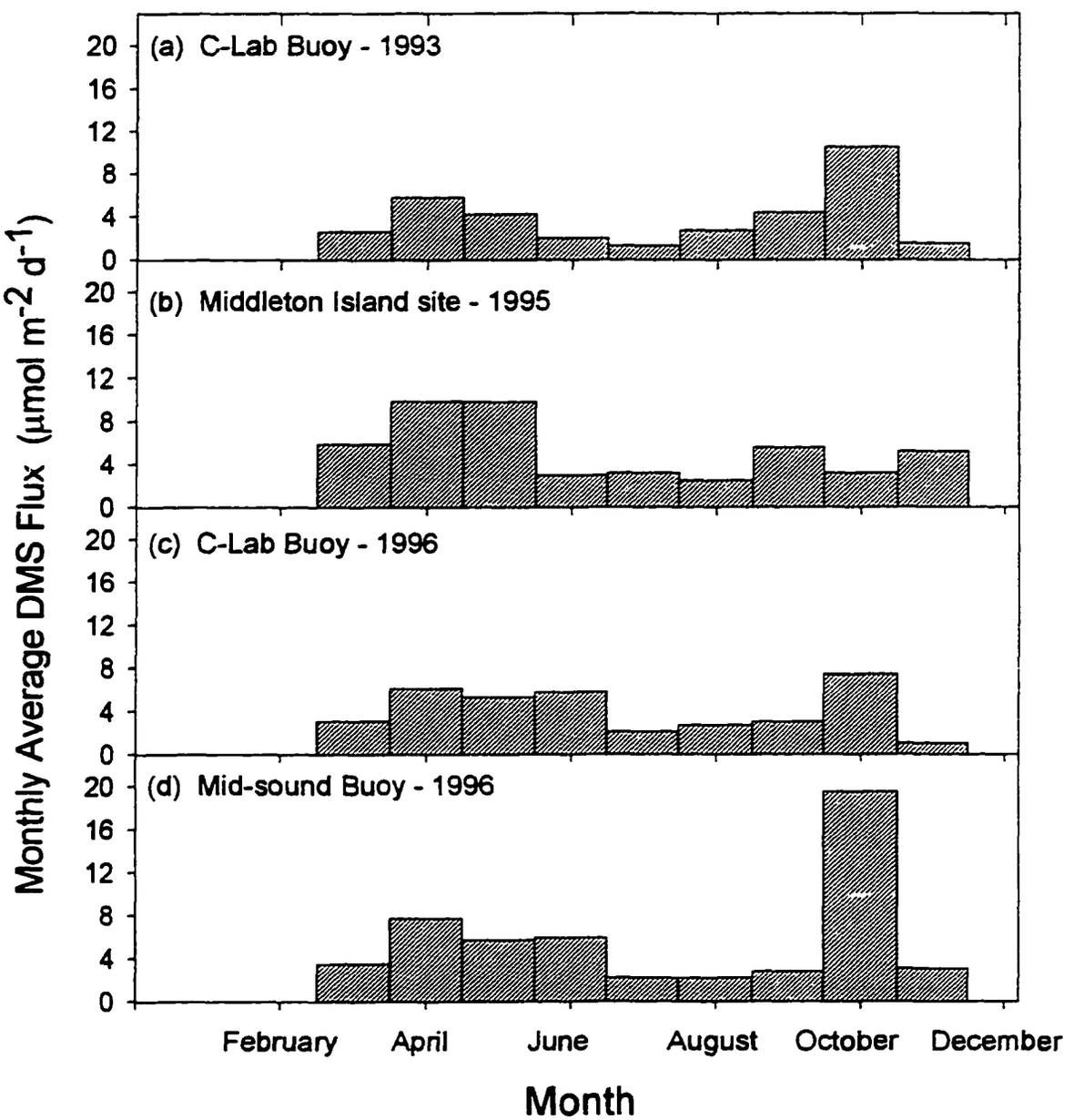

Figure 4.5 - Model results showing average monthly DMS flux for (a) C-Lab Buoy - 1993, (b) Middleton Island site - 1995, (c) C-Lab Buoy - 1996, and (d) Mid-sound Buoy - 1996.

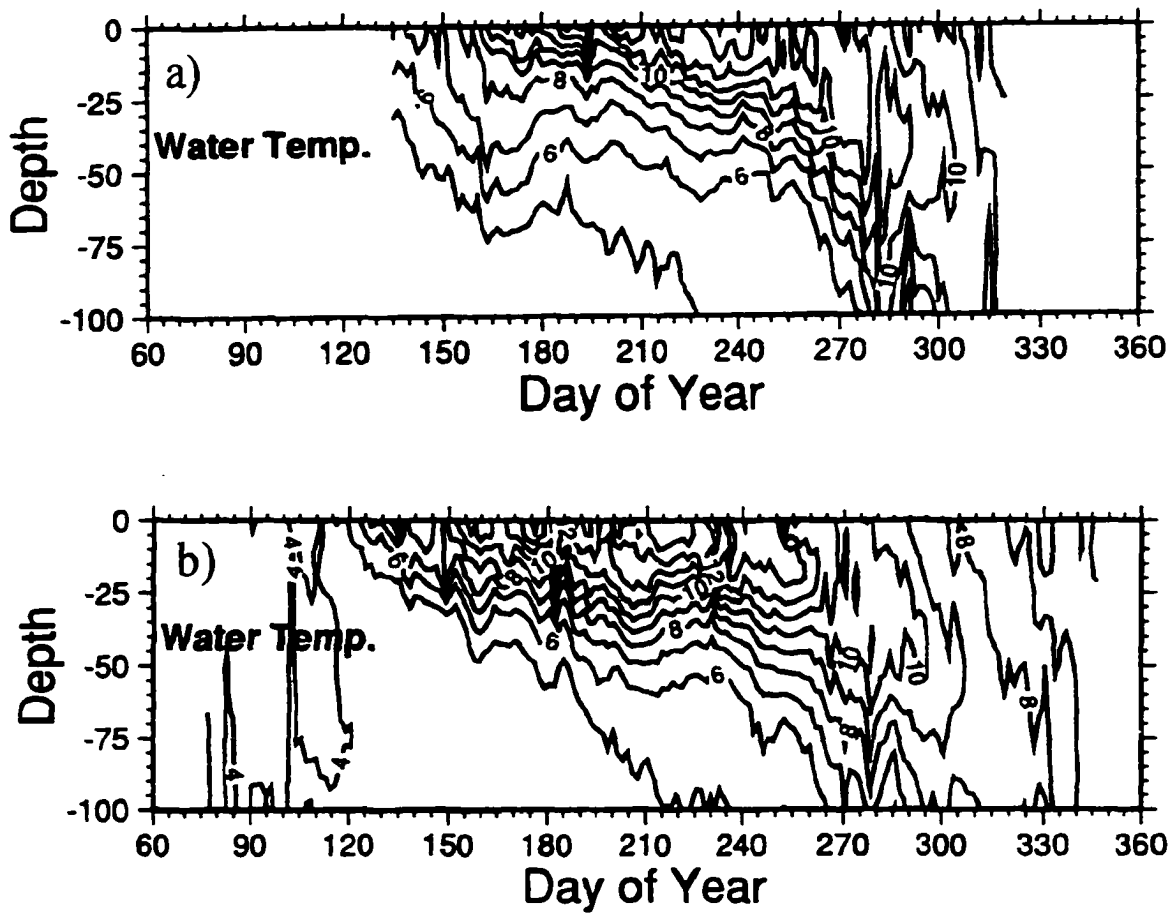

Figure 4.6 - Time series of seawater temperature profiles from C-Lab Buoy (a) 1993, and (b) 1996. Depths are in meters.

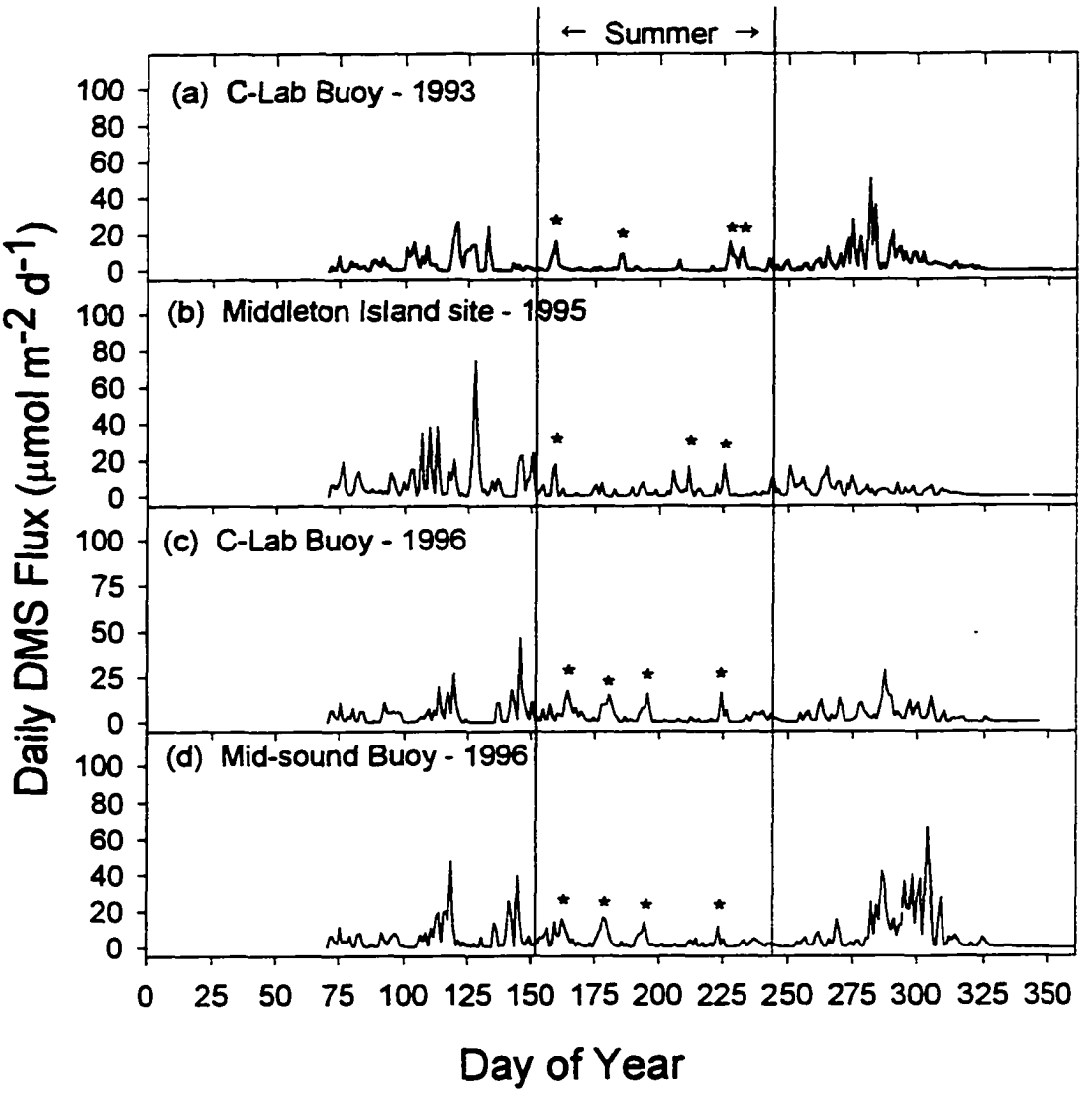

Figure 4.7 - Model result showing daily DMS flux for (a) C-Lab Buoy - 1993, (b) Middleton Island site - 1995, (c) C-Lab Buoy - 1996, and (d) Mid-sound Buoy - 1996. The asterisks (*) indicate wind events discussed in the text.

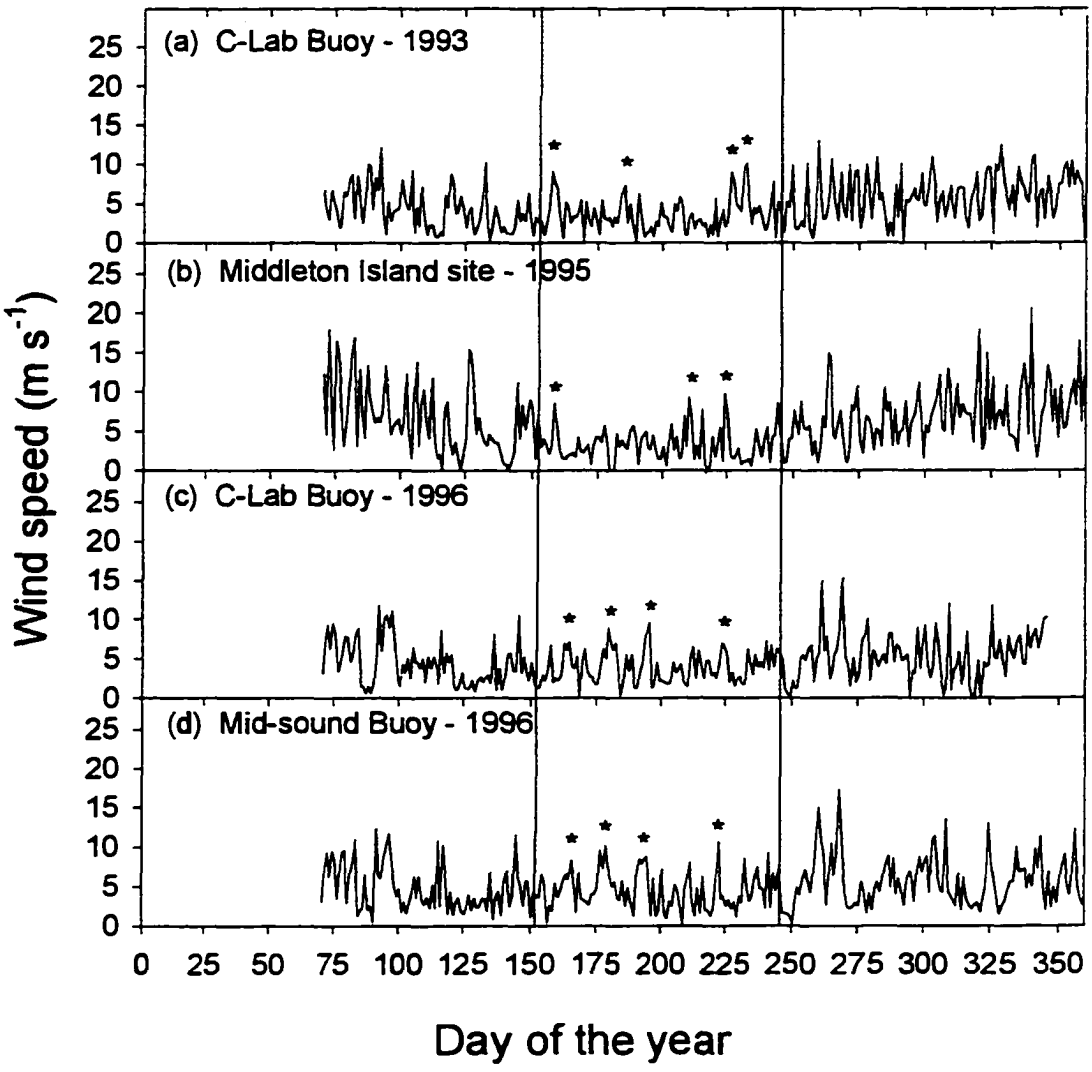

Figure 4.8 - Time series of actual wind speeds from (a) C-Lab Buoy - 1993, (b) Middleton Island site - 1995, (c) C-Lab Buoy - 1996, and (d) Mid-sound Buoy - 1996. The asterisks (*) indicate wind events discussed in text.

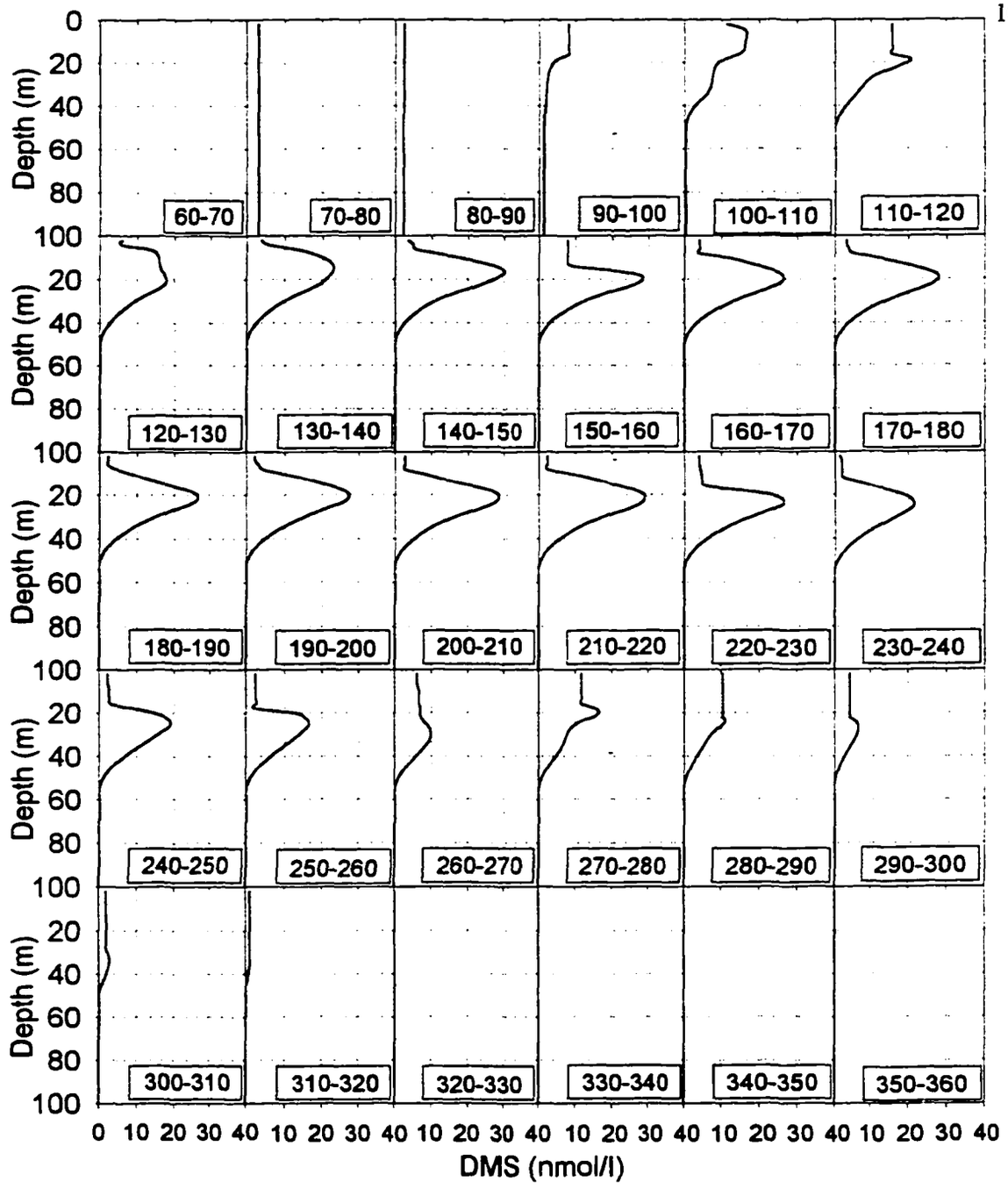

Figure 4.9 - Seawater profiles of DMS from the C-Lab Buoy - 1993 model run.

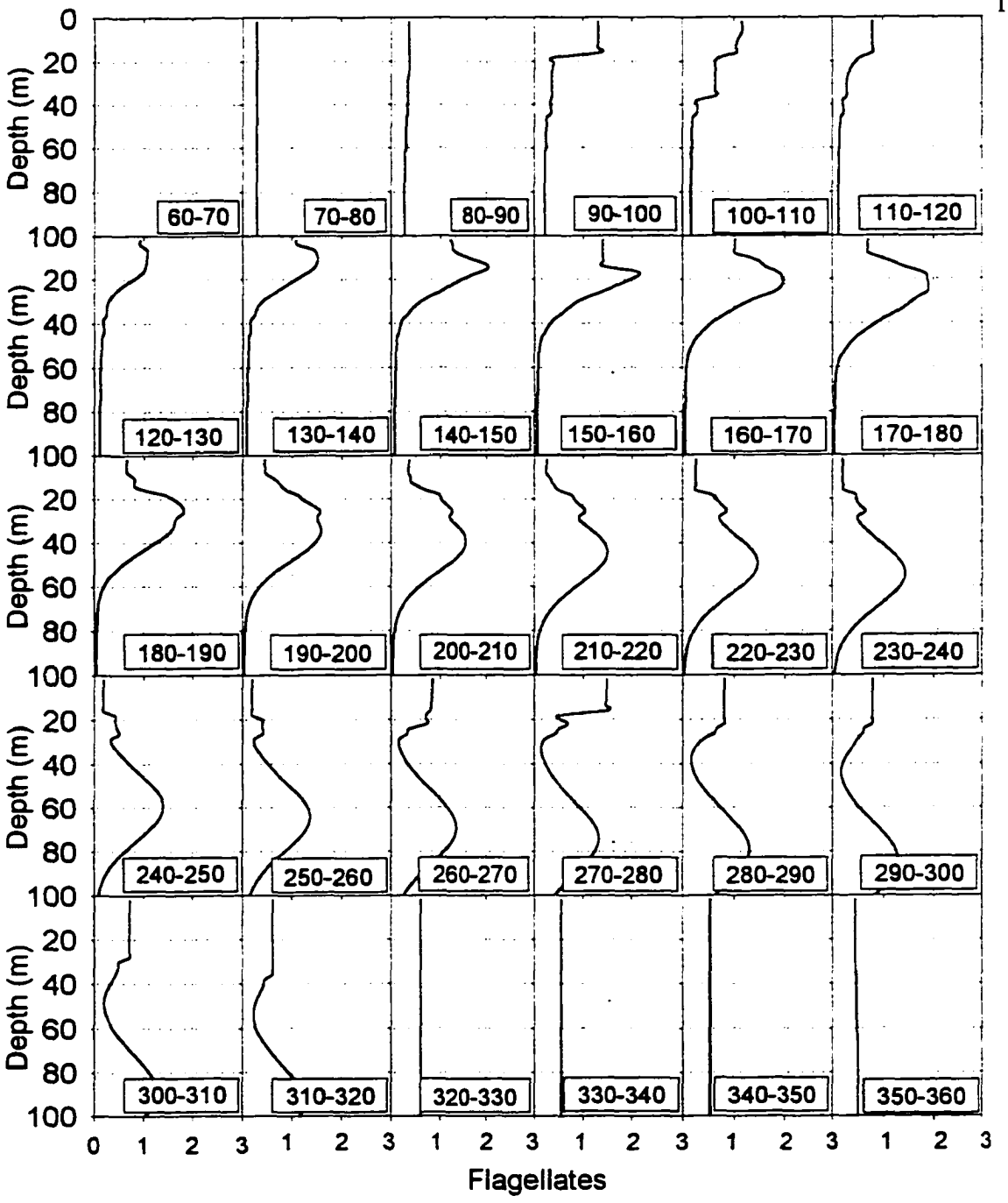

Figure 4.10 - Seawater profiles of flagellated phytoplankton from the C-Lab Buoy - 1993 model run.

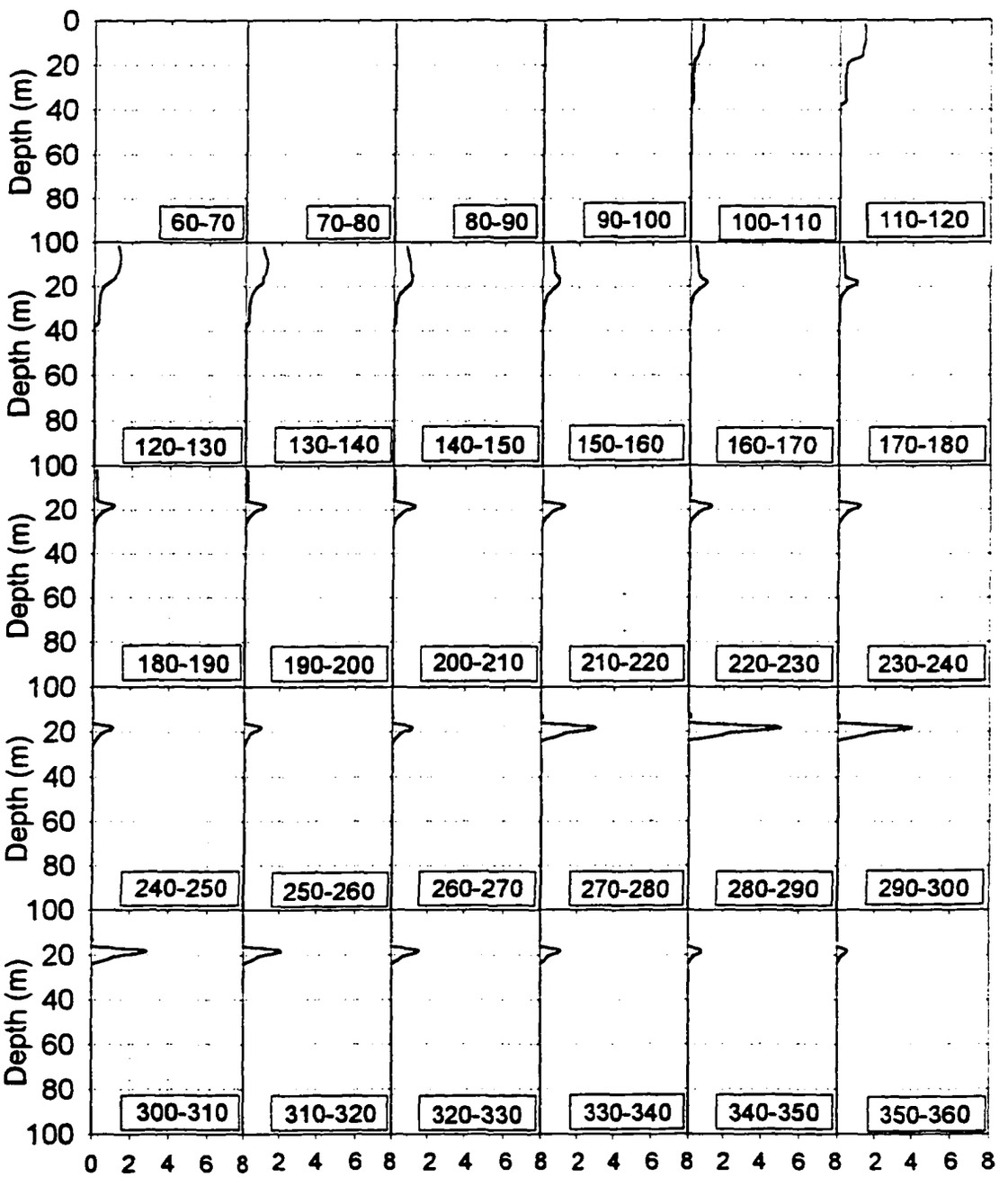

Figure 4.11 - Seawater profiles of pseudocalanus zooplankton from the C-Lab Buoy - 1993 model run.

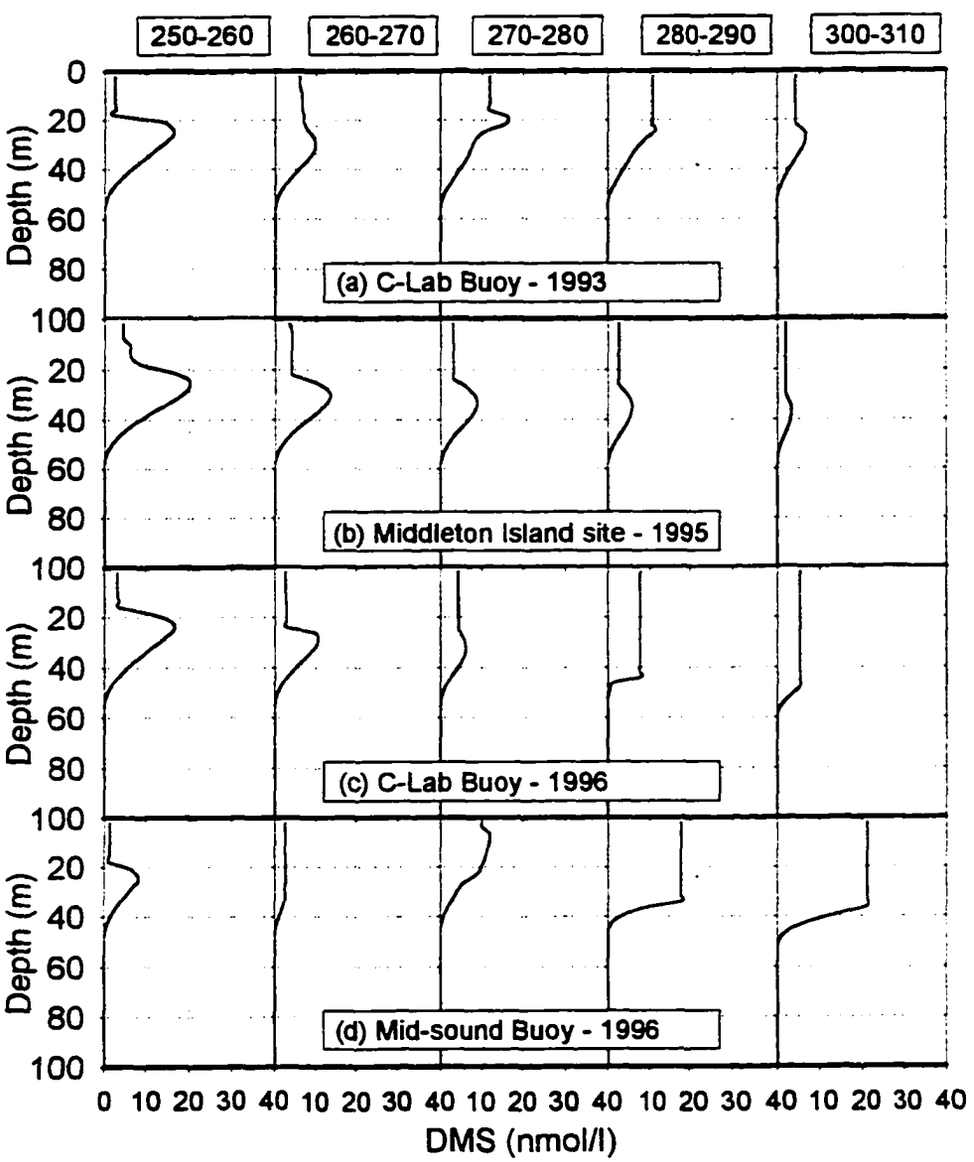

Figure 4.12 - Model results showing DMS seawater profiles between day 250 and 310 (September 7 through November 4) for the (a) C-Lab Buoy - 1993, (b) Middleton Island site -1995, (c) C-Lab Buoy - 1996 and (d) Mid-sound Buoy - 1996 model runs.

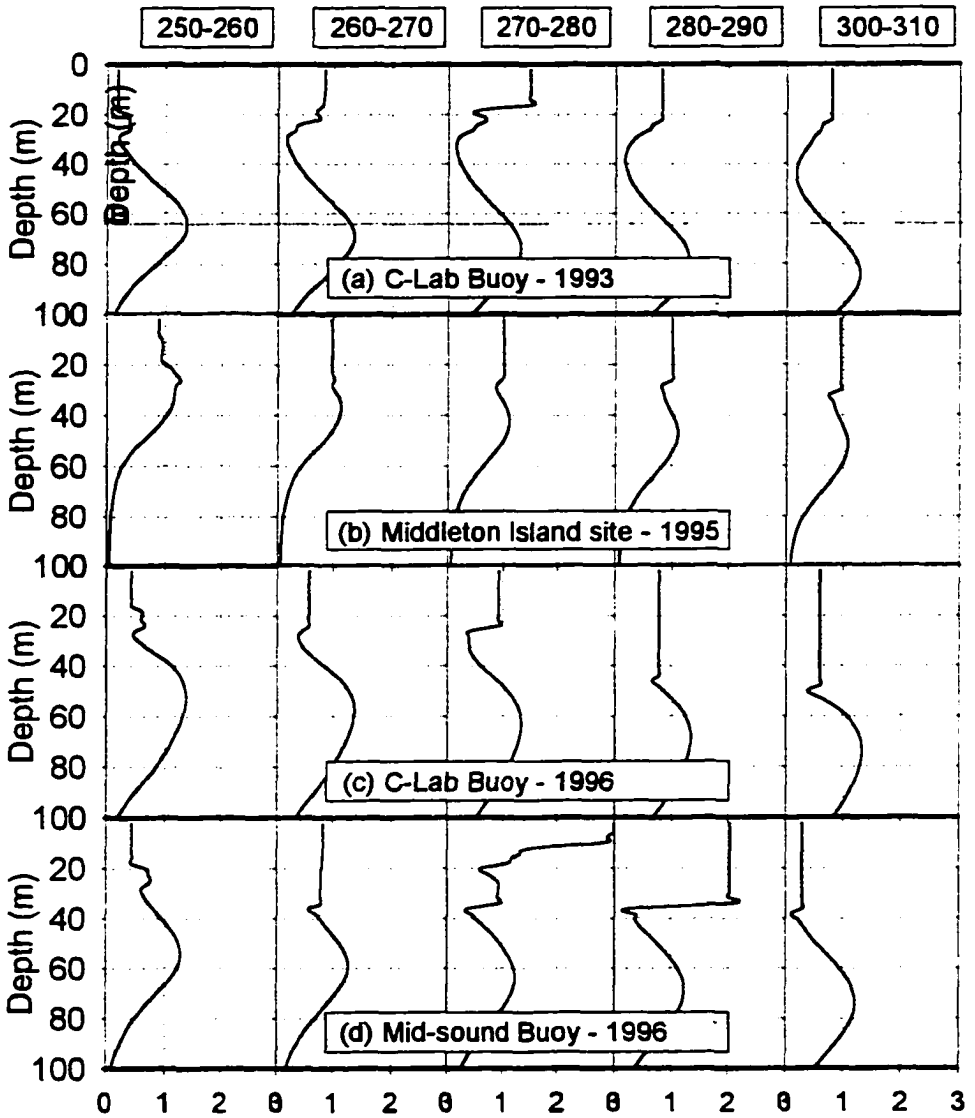

Figure 4.13 - Model results showing flagellate seawater profiles between day 250 and 310 (September 7 through November 4) for the (a) C-Lab Buoy - 1993, (b) Middleton Island site -1995, (c) C-Lab Buoy - 1996 and (d) Mid-sound Buoy - 1996 model runs.

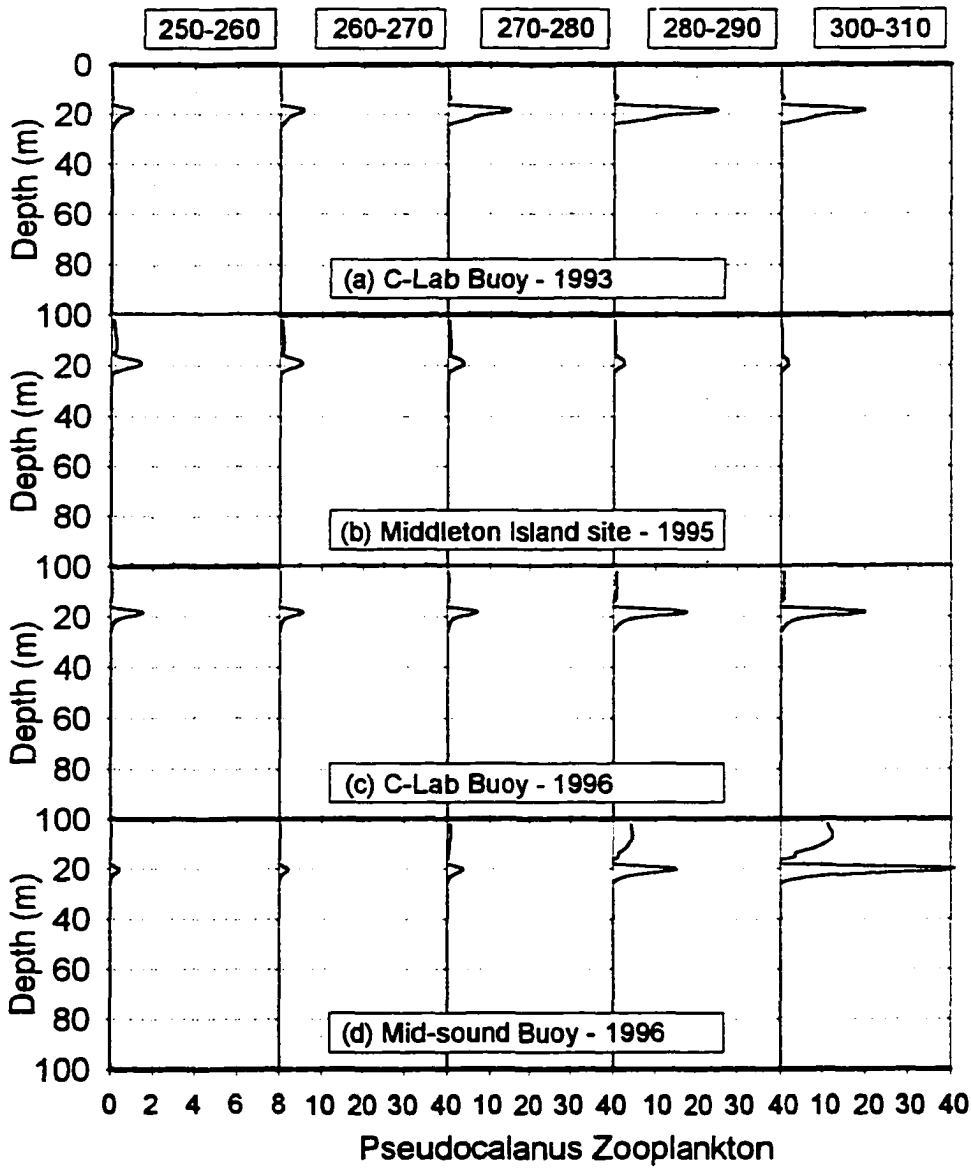

Figure 4.14 - Model results showing pseudocalanus zooplankton seawater profiles between day 250 and 310 (September 7 through November 4) for the (a) C-Lab Buoy - 1993, (b) Middleton Island site -1995, (c) C-Lab Buoy - 1996 and (d) Mid-sound Buoy - 1996 model runs.

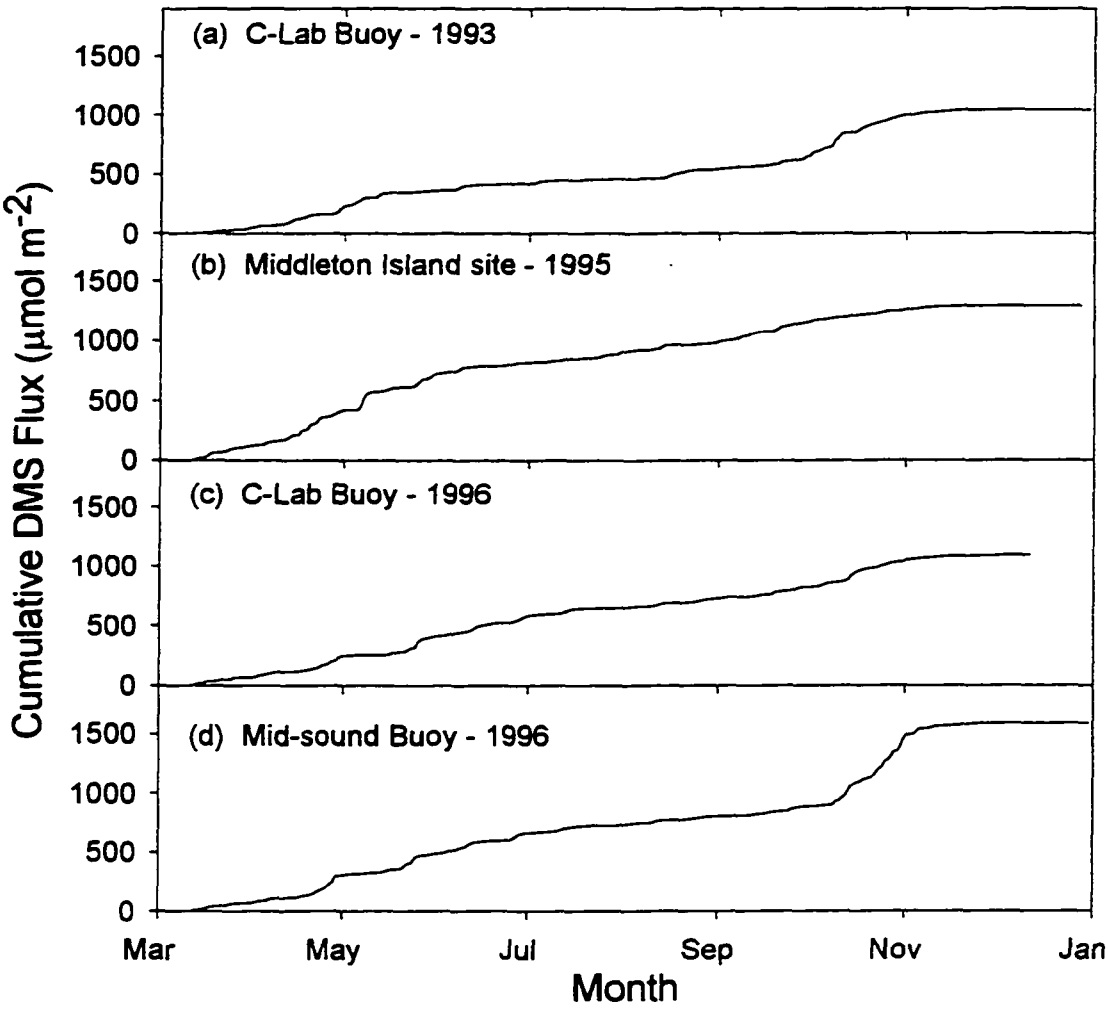

Figure 4.15 - Model results showing cumulative DMS flux for (a) C-Lab Buoy - 1993, (b) Middleton Island site - 1995, (c) C-Lab Buoy - 1996, and (d) Mid-sound Buoy - 1996.

References

Andreae, M. O., The ocean as a source of atmospheric sulfur compounds, in: The role of air-sea exchange in geochemical cycling, *edited by* Buat-Menard, pp 331-362, D. Reidel, Norwell, Mass., 1986.

Andreae, M. O., Ocean-atmosphere interactions in the global biogeochemical sulfur cycle, *Marine Chemistry, 30,* 1-29, 1990.

Andreae, M. O., R. J. Ferek, F. Bermond, K. P. Byrd, R. T. Engstron, S. Hardin, P. D. Houmere, F. LeMarrec, and H. Raemdonck, Dimethyl sulfide in the marine atmosphere, *Journal of Geophysical Research, 90,* (D7), 12,891-12,900, 1985.

Ayers, G. P., S. T. Bentley, J. P. Ivey, and B. W. Forgan, Dimethylsufide in marine air at Cape Grim, 41 degrees S, *Journal of Geophysical Research, 100,* (D10), 21,013-21,021, 1995.

Barnard, W. R., M. O. Andreae, and R. L. Iverson, Dimethylsulfide and *Phaeocystis poucheti* in the southeastern Bering Sea, *Continental Shelf Research, 3,* (2), 103-113, 1984.

Barnard, W. R., M. O. Andreae, W. E. Watkins, H. Bingemer, and H. W. Georgii, The flux of dimethylsulfide from the oceans to the atmosphere, *Journal of Geophysical Research, 87,* (C11), 8787-8793, 1982.

Bates, T. S., J. D. Cline, R. H. Gammon, and S. R. Kelly-Hansen, Regional and seasonal variations in the flux of oceanic dimethylsulfide to the atmosphere, *Journal of Geophysical Research, 92,* (C3), 2930-2938, 1987.

Bates, T. S., R. P. Kiene, G. V. Wolfe, P. A. Matrai, F. P. Chavez, K. R. Buck, B. W. Blomquist, and R. L. Cuhel, The cycling of sulfur in surface seawater of the northeast Pacific, *Journal of Geophysical Research, 99,* (C4), 7835-7843, 1994.

Bates, T. S., B. K. Lamb, A. Guenther, J. Dignon, and R. E. Stoiber, Sulfur emissions to the atmosphere from natural sources, *Journal of Atmospheric Chemistry, 14,* 315-337, 1992.

Bigg, E. K., J. L. Gras, and C. Evans, Origin of Aitken particles in remote regions of the Southern Hemisphere, *Journal of Atmospheric Chemistry, 1,* (2), 203-214, 1984.

Bonsang, B., B. C. Nguyen, A. Gaudry, and G. Lambert, Sulfate enrichment in marine aerosols owing to biogenic gaseous sulfur compounds, *Journal of Geophysical Research , 85,* (C12), 7410-7416, 1980.

Brimblecombe, P., and D. Shooter, Photo-oxidation of dimethylsulphide in aqueous solution, *Marine Chemistry, 19,* 343-353, 1986.

Bürgermeister, S., and H. W. Georgii, Distribution of methanesulfonate, NSS sulfate and dimethylsulfide over the Atlantic and the North Sea, *Atmospheric Environment, 25A,* (3/4), 587-595, 1991.

Charlson, R. J., J. E. Lovelock, M. O. Andreae, and S. G. Warren, Oceanic phytoplankton, atmospheric sulphur, cloud albedo and climate, *Nature, 326,* 655-661, 1987.

Clarke, A. D., The Pacific marine aerosol: Evidence for natural acid sulfates, *Journal of Geophysical Research, 92,* (D4), 1987.

Dacey, J. W. H., and S. G. Wakeham, Oceanic dimethylsulfide: Production during zooplankton grazing on phytoplankton, *Science, 233,* 1314-1316, 1986.

Daly, K. L., and G. R. DiTullio, Biogenic production of dimethyl sulfide: Krill grazing, *Antarctic Journal, Review*, 141-142, 1993.

Eslinger, D. L. Florida State University, Tallahassee, FL, 1990.

Eslinger, D. L., and R. L. Iverson, The effects of convective and wind mixing on springtime phytoplankton dynamics in the southeastern Bering Sea shelf, *Continental Shelf Research*, in press.

Ferek, R. J., and J. A. Herring, Ground-based measurement of DMS in tiie Arctic atmosphere at Barrow during summer 1991, *Climate Monitoring and Diagnostics Laboratory*, (20), 1991.

Frouin, R., D. W. Lingner, C. Gautier, K. S. Baker, and R. C. Smith, A simple analytical formula to compute clear sky total and photosynthetically available solar irradiance at the ocean surface, *Journal of Geophysical Research, 94*, 9731-9742, 1989.

Gabric, A., N. Murray, L. Stone, and M. Kohl, Modelling the production of dimethylsulfide during a phytoplankton bloom, *Journal of Geophysical Research, 98*, (C12), 22,805-22,816, 1993.

Gibson, J. A. E., R. C. Garrick, H. R. Burton, and A. R. McTaggart, Dimethylsulfide and the alga *Phaeocystis pouchetii* in antarctic coast waters, *Marine Biology*, 339-345, 1990.

Hood, D. W., and E. J. Kelley, *Oceanography of the Bering Sea: With Emphasis on Renewable Resources*, Institute of Marine Sciences, Fairbanks, Alaska, 1974.

Keller, M., Dimethyl sulfide production and marine phytoplankton: The importance of species composition and cell size, *Biological Oceanography, 6*, 375-382, 1989.

Kiene, R. P., Dynamics of dimethyl sulfide and dimethylsulfoniopropionate in oceanic water samples, *Marine Chemistry, 37*, 29-52, 1992.

Kiene, R. P., and T. S. Bates, Biological removal of dimethyl sulphide from sea water, *Nature, 345*, 702-705, 1990.

Kiene, R. P., and S. K. Service, Decomposition of dissolved DMSP and DMS in estuarine waters: Dependence on temperature and substrate concentration, *Marine Ecology Progress Series, 76*, 1-11, 1991.

Kwint, R. L. J., and K. J. M. Kramer, Dimethylsulphide production by plankton communities, *Marine Ecology Progress Series, 121*, 227-237, 1995.

Leck, C., U. Larsson, L. E. Bagander, S. Johansson, and S. Hajdu, Dimethyl Sulfide in the Baltic Sea: Annual Variability in Relation to Biological Activity, *Journal of Geophysical Research, 95*, (C3), 3353-3363, 1990.

Leck, C., and H. Rodhe, Emissions of marine biogenic sulfur to the atmosphere of northern Europe, *Journal of Atmospheric Chemistry, 12*, pp. 63-86, 1991.

Liss, P. S., Gas-transfer: Experiments and geochemical implications, In: Air-sea Exchange of Gases and Particles, pp 241-298, D. Reidel, Norwell, Mass., 1983.

Liss, P. S., G. Malin, S. M. Turner, and P. M. Holligan, Dimethyl sulphide and *Phaeocystis*: A review, *Journal of Marine Systems, 5*, 41-53, 1994.

Liss, P. S.; Merlivat, L. in *The Role of Air-Sea Exchange in Geochemical Cycling; edited by* P. Buat-Ménard, D. Reidel: Norwell, Mass., 1986; pp 113-127.

Matrai, P. A., and M. D. Keller, Dimethylsulfide in a large-scale coccolithophore bloom in the Gulf of Maine, *Continental Shelf Research, 13*, (8/9), 831-843, 1993.

McTaggart, A. R., and H. Burton, Dimethyl sulfide concentrations in the surface waters of the australasian antarctic and subantarctic oceans during an austral summer, *Journal of Geophysical Research, 97,* (C9), 14,407-14,412, 1992.

Nguyen, N. C., S. Belviso, N. Mihalopoulos, J. Gostan, and P. Nival, Dimethyl sulfide production during natural phytoplankton blooms, *Marine Chemistry, 24,* 133-141, 1988.

Pollard, R. T., P. B. Rhines, and R. Y. Thompson, The deepening of the wind-mixed layer, *Geophysical Fluid Dynamics, 4,* 381-404, 1973.

Pomeroy, L. R., and W. J. Wiebe, Energetics of microbial food webs, *Hydrobiologia, 159,* 7-18, 1988.

Shaw, G. E., Bio-controlled thermostatis involving the sulfur cycle, *Climatic Change, 5,* 297-303, 1983.

Shooter, D. B. P., Dimethylsulphide oxidation in the ocean, *Deep-Sea Research, 36,* 577-585, 1989.

Simo, R., J. O. Grimalt, C. Pedros-Alio, and J. Albaiges, Occurrence and transformation of dissolved dimethyl sulfur species in stratified seawater (western Mediterranean Sea), *Marine Ecology Progress Series, 127,* 291-299, 1995.

Stefels, J., and W. H. M. van Boekel, Production of DMS from dissolved DMSP in axenic cultures of the marine phytoplankton species *Phaeocystis* sp., *Marine Ecology Progress Series, 97,* 11-18, 1993.

Taylor, B. F.; Kiene, R. P. *Biogenic Sulfur in the Environment*; Saltzman, E. S.; Cooper, W. J., American Chemical Society: Washington, DC, pp 202-221, 1989.

Thompson, R. O. R. Y., Climatological numerical models of the surface mixed layer of the ocean, *Journal of Physical Oceanography, 5,* 496-503, 1976.

Turner, S. M., G. L. P. S. Malin, D. S. Harbour, and P. M. Holligan, The seasonal variation of dimethyl sulfide and dimethylsulfoniopropionate concentrations in nearshore waters, *Limnological Oceanography, 33,* (3), 364-375, 1988.

Turner, S. M., Malin, G., and Liss, P. S., Dimethyl sulfide and (dimethylsulfonio)propionate in European coastal and shelf waters, In: *Biogenic Sulfur in the Environment, edited by* Saltzman, E. S. and W. J. Cooper, pp 183-200, American Chemical Society, Washington, DC, 1989.

Vairavamurthy, A., M. O. Andreae, and R. L. Iverson, Biosynthesis of dimethylsulfide and dimethylpropiothetin by *Hymenomonas carterae* in relation to sulfur source and salinity variations, *Limnological Oceanography, 30(1),* 59-70, 1985.

Wakeham, S. G., and Dacey, J. W. H., in Biogeochemical cycling of dimethyl sulfide in marine environments, *Biogenic Sulfur in the Environment*; edited by Saltzman, E. S.; W. J. Cooper, pp 152-166, American Chemical Society, Washington, DC, 1989.

Chapter 5

On the Possibility of Remotely Sensing Global Dimethyl Sulfide Sea-to-Air Flux[4]

Abstract

Biogenic emissions of sulfur from the ocean surface is believed to be a significant contribution to the atmospheric aerosol burden, thus playing a significant role on climate. The possibility exists for using remotely-sensed data to locate sources, map distributions, and estimate global scale fluxes of marine sulfur flux. By definition, estimates of surface trace gas flux from satellites are indirect. Empirical algorithms must be derived using direct surface flux measurements. This technology does not currently exist and may be many years from coming to fruition. We discuss the possibilities of developing a satellite based DMS flux capability and describe a new technique that can be used to develop the necessary empirical relationships. We have demonstrated the feasibility of using a sulfur chemiluminescence detector (SCD) for measuring surface sulfur gas flux directly from the ground. We also have estimated ocean surface sulfur gas flux using two related, indirect methods, known as a variance method and the inertial-dissipation method. These methods can be used in the Arctic, where the ocean to atmosphere flux may be a significant fraction of global biogenic sulfur emissions.

Introduction

Natural emissions of sulfur gases to the atmosphere are comparable in magnitude to combined anthropogenic sulfur gas emissions (for example, Andreae and others 1985;

---

[4]Jodwalis, C. M. and R. L. Benner, On the possibility of remotely sensing dimethyl sulfide sea-to-air flux, 1995, *Polar Record* **31**(177), 251-256.

Cullis and Hirschler 1980; Möller 1984; Michida and others 1992; Toon and others 1987). The dominant natural sulfur source is believed to be dimethyl sulfide ($(CH3)_2S$ or DMS) from the oceans, originating as a metabolic by-product of phytoplankton (Dacey and Wakeham 1986). Uncertainty in the magnitude of this flux exists because no direct measurements have been made, leading to potentially large experimental errors. In addition, DMS emissions are highly variable in both space and time, making it difficult to extrapolate to yearly averages. Because of the high variability, ranging over a couple orders of magnitude (Thompson and others 1992), even thousands of DMS flux estimates are inadequate for determining a global flux. Advantages of spatial and temporal resolution offered by remote sensing makes it the method of choice for estimating global fluxes.

The major constituent of remote marine non-sea salt aerosols, in number concentrations, is sulfate (for example, Clarke and others 1987). Oceanic emission of DMS provides the sulfur for most of this sulfate (Bonsang 1980). The aerosols which result from the oxidation of DMS may impact climate directly through light scattering (Shaw 1983) or indirectly by affecting cloud formation and radiative properties (Charlson 1987, 1994). If this is true, the impact on global climate may be significant.

High latitude ocean regions may make a significant contribution to the global sulfur cycle. There are several lines of indirect evidence to suggest this. (1) Lewis (1989) shows a global view of chlorophyll a concentrations (an indicator of phytoplankton biomass) in the oceans. The picture is a composite which represents averages of data from NASA's Nimbus 7 satellite coastal zone color scanner (CZCS) collected over 18 months. The high latitude oceans, especially coastal areas, show high pigment concentrations relative to mid-latitudes and open oceans. Although the color of the ocean does not directly correlate to magnitude of DMS surface flux, it is reasonable to attempt to quantify the flux from areas of high biological productivity. (2) Researchers on flights over the Arctic Ocean, (Ferek and others 1991), measured DMS concentrations exceeding

200 pptv on several occasions. These levels were the highest ever measured by this group. Generally DMS concentrations in the marine boundary layer are 20 to 50 pptv. (3) Several cruises in the Pacific Ocean found DMS concentrations in seawater from 50 to 65 degrees N latitude among the highest values measured (Bates 1987). Again, these values suggest a potentially large DMS source in northern oceans.

Polar and sub-polar regions may be particularly well suited for a remote sensing approach to sea-to-air sulfur flux which is based on ocean color measurements. In the Bering Sea very strong correlations between phytoplankton cell density and DMS concentrations in seawater have been found (Barnard 1984). This area has high densities of the phytoplankton species Phaeocytis poucheti, also found in Antarctic waters. Similar studies of this species in Antarctic waters show a similar strong correlation (Gibson and others 1990).

Methods

The possibility of using remotely-sensed data to locate sources and map distributions of marine sulfur flux is new, but not untried. Thompson and others (1990) have used remote sensing to estimate sulfur gas sea-to-air flux for a region in the tropical North Atlantic. Their approach was based on empirical relationships between; 1) chlorophyll pigment concentration and DMS in seawater, and 2) wind speed and air-sea exchange rate. As validation, they used photochemical model predictions of sea-to-air sulfur flux. What we offer in this paper is; 1) a means of validating their approach using two indirect methods which are independent of the method used for estimating sulfur gas sea-to-air flux using DMS seawater concentrations, 2) a description of a direct technique for measuring sulfur gas sea-to-air flux which can be used to more accurately validate a remote sensing approach. Even more importantly, at this stage, a direct measurement technique is needed to quantify the relationship between flux and the important parameters which affect the flux. We say this because parameters other than ocean color and wind

speed may be important. What we propose is a concerted effort to find out what these parameters are. For this, a direct measurement technique, allowing accurate measurements is necessary.

Using the remote sensing approach of Thompson and others (1992), DMS concentrations in seawater are estimated from remotely sensed chlorophyll pigment concentrations, through an empirical relationship. The derived DMS concentrations in surface seawater are used to estimate the flux using the stagnant boundary layer model for air-sea gas exchange. The stagnant boundary layer model of Liss and Slater (1974) for air- sea gas exchange is most commonly used for estimating sea-to-air DMS flux. It states that:

$$flux = vt[DMS]_{seawater} \quad (1)$$

where v_t is the transfer velocity. We refer to the method based on this model as the stagnant boundary layer method.

Usually transfer velocities are calculated from correlations of wind speed with transfer velocities determined using the radon deficit or radiocarbon methods, making adjustments for the diffusivity of the gas at different ocean surface temperatures. Erickson and others (1990) state that an uncertainty of approximately 40% in the DMS transfer velocity calculation exists, because the diffusivity of DMS in seawater has never been measured. Another uncertainty in this approach to calculating transfer velocities is that parameters other than wind speed may be important, such as; turbulence at the air-water interface, boundary layer stability, surfactants, and bubbles, some of which are not "intimately linked" to wind speed (Wanninkhof, 1992). Also there is uncertainty in the correlation of wind speeds with the transfer velocity. These correlations are difficult to determine because the time scale for wind speed variations (on the order of hours) is much shorter than the time scales used to determine the transfer velocities (Smethie and others 1985). As an alternate means of estimating transfer velocities, wind tunnel studies have

been made (Liss and Merlivat 1986). Uncertainties exist in these estimates due to the difficulties of truly simulating the natural ocean environment. Many researchers believe that most of the uncertainty in the stagnant boundary layer method lies in the calculation of the transfer velocities, which have been estimated to be uncertain by about a factor of 2 (Andreae 1986; Bates and others 1987).

Chlorophyll pigment concentrations may or may not be an important parameter for remotely measuring DMS sea-to-air flux. Generally speaking, higher DMS seawater levels occur in waters of higher biological productivity (Andreae and Barnard 1984). But, often the correlation between DMS concentrations in seawater and phytoplankton biomass is weak (Thompson and others 1990) and in some instances does not exist at all (Matrai and others 1993). One explanation for this is that the production rate of DMS varies over three orders of magnitude depending on the phytoplankton species (Charlson and others 1987). Lack of correlation could also be due to seawater DMS concentrations not being in a steady-state. That is, the removal rate of DMS from seawater can change without a concomitant change in production rate. For example, in some locations, bacteria and other microbes may remove seawater DMS, which can affect a correlation between seawater DMS and phytoplankton biomass. Another sink could be the oxidative breakdown of DMS in seawater to dimethyl sulfoxide (DMSO). On the other hand, DMS release to seawater increases substantially due to zooplankton grazing (Dacey and Wakeham 1986), further complicating the relationship between ocean color and seawater DMS concentration.

Instead of the commonly used stagnant boundary layer method to estimate sea-to-air sulfur gas flux, we used a variance method and the inertial-dissipation method. Both methods are independent of the stagnant boundary layer method. The variance and inertial-dissipation methods are related, since both utilize measurements of turbulence driven concentration fluctuations to estimate flux. This requires a real-time detection system with adequate sensitivity and time resolution to measure turbulent scale

fluctuations. The sulfur chemiluminescence detector (SCD) used meets these requirements because it offers high sensitivity with fast response.

In the remote marine boundary layer, the dominant source of sulfur gas is the ocean. A vertical sulfur gas flux from the ocean surface results. Because of this flux, as the wind blows air past the stationary sensor, turbulent eddies manifest themselves as fluctuations in the sulfur time series. The more intense the fluctuation, the greater the variance in the time series. Turbulent fluctuations in the atmospheric sulfur gas concentration time series can give us information about the flux since turbulence is responsible for the vertical transport of conserved quantities in the boundary layer.

A power spectrum of the sulfur gas time series gives us a measure of the intensity (often called spectral density or power) of the turbulence for each turbulent eddy size. The inertial-dissipation method requires a measure of the intensity of the turbulence for eddy sizes in the inertial subrange region of the turbulence spectrum. While the variance method requires a measure of the variance in sulfur gas concentrations for the eddy frequency range important for turbulent transfer. In addition, both methods require an evaluation of atmospheric stability and semi-empirical relationships relating the variance to flux. Fairall and Larsen (1986) provide an in-depth description of the inertial-dissipation method. For a detailed description of the variance method see Lenschow (1993) or Kaimal and Finnigan (1994). Both methods have been used successfully to estimate surface fluxes of other scalar constituents in the boundary layer (Debruin, 1993; Edson and others 1991; Weseley 1988).

The variance and inertial-dissipation methods are not plagued with the uncertainties and assumptions mentioned earlier in this paper for the stagnant boundary layer method, but they have some of their own. To use both the variance and inertial-dissipation methods we made the following assumptions: (1) a homogeneous oceanic source of sulfur gases existed, (2) oceanic DMS was the dominant sulfur species resulting in turbulence driven sulfur concentration fluctuations, and (3) horizontal

homogeneity of flow in the atmospheric boundary layer existed under steady-state conditions for a time scale less than one hour.

It is important to keep in mind that our flux estimates are based on measurements of the concentration fluctuations, not absolute concentrations. Carbonyl sulfide, present at background levels throughout the boundary layer, is measured by the SCD. But, because it is long-lived (life-time of years) and the oceanic source is very small relative to that of DMS (Toon and others 1987), it results in very small fluctuations in the sulfur gas concentration time series. Also, our flux estimations were made during periods when the air sampled was not significantly influenced by air masses of continental origin. Under these conditions, sulfur dioxide flux to the surface would be small relative to the DMS flux from the surface. If we assume that DMS flux is the dominate sulfur gas flux, then our flux estimates correspond to DMS flux from the ocean to the atmosphere.

Discussion

What are the important parameters?

In light of the uncertainties known in the relationships between: 1) ocean color and DMS seawater concentrations, and 2) wind speed and transfer velocities, determining which parameters are important in sulfur gas sea-to-air flux needs to be done before any remote sensing approach can be successful on a global scale. Ocean color does not always correlate with DMS seawater concentrations. But considering other parameters that may be important along with ocean color, a correlation may exist. For example, if per cent phytoplankton speciation is known along with the DMS production rate of each species, a correlation may be seen. Considering other variables associated with oceanic productivity may also improve correlations based on ocean color. These could include illumination, surface ocean nutrient supply, salinity, and sea surface temperature; some of which can be remotely measured. Also, as mentioned in the introduction, production rate of DMS may be increased by zooplankton grazing, making knowledge of zooplankton density necessary

in such situations. Further investigations are needed to determine how important these parameters are and if other important parameters exist. Perhaps there is a parameter other than ocean color which is strongly correlated to DMS seawater concentrations. Erickson and others (1990) have used an alternative correlation of the flux of DMS with incident solar radiation to estimate global DMS flux. Likewise, the correlation between DMS seawater concentrations and DMS flux may be improved upon by considering parameters in addition to or other than wind speed. As mentioned earlier, sea state, boundary layer stability, surfactants, bubbles, and DMS removal mechanisms (for example, oxidative breakdown) may be important, justifying further investigation.

Indirect sea-to-air sulfur flux measurements

Measurements were taken of real-time total gaseous sulfur concentrations in the atmosphere from a stationary ship in the Atlantic Ocean, near the Azores. The instrument used was a Sulfur Chemiluminescence Detector (SCD) with a sampling frequency of one hertz. For a complete description of the instrument see Benner and Stedman (1990), and Benner (1994). From this data we estimated sulfur gas sea-to-air flux for five one-hour sampling periods on two different days. The range of results using the variance method and the inertial-dissipation method were 21 to 27 μmoles of sulfur $m^{-2} \cdot d^{-1}$ and 11 to 17 μmoles of sulfur $m^{-2} \cdot d^{-1}$, respectively. Propagation of error analysis shows that the uncertainty in these two methods is approximately 30 to 35 per cent. This could account for the different range of results for these two methods, but more work is needed to further investigate the discrepancy.

The ranges were substantially higher than those found previously in this region of the world using the stagnant boundary layer method based on seawater DMS concentrations (Barnard and others 1982; Berresheim, 1991; Van Valin, 1987). The difference in results is not surprising considering the spatial, diurnal and seasonal variability of DMS fluxes. To make an accurate comparison of results from the methods we used to those of the stagnant boundary layer method, measurements need to be made

simultaneously at the same location. Verification of the stagnant boundary layer method is needed because it may have significant systematic errors.

Direct Measurement Technique

The eddy-correlation flux is the average of the instantaneous products of the vertical wind velocity and the constituent concentration. It can be expressed as :

$$flux = \overline{(w'c')} \qquad (2)$$

where the overbar denotes an average, and w' and c' are deviations from the average values of vertical wind speed and constituent concentration, respectively. w' and c' are also defined as the turbulent components of the vertical wind speed and constituent concentration. Figure 5.1 illustrates this technique using hypothetical data. In simple terms, the flux is the sum of concentrations in upward and downward moving eddies. For example, consider the time interval between 0 and 2. During this time, the vertical wind speed is positive (i.e. upward moving eddies) and the constituent concentrations in these upward moving eddies is higher than average. Therefore, the average of the instantaneous products of the two is positive, i.e. a flux upward. The time interval between 2 and 4 also shows an upward flux due to lower than average constituent concentrations in downward moving eddies. The remaining time interval of this plot shows a downward flux which is a result of higher than average constituent concentrations in downward moving eddies.

The eddy-correlation technique requires a real-time, fast-response instrument, sensitive enough to detect boundary layer concentrations. For example, in the remote ocean boundary layer, an analytical technique capable of resolving a few 10's of pptv change in concentration in less than one second is required. The SCD is a recently-developed system that meets this rigorous and previously unobtainable requirement. Concurrent measurements of vertical wind velocity are usually made using a sonic anemometer. This technique has been used successfully for direct flux measurements (Lenschow 1981).

The current data provide two pieces of evidence showing that the SCD is capable of measuring turbulent scale sulfur gas concentration fluctuations in the atmosphere and, therefore, can be used for eddy correlation flux measurements. First the -5/3 slope, indicative of the inertial subrange region of the turbulence spectrum (Stull 1993), is resolved in the power spectrum of the sulfur time series displayed in Figure 5.2. This shows that the concentration fluctuations measured in the sulfur time series were in fact due to turbulence driven concentration fluctuations in the atmosphere. The second piece of evidence comes from measurements of the ship's cabin air. Assuming the cabin air is thoroughly mixed, the sulfur time series of the cabin air is a measure of the instrument noise. Comparing the time series for the cabin air with that of atmospheric measurements, Figure 5.3 displays a signal-to-noise ratio of 5 to 1. If the air in the cabin was not thoroughly mixed, the signal-to-noise ratio would be larger still.

Summary

In a remote sensing approach there are essentially two problems that need to be overcome. One is determining the relationship between ocean color and DMS seawater concentrations. For this, the effect of ecosystem dynamics (for example, nutrient levels, sinks other than emission to the atmosphere) and phytoplankton speciation needs to be determined and quantified. Matrai and others (1993) suggest that phytoplankton blooms should probably be the first place to study an ocean color-DMS relationship. The other problem is the relationship between seawater concentrations of DMS to sea-to-air DMS flux. We believe variables in addition to the ones considered in the stagnant boundary layer method are important in air-sea exchange (for example, sea state, bubble bursting).

Once these relationships are determined, an empirical algorithm can be determined making a remote sensing approach to measuring sea-to-air DMS flux possible. A direct measurement method is needed to accomplish this with acceptable accuracy and to validate the stagnant boundary layer method estimates of DMS sea-to-air flux, which may

be part of a remote sensing approach. For the present, the indirect methods we have used to estimate flux can be used to investigate and validate a remote sensing approach.

Conclusion

The study demonstrated the feasibility of using a SCD for direct ocean surface sulfur flux measurements. We also have obtained sea-to-air flux estimates using a variance method and the inertial-dissipation method over the Atlantic Ocean, near the Azores. Values ranged from 21 to 28 μmoles · m^{-2} ·d^{-1} and 11 to 17 μmoles · m^{-2} ·d^{-1}, respectively.

Because of the spatial and temporal inhomogeneity of the system, determining the global emission of oceanic DMS is a difficult problem. In our opinion, remote sensing is the obvious way of resolving this problem. There will be opportunities to use a remote sensing approach on a global scale for measuring DMS sea-to-air flux in the Arctic, with the deployment of NASA's SeaWiFs satellite in May of 1995. This satellite will offer global coverage of ocean color twice daily in the northern latitudes. But, before satellites can help much, the empirical relationships between ocean color, DMS seawater concentrations and DMS sea-to-air flux need to be established.

Acknowledgments

We would like to thank Byron Blomquist for his efforts in providing logistical support during the field campaign, Chris Fairall for providing a computer program used in our data analysis, the captain and crew of the RV/Oceanus, Don Lenschow and Chris Fairall for helpful discussions and the anonymous reviewers for helpful comments. This work was supported by the Office of Naval Research Ocean Chemistry Program under grant ONR N00014-92-J- 1296.

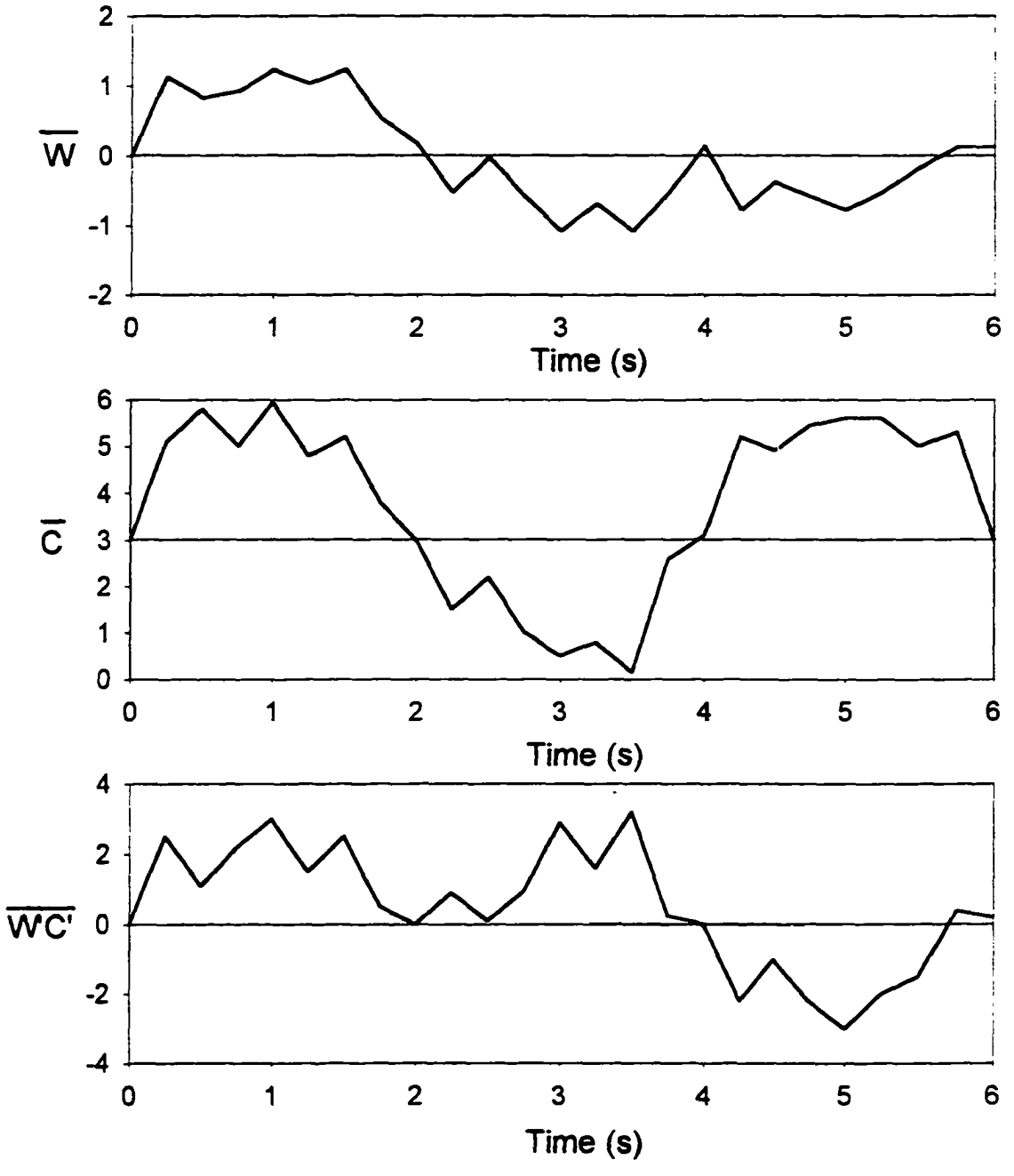

Figure 5.1 - An illustration of the eddy correlation technique using hypothetical data. The flux is the average of the instantaneous products of the vertical wind velocity and constituent concentration.

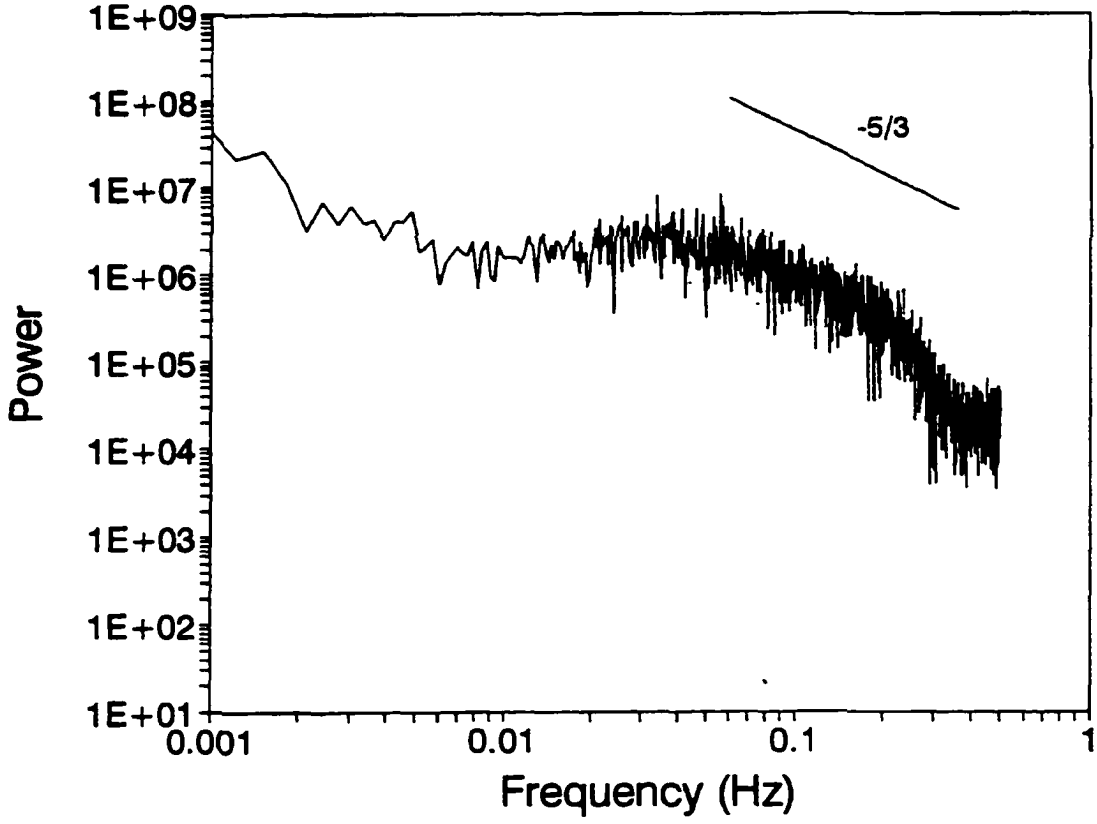

Figure 5.2 - A power spectrum of sulfur gas concentration fluctuations. The -5/3 slope indicates that the sulfur detection system resolved fluctuations driven by turbulence in the atmosphere. The fall of response above approximately 0.2 Hz is caused by attenuation in sample line, instrument response or both.

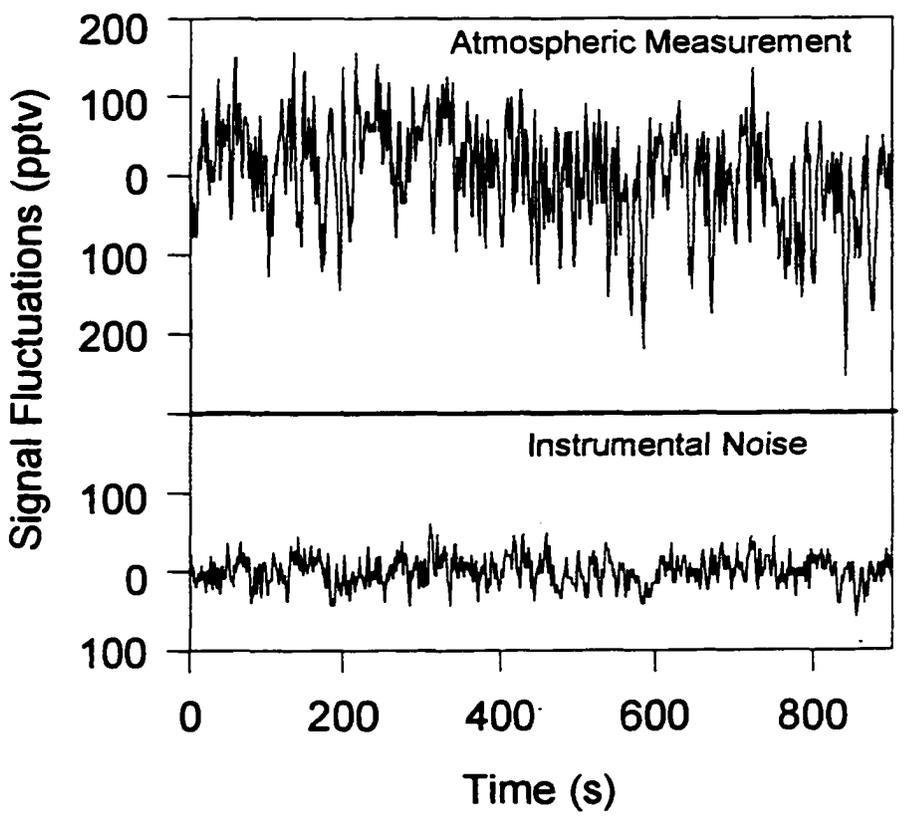

Figure 5.3 - A segment of the sulfur gas time series for both the ship's cabin air and the atmosphere. This shows a signal-to-noise ratio of approximately five to one, which is more than adequate for flux measurements.

References

Andreae, M. O., and W.R. Barnard. 1984. Exchange of dimethyl sulfide from ocean to atmosphere. *Marine Chemistry* 14: 267-279.

Andreae, M.O., R.J. Ferek, F. Bermond, K.P. Byrd, R.T. Engstrom, S. Hardin, P.D. Houmere, F. LeMarrec, H. Raemdonck, and R.B. Chatfield. 1985. Dimethylsulfide in the marine atmosphere. *Journal of Geophysical Research* 90: 12,891-12,900.

Andreae, M.O. 1986. The ocean as a source of atmospheric sulfur compounds. In: Buat-Ménard, P. (editor). The role of air-sea exchange in geochemical cycling. Boston:Reidl, 331-362.

Barnard, W.R., M.O. Andreae, and W.E. Watkins. 1982. The flux of dimethylsulfide from the oceans to the atmosphere. *Journal of Geophysical Research* 87: 8787-8793.

Barnard, W.R., M.O. Andreae, and R. Iverson. 1984. Dimethylsulfide and Phaeocystis Poucheti in the southeast Bering Sea. *Continental Shelf Research* 3:103-113.

Bates, T.S.,

Cline, J.D., R.H. Gammon, and S.R. Kelly-Hansen. 1987. Regional and seasonal variations in the flux of oceanic dimethylsulfide to the atmosphere. *Journal of Geophysical Research* 92: 2930-2938.

Benner, R.L., and D.H. Stedman. Field evaluation of the sulfur chemiluminescence detector. 1990. *Environmental Science and Technology* 24: 1592-1596.

Benner, R.L., and D.H. Stedman. 1994. Chemical Mechanism and Efficiency of the Sulfur Chemiluminescence Detector. *Applied Spectroscopy* 48 (7): 848-851.

Bonsang, B., B.C. Nguyen, A. Gaudry, and G. Lambert. 1980. Sulfate enrichment in marine aerosols owing to biogenic sulfur compounds. *Journal of Geophysical Research* 85:7410-7416.

Berresheim, H., M.O. Andreae, R.L. Iverson, and S.M. Li. 1991. Seasonal variations of dimethylsufide emissions and atmospheric sulfur and nitrogen species over the western north Atlantic Ocean. *Tellus* 43B: 353-372.

Charlson, R.J., J.E. Lovelock, M.O. Andreae, and S.G. Warren. 1987. Oceanic phytoplankton, atmospheric sulfur, cloud albedo, and climate. *Nature* 349: 655-661.

Charlson, R.J. and T.M.L. Wigley. 1994. Sulfate aerosol and climatic change. *Scientific American* February: 48-57.

Clarke A.D., N.C. Ahlquist, and D.S. Covert. 1987. The pacific marine aerosol: evidence for natural acid sulfates. *Journal of Gephysical Research* 92D: 4179-4190.

Cullis, C.F., and M.M. Hirschler. 1980. Atmospheric sulphur: natural and man-made sources. *Atmospheric Environment* 14: 1263-1278.

Dacey, J.W., and S.G. Wakeham. 1986. Oceanic dimethyl sulfide: Production during zooplakton grazing on phytoplankton. Science 233: 1314-1326.

De Bruin, H.A., Kohsiek, W., and B.J.J.M. Van Den Hurk. 1993. A verification of some methods to determine the fluxes of momentum, sensible heat, and water vapour using standard deviation and structure parameter of scalar meteorological quantities. *Boundary Layer Meteorlogy* 63: 231-257.

Edson, J.B., C.W. Fairall, P.G. Mestayer, and S.E. Larsen. 1991. A study of the inertial-dissipation method for computing air-sea fluxes. *Journal of Geophysical Research* 96: 10,689-10,711.

Erickson, D.J., J. Ghan, and J.E. Penner. 1990. The oceanic source of DMS to the atmosphere. *Journal of Geophysical Research* 95: 7543-7552.

Fairall, C.W., and S.E. Larsen. 1986. Fluxes at the air-ocean interface. *Boundary-Layer Meteorology* 34: 287-301.

Gibson, J.A.E., R.C. Garrick, H.R. Burton and A.R. McTaggart. 1990. Dimethylsulfide and the alga Phaeocystis pouchetii in antarctic coastal waters. *Marine Biology* 104: 339- 346.

Kaimal, J.C., and J.J. Finnigan. Atmospheric Boundary Layer Flows. New York: Oxford University Press.

Liss, P.S., and P.G. Slater. 1974. Flux of gases across the air-sea interface. *Nature* 24: 181-184.

Liss, P.S., and L. Merlivat. 1986. Air-sea gas exchange rates: introduction and synthesis. In: Buat-Ménard (editor). The role of air-sea exchange in geochemical cycling. Boston: Reidl.

Matrai, P.A., W.M. Balch, D.J. Cooper, and E.S. Saltzman. 1993. Ocean color and atmospheric dimethyl sulfide: On their mesoscale variability. *Journal of Geophysical Research* 98: 23,469-23,476.

Michida, M., S. Tanaka, and Y. Hashimoto. 1992. Concentrations of sulfur compounds (MSA, SO2, NSS-SO2-4,) in the marine atmosphere, and estimation of biogenic sulfur emission from the sea. In: Proceedings of the NIPR Symposium on Polar Meteorology and Glaciology. Tokyo, Japan 5: 174. Abstract only.

Möller, D. 1984. Estimation of the global man-made sulphur emission. *Atmospheric Environment* 18: 19-27.

Shaw, G.E. 1983. Bio-controlled thermostatis involving the sulfur cycle. *Climatic Change* 5:297-303.

Stull, R.B. 1993. An introduction to boundary layer meteorlogy. Page 391. Norwell, Massachusetts: Kluwer Academic.

Thompson, A.M., W.E. Esaias, and R.L. Iverson. 1990. Two approaches to determining the sea-to-air flux of dimethyl sulfide: satellite ocean color and a photochemical model with atmospheric measurements. *Journal of Geophysical Research* 95: 20,551-20,558.

Toon, O.B., J.F. Kasting, R.P. Turco, and M.S. Liu. 1987. The sulfur cycle in the marine atmosphere. *Journal of Geophysical Research* 68: 943-963.

Van Valin, C.C., H. Berresheim, M.O. Andreae, and M. Luria. 1987. Dimethyl sulfide over the western Atlantic Ocean. *Geophysical Research Letters* 14:715-718.

Wanninkhof, R. 1992. Relationship between wind speed and gas exchange over the ocean. *Journal of Geophysical Research* 97(C5): 7373-7382

Chapter 6

Conclusion

Of the four major biogeochemical cycles (C, N, O, S), the sulfur cycle is perhaps the least studied and most poorly understood. The most important pathway of sulfur through the atmosphere starts with its entry as a low oxidation state gas from both anthropogenic and natural sources. Examples include SO_2 from fossil fuel combustion or DMS from phytoplankton. Once in the atmosphere, this sulfur is eventually oxidized to sulfate and then removed by both wet and dry deposition. The whole process lasts several days, resulting in widely varying atmospheric sulfur gas mixing ratios and sulfate aerosol distributions over the globe. Without accurate sulfur surface flux measurements, it is difficult to study the production, transport, distribution, chemical transformations and removal of sulfur gases and aerosols in the atmosphere.

One, if not the major, uncertainty in understanding the atmospheric sulfur cycle is the surface flux of sulfur species. Only the anthropogenic contribution is known to a high degree of accuracy, since the anthropogenic sources are well-known and relatively easy to quantify. Global natural emissions of sulfur are believed to be comparable in magnitude to anthropogenic emissions, although they are more difficult to sum because of the high spatial and temporal variability of the wide variety of sources, the lack of adequate geographical coverage of data, and the difficulty in measuring rates of transfer across the air-sea interface. The latter factor is especially important, since the major natural source of sulfur to the atmosphere is the oceans.

The ocean sources of sulfur to the atmosphere include sea-salt sulfate and volatile sulfur compounds. On a mass flux basis, sea salt-sulfate from sea spray appears significant as shown in Figure 6.1. However, being already in a fully oxidized, stable state, sea-salt sulfate does not alter the chemistry of the atmosphere and is thus of little geochemical importance. This is evident if we use the change in oxidation state of sulfur as a surrogate for the importance of the sulfur-containing compounds in the atmosphere. The oxidation

state of sulfur in sea salt is +6, the highest possible, so the potential to change is 0. Conversely, volatile dimethyl sulfide emitted from the oceans has a sulfur oxidation state of -2. It is very likely that this sulfur will be oxidized to a +6 oxidation state in the atmosphere, effecting a change in oxidation state of 8. Figure 6.1 and Figure 6.2 drive home the point that sea salt sulfate is of relatively little importance to the sulfur chemistry of the atmosphere.

We have worked to lessen the uncertainty in quantifying natural sulfur emissions on two fronts. First, we have developed two new techniques for measuring sulfur gas surface flux and have used them in the field to estimate DMS sea-to-air flux. Both methods provide an independent check of the commonly used stagnant boundary layer (SBL) method. Second, we have set out to evaluate the magnitude of the northern ocean source of sulfur to the atmosphere. This involves measurements of DMS mixing ratios in marine boundary layer air and a modeling study of DMS ocean mixing, biological production and sea-to-air flux.

Real-time total gaseous sulfur concentrations were measured (sampling frequency 1 Hz) from the R/V *Oceanus* as part of the Atlantic Stratocumulus Transition Experiment/Marine Aerosol and Gas Exchange (ASTEX/MAGE) field campaign in the Azores during June of 1992. Our field measurements demonstrate, for the first time, that the sulfur chemiluminescence detector (SCD) is capable of resolving turbulence-driven sulfur gas concentration fluctuations in the atmosphere. We know of no other instrument with this capability. Since turbulence is responsible for the vertical transport of trace chemical species in the boundary layer, fluctuations in sulfur gas concentrations due to turbulence bear a unique, though indirect, relationship to the sulfur surface flux for a given set of turbulent mixing parameters. We used these data with two established micrometeorological methods based on turbulence statistics - the variance and inertial-dissipation methods - to estimate DMS sea-to-air flux. This is the first time that these two methods have been used to estimate sulfur surface flux, although they have been used for

other scalar constituents. Both methods appear to be more accurate than the commonly used stagnant boundary layer (SBL) model for estimating DMS sea-to-air flux. Values from five 1-hour measurement periods on two different days ranged from 21 to 28 μmole $m^{-2} d^{-1}$ and 11 to 17 μmole $m^{-2} d^{-1}$, respectively. These values are above the range of 1 to 13 μmole $m^{-2} d^{-1}$ reported during ASTEX/MAGE (Blomquist et al., 1996) based on the product of the transfer velocity and the DMS concentration in surface seawater using the SBL model of air-sea exchange. However, studies of *Putaud and Nguyen* (1996), suggest that empirically determined transfer velocities used to estimate DMS sea-to-air flux may be too low, by a factor of 2. And, recently, *Yvon et al*, (1996), using a photochemical box model and the observed amplitude of the atmospheric DMS diel cycle, concluded that sea-to-air DMS flux is higher than was previously thought. Our results and those of *Putaud and Nguyen* (1996) and *Yvon et al.* (1996) suggest that DMS sea-to-air flux estimates and emission rates, which have been almost exclusively based on the SBL model of air-exchange, are biased low. More work and better techniques, such as a direct flux measurement technique, are needed to resolve the discrepancies between the methods.

Real-time sulfur gas measurements also provide information on the horizontal inhomogeneity of sulfur gas concentrations in the marine boundary layer due to turbulent mixing. Who cares about this? Anyone who wants to collect a sample representative of an air mass must consider how long they need to collect the sample to get a result representative of the airmass. The question of how long is often asked, but we know of no one who has systematically tried to answer the question as we have. Fourier-transform processing of the sulfur gas concentration time series from the Azores study provides information on the horizontal inhomogeneity. The resulting power spectrum of the time series shows the contribution of each eddy size to the total variance. A plot of the fraction of total variance in sulfur concentration fluctuations as a function of sampling time reveals the time period necessary to collect a representative sample. From our measurements, we

have determined that air samples should be integrated for 1000 s for ground-based measurements. The size scale of sampling can be estimated by multiplying by wind speed.

Upon completion of the Azores research, we had two new flux methods ready for the next field experiment. We decided then to focus on sulfur emissions from northern oceans, particularly those surrounding Alaska, for many reasons. High primary productivity in these ocean regions, and the few existing field measurements of DMS in air above the Arctic Ocean and in surface seawater of the north Pacific Ocean, suggested a significant source of sulfur to the atmosphere. The new flux methods that we proved successful in a field setting in the Azores may be used in the Arctic. And, although the recommended sulfur gas sample integration time of 1000 s is derived from data near the Azores, it could also be appropriate for sampling over northern oceans. At the very least, this duration is a starting point rather than a guess as to how long a sample should be integrated.

To set the stage for measuring DMS sea-to-air flux from northern oceans, we initiated a screening study to evaluate the magnitude, seasonality and spatial variability of the DMS source strengths from ocean regions around Alaska. Atmospheric DMS mixing ratios in the MBL were measured from a ship on the Bering and Chukchi Seas and from a land-based research station overlooking Katchemak Bay. Our main objective with this project was to increase the relatively small database of atmospheric DMS mixing ratios above northern oceans. A mobile laboratory at Katchemak Bay allowed us to set up the gas chromatograph - sulfur chemiluminescence detector (GC-SCD) on site and thus make ambient measurements of DMS. Since the GC-SCD used to quantify DMS was not compact or rugged enough to withstand strong seas and the sampling conditions available to us on the Bering and Chukchi Seas, we developed a sample collection system for trapping DMS. We found this portable sample collection system to be an effective tool for sampling in remote regions, at minimal cost and with few logistical complications.

Typically, DMS mixing ratios in the MBL are between 20 and 200 pptv. Most of

the mixing ratios we measured above the Bering and Chukchi Seas fall within this range, with a few on the high end, above 150 pptv. Several features from the DMS data are especially interesting. One is that relatively high values (>150 pptv) are seen in September, not considered a very productive time of the year for Arctic organisms. The highest value, 650 pptv, was found in a sample collected directly at the ice edge. Also, the data suggest a gradient in DMS mixing ratios that decreases from west to east. The reason for the gradient could lie in the biology of the currents flowing north through the Bering Strait. Waters that flow north from the western Bering Sea and coast of Siberia to the western Chukchi Sea are nutrient rich, characterized as having high primary productivity. On the contrary, currents flowing north along the coast of Alaska are relatively low productivity and nutrient poor. Last, DMS is not the only volatile sulfur compound present in significant quantities. DMDS appears to be present in about half of the samples collected and in many samples the amount rivals that of DMS. To our knowledge, there are no literature reports of such high levels of DMDS in MBL air.

The DMS MBL mixing ratios from the Katchemak Bay site display an even wider range of values than from over the Bering and Chukchi Seas. On eleven days, the mixing ratios ranged from 11 to 1,950 pptv, although most of the values were below 200 pptv. Variability of DMS mixing ratios could result from a combination of many factors, including: (1) marine source strength; (2) meteorological parameters, such as boundary layer mixing height, or wind speed, which affects mass transfer rates; (3) pathway of air mass and time it spent over the ocean, (4) the sampling height; and (5) influence of the coastal environment. We suspect that tidal heights may have a major influence on MBL DMS mixing ratios at this and other coastal sites, since the three highest mixing ratios of the field campaign, 1860, 1790 and 1950 pptv, were measured during three of the four minus tide events when samples were collected. As in the Bering and Chukchi Sea MBL samples, DMDS was found in many of the samples collected and analyzed in MBL air from over Katchemak Bay.

Little is known about sulfur gas emissions from northern oceans. We are still in the early stages of this research. DMS field measurements that do exist, including the results of this study, support the hypothesis that ocean areas around Alaska may contribute significantly to the global sulfur budget. Our results call for a more thorough look into DMS and DMDS emissions from ocean regions around Alaska, potentially a significant source of sulfur to the atmosphere.

High variability in MBL DMS mixing ratio is not limited to northern ocean regions surrounding Alaska. Time series of atmospheric DMS in the MBL from many locations around the world show considerable variability (*Andreae et al.*, 1985). Changes in hundreds of pptv are common from one day to the next. Although there are many factors that may influence MBL DMS mixing ratios, we know of no study in which the authors rigorously evaluate the reasons for the high variability.

We propose that perhaps these sudden excursions are linked to ocean mixed-layer dynamics. That is, stormy, high-wind events bring DMS from depth to the surface, making more DMS available to the atmosphere. To test this hypothesis, we developed a model of DMS ocean mixing, production and sea-to-air flux, known as the DMS model.

Our goals with the DMS modeling exercise are to quantify the role of ocean mixed-layer dynamics and biological activity on DMS sea-to-air flux; and evaluate which parameters are important to DMS sea-to-air flux. The results may help to (1) improve design of field experiments; (2) improve accuracy of regional DMS sea-to-air flux estimations; (3) extend DMS flux estimates to climatic regimes or extreme whether conditions not conducive to sampling; and (4) indicate areas where measurements need to be made.

DMS seawater concentrations drive the flux of DMS from the sea to the air. A complex food web including bacteria, phytoplankton and zooplankton governs the distribution and concentrations of DMS in seawater. Dynamic, bio-mediated processes result in typically wide fluctuations of DMS in seawater.

Our modeling of ocean mixing, biological production and DMS sea-to-air flux indicates that biological consumption and production are very important parameters in controlling seawater DMS concentrations and, ultimately, DMS sea-to-air fluxes. Unfortunately, these parameters have very large uncertainties and little field data on them exists, particularly at high latitudes. The importance of biological consumption and production in the oceanic DMS cycle calls for more research.

Preliminary model results indicate that (1) pulses in flux correspond to high wind speed and deep mixing events; and (2) there is a fall DMS "mixing bloom" at northern latitudes. These results show that ocean mixed-layer dynamics play a significant role in DMS sea-to-air flux. Field measurement campaigns and estimates of the contribution of northern latitude oceans to the global sulfur budget need to include measurements during these mixing events to obtain unbiased DMS sea-to-air flux estimates.

Where do we go from here? The DMS model gives us a tool to investigate and help to understand the spatial and temporal variability of DMS sea-to-air flux. The new flux estimation methods will be useful in validating the DMS model and estimating DMS sea-to-air flux from northern oceans. A direct flux measurement technique needs to be developed to resolve the discrepancies between the existing indirect flux measurement techniques. The SCD used in the Azores shows potential as a direct sulfur flux measurement device, using the eddy correlation method. This method could aid in developing the empirical algorithms needed for a remote-sensing approach to measuring DMS sea-to-air flux. In our opinion, remote sensing is the obvious way to determine regional and global fluxes for dimethyl sulfide, a gas with highly variable sources.

In closing, we list a summary of contributions from this doctoral research:

- The development of new techniques for sulfur flux estimates from the ocean.
- The determination of sample integration times necessary for a representative sulfur gas sample in the MBL.

- The development of a new DMS ocean flux model that
  - integrates experimental and modeling capabilities to bring out the best in both.
  - highlights importance of ocean mixed layer dynamics for DMS flux.
- Support for the hypothesis that northern oceans may contribute more to the sulfur in the atmosphere than previously thought.
- Creation of a foundation for the development of a remote sensing approach to measuring DMS flux.

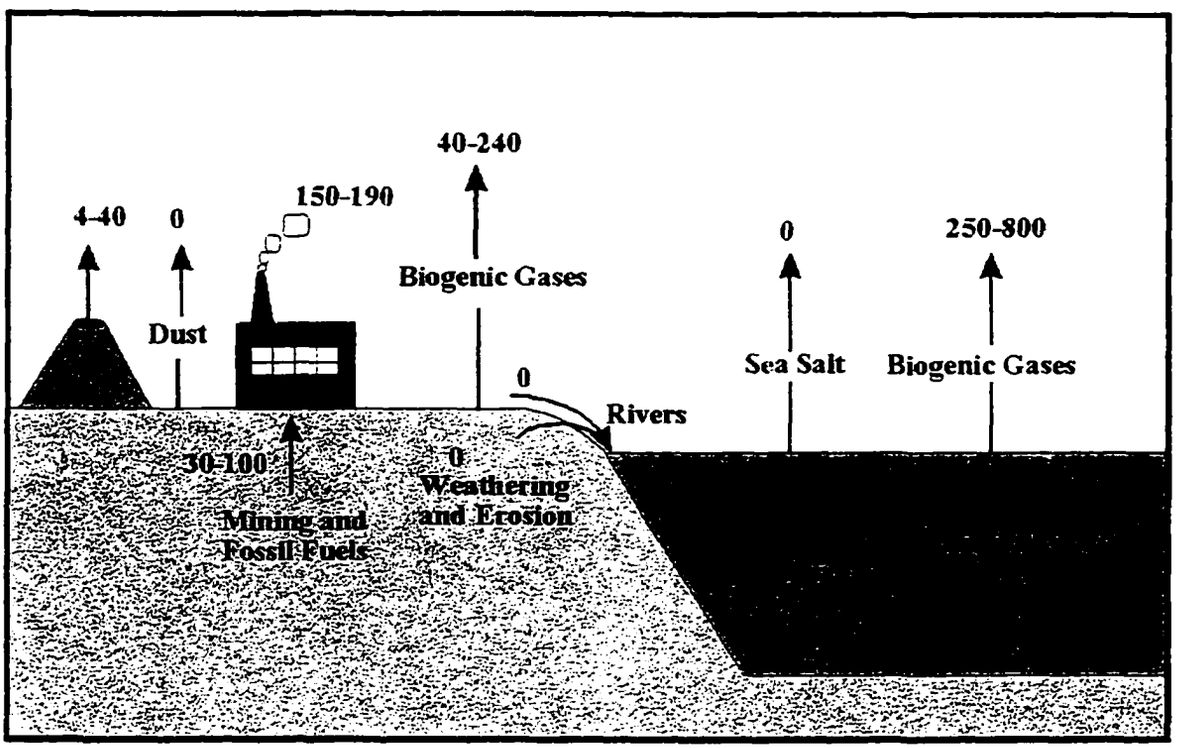

Figure 6.2 - The global S cycle. All values are in 10^{12} g S / yr multiplied by change in oxidation number of S.

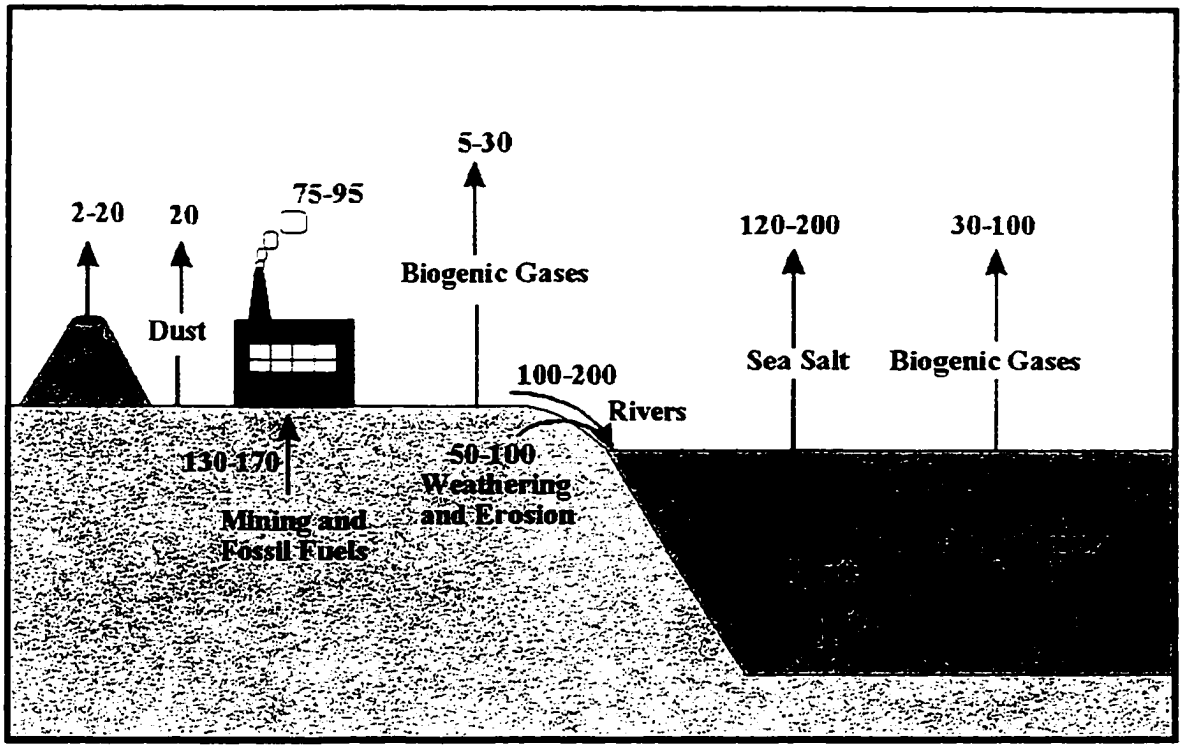

Figure 6.1 - The global S cycle. All values are 10^{12} g S / yr.

Appendix A

The following figures refer to chapter 4 of this thesis.

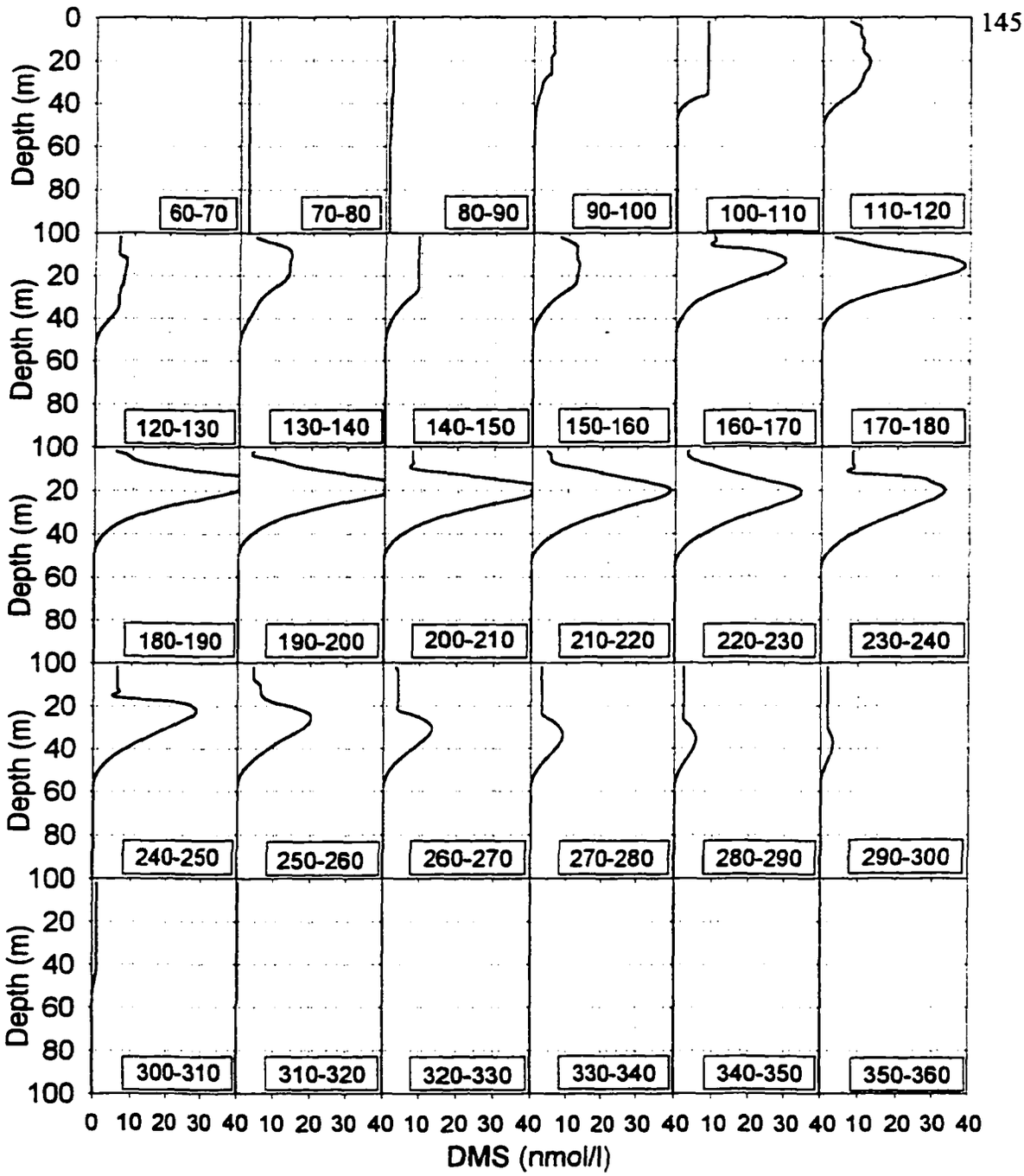

Figure A.1 - Seawater profiles of DMS from the Middleton Island site - 1995 model run.

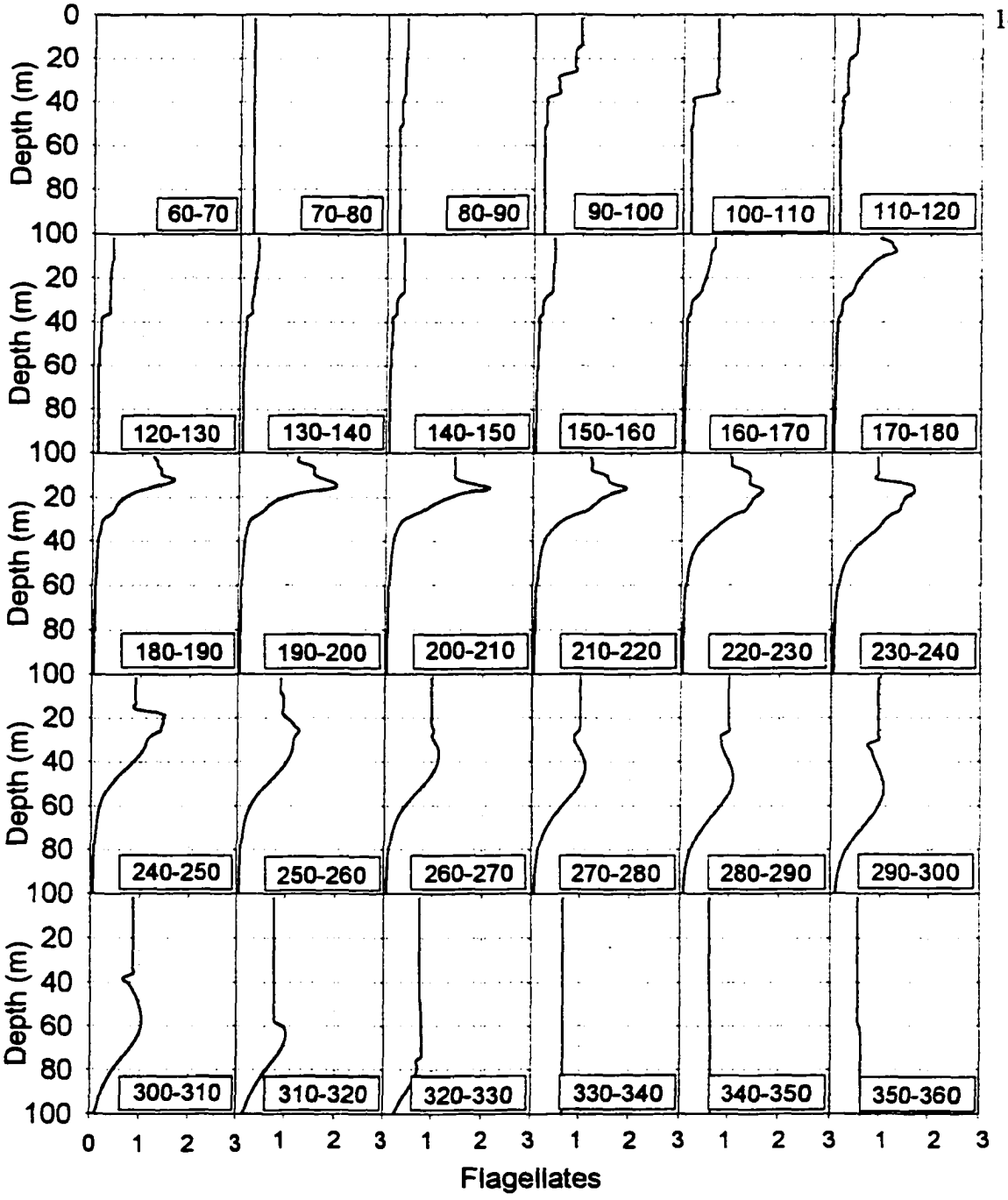

Figure A.2 - Seawater profiles of flagellated phytoplankton from the Middleton Island site - 1995 model run.

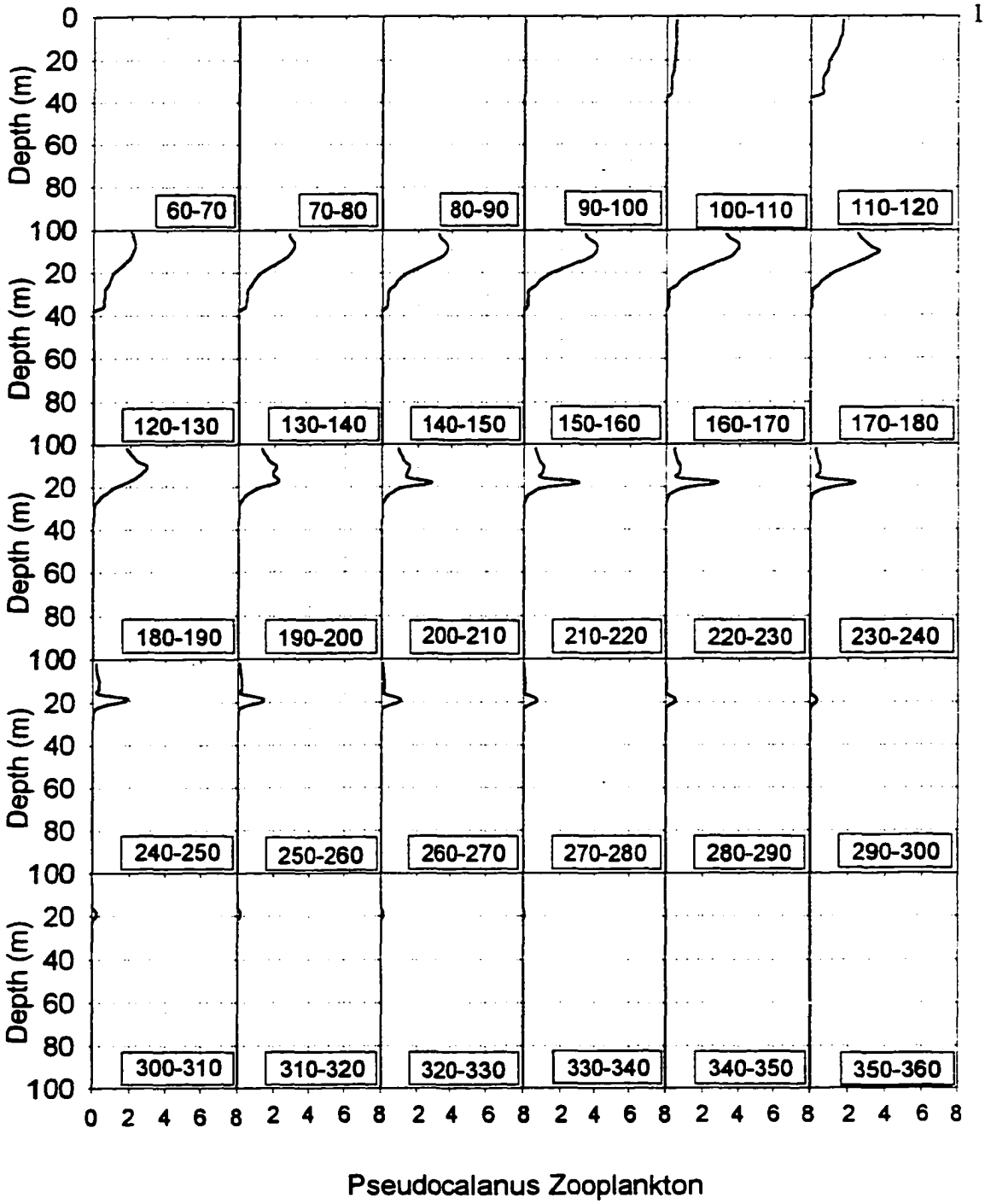

Figure A.3 - Seawater profiles of pseudocalanus zooplankton from the Middleton Island site - 1995 model run.

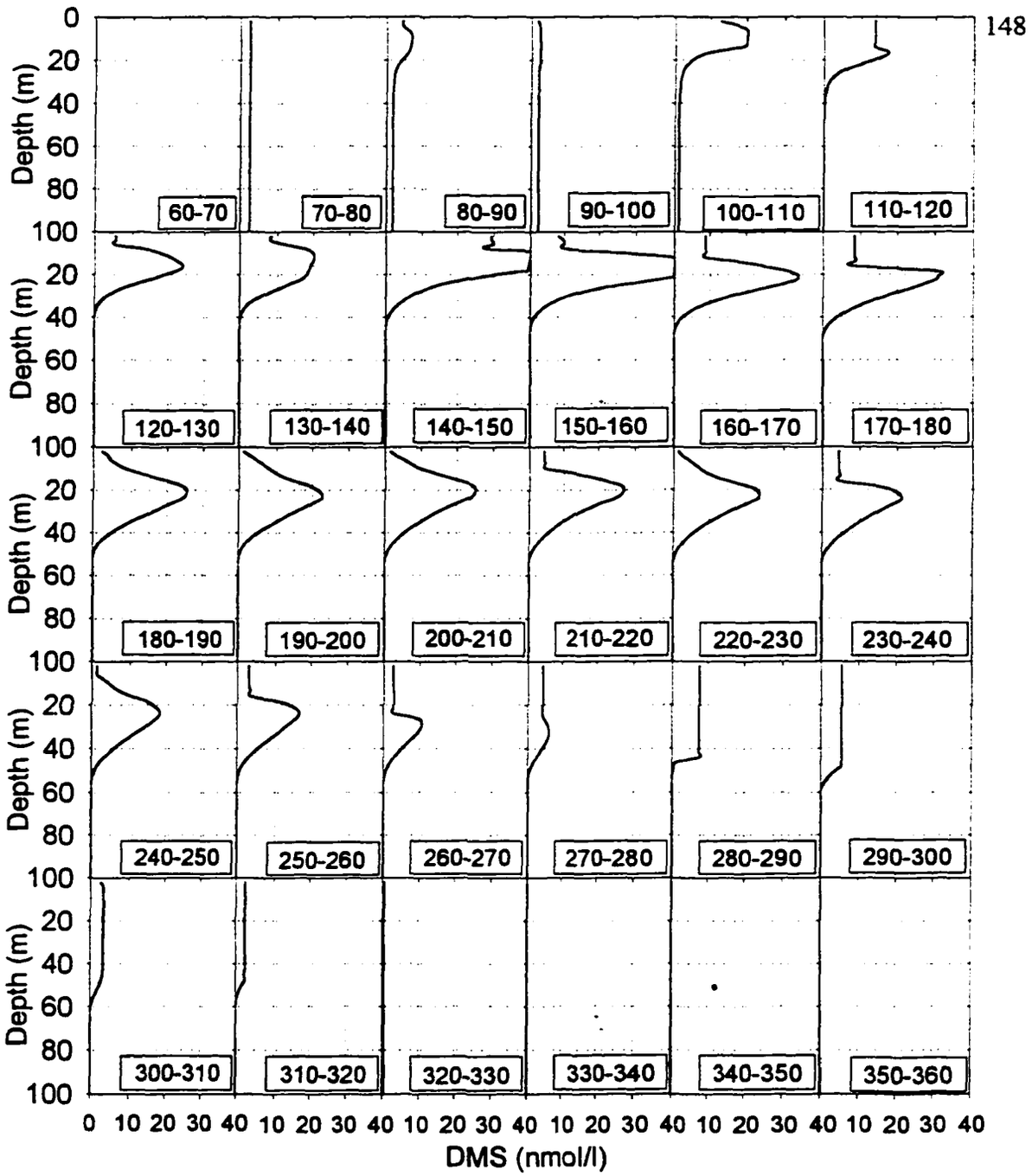

Figure A.4 - Seawater profiles of DMS from the C-Lab Buoy - 1993 model run.

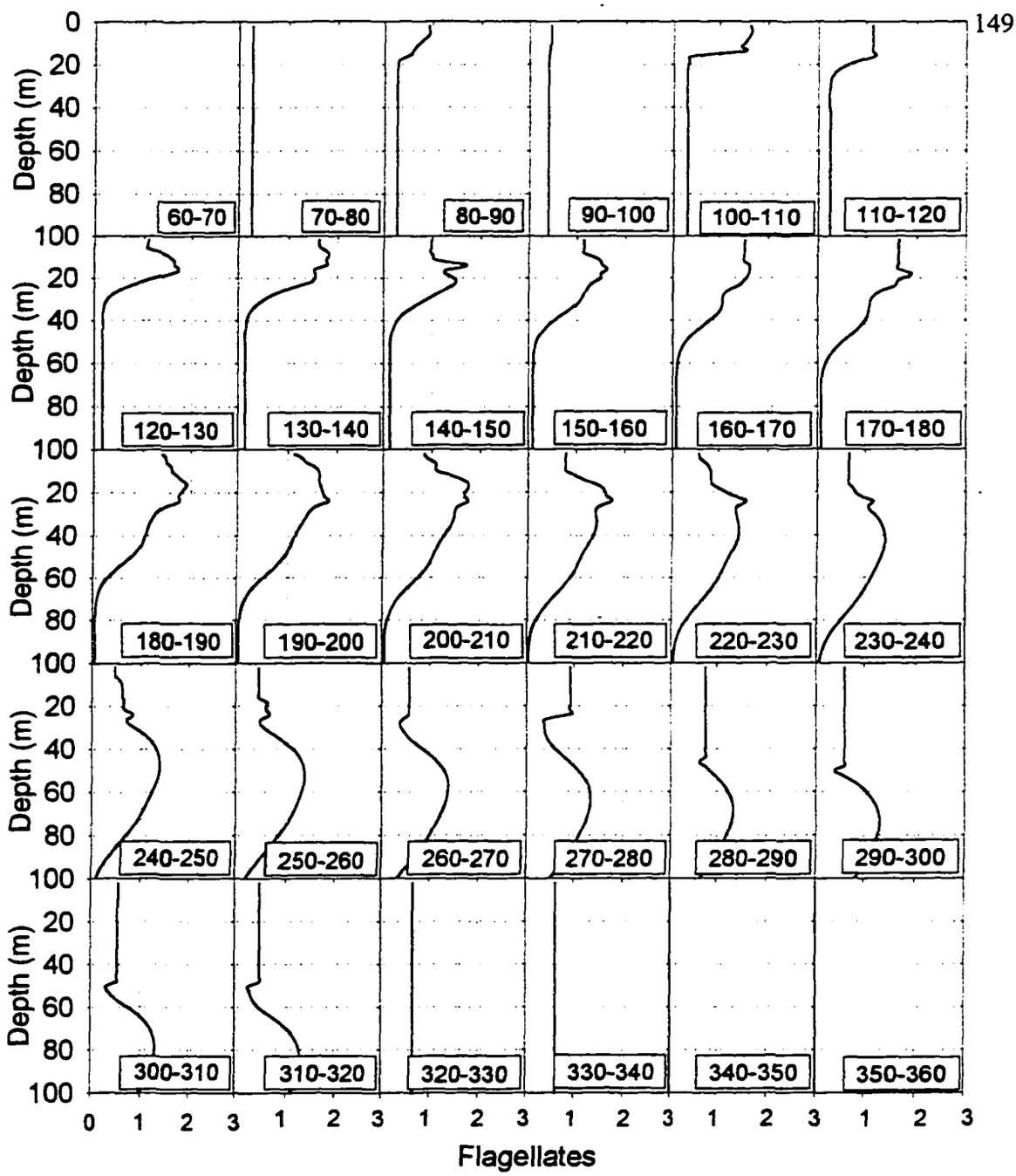

Figure A.5 - Seawater profiles of flagellated phytoplankton from the C-Lab Buoy - 1993 model run.

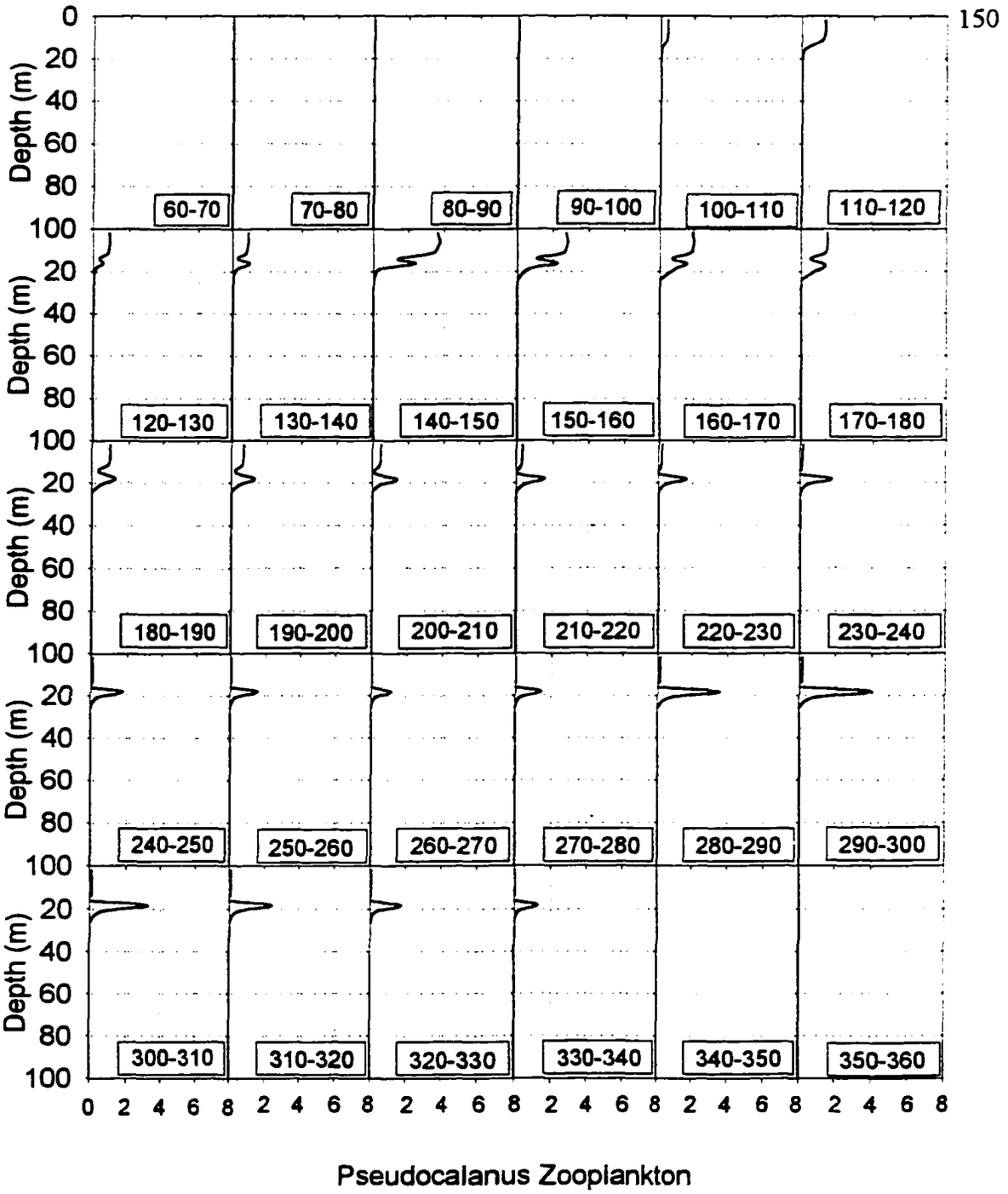

Figure A.6 - Seawater profiles of pseudocalanus zooplankton from the C-Lab Buoy - 1993 model run.

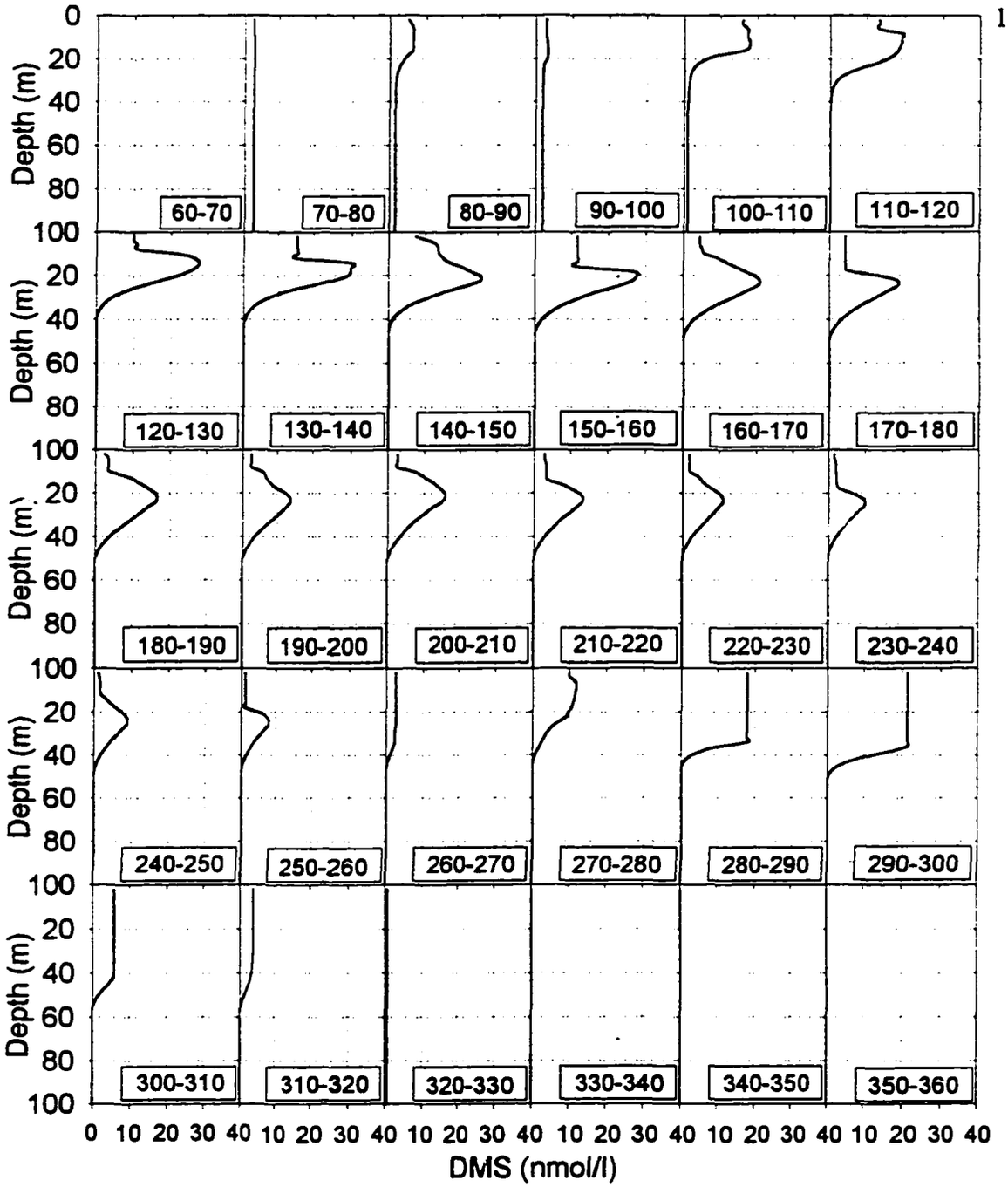

Figure A.7 - Seawater profiles of DMS from the Mid-sound Buoy - 1996 model run.

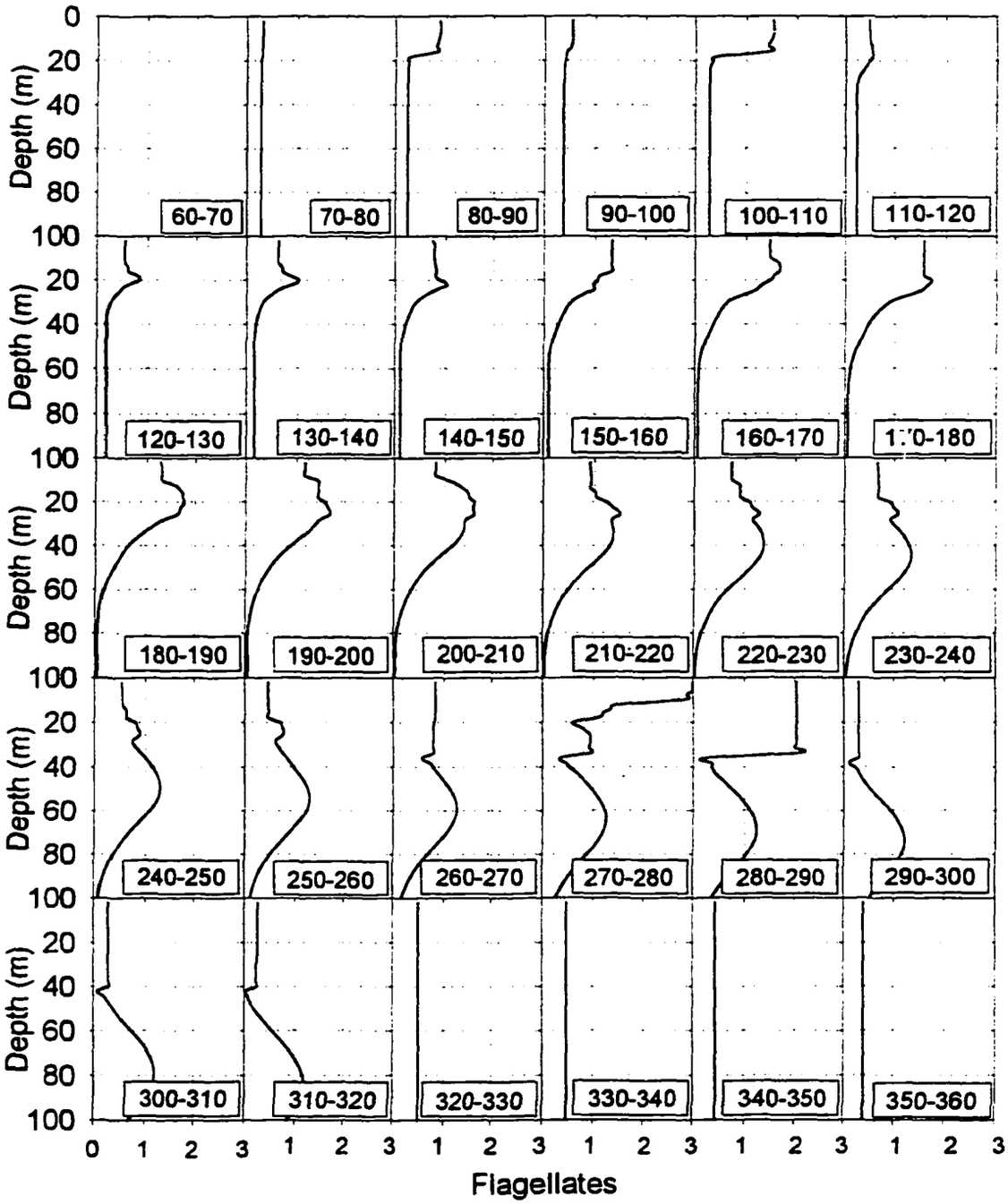

Figure A.8 - Seawater profiles of flagellated phytoplankton from the Mid-sound Buoy - 1996 model run.

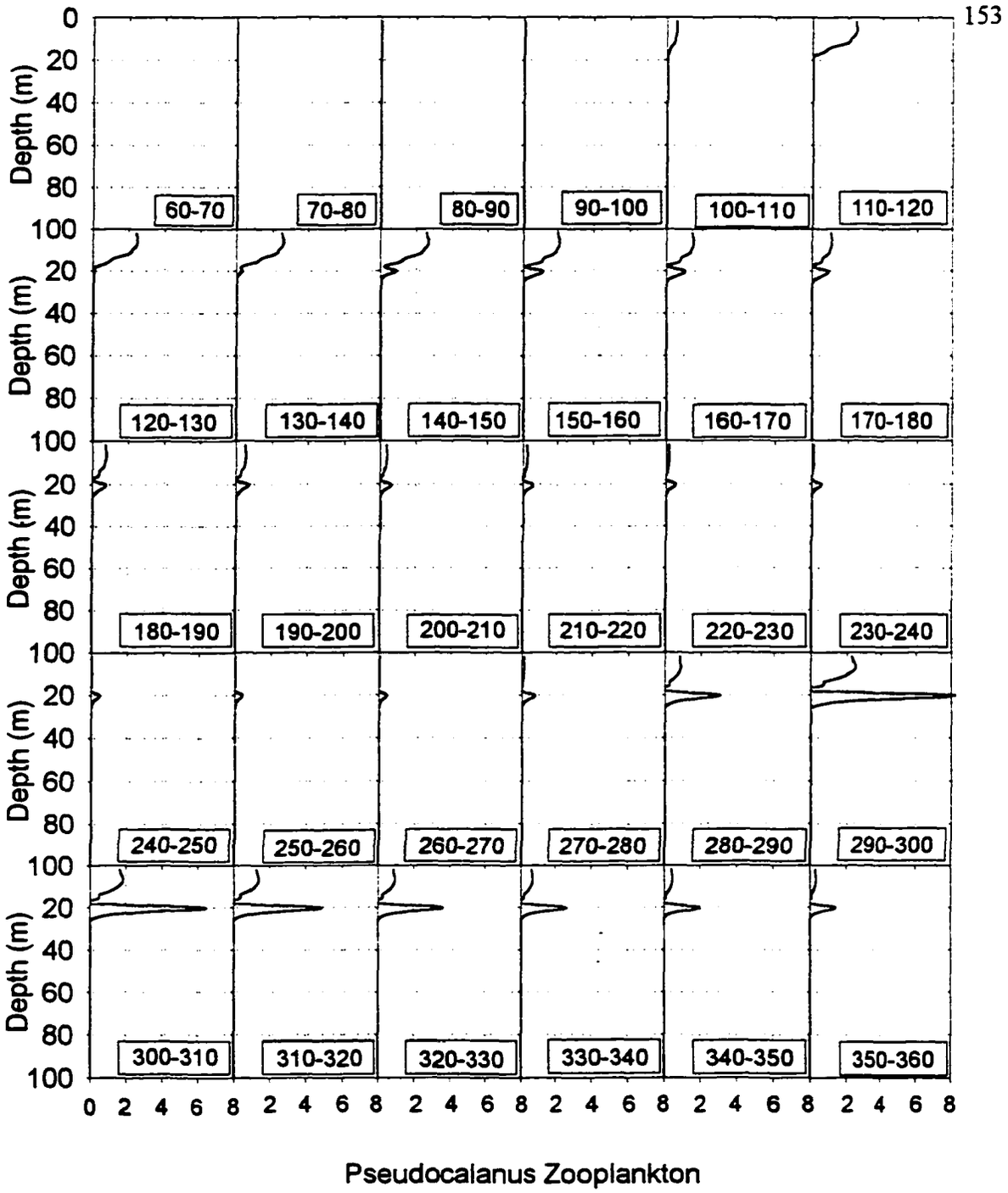

Figure A.9 - Seawater profiles of pseudocalanus zooplankton from the Mid-sound Buoy - 1996 model run.

IMAGE EVALUATION TEST TARGET (QA-3)

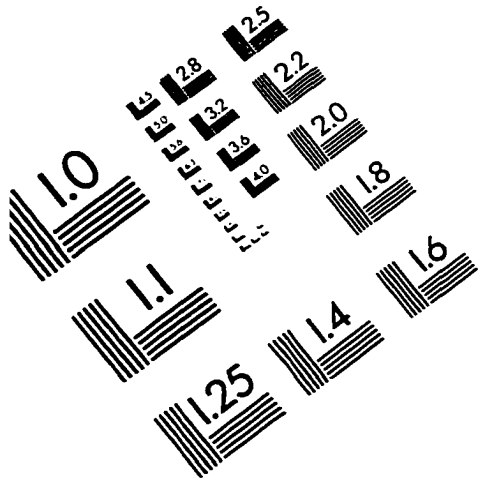

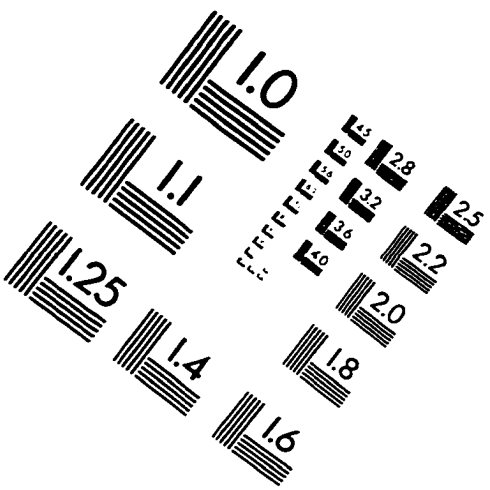

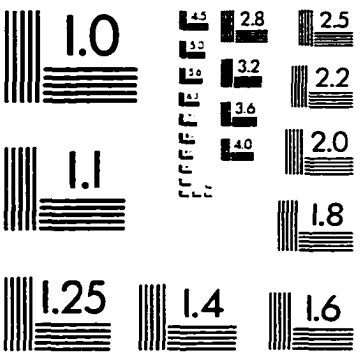

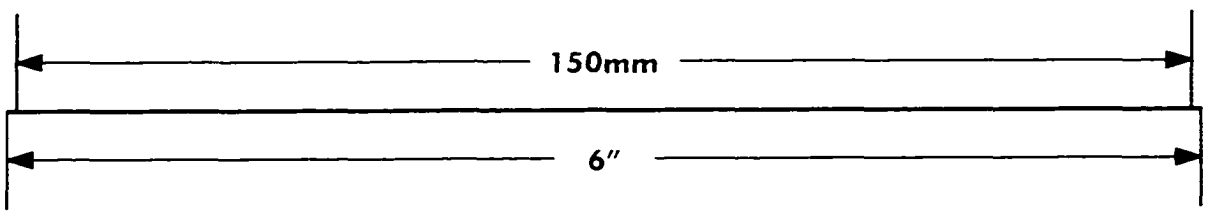

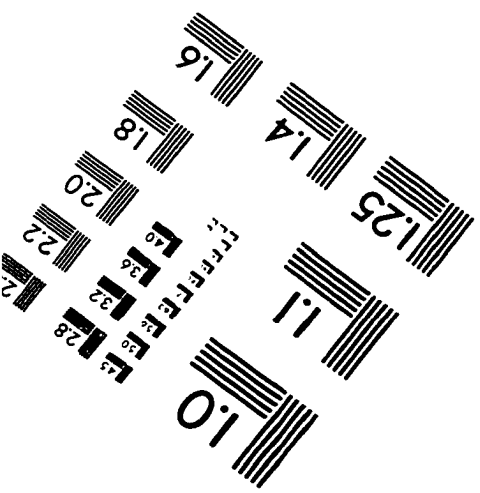

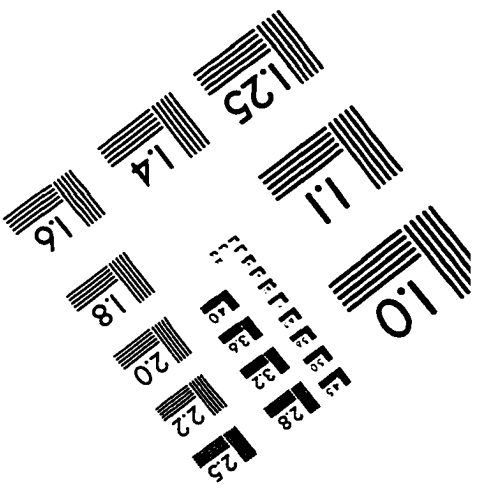

APPLIED IMAGE, Inc
1653 East Main Street
Rochester, NY 14609 USA
Phone: 716/482-0300
Fax: 716/288-5989